NOAA Technical Memorandum NOS CS 45

VDATUM WITH SPATIALLY VARYING UNCERTAINTY IN THE NORTHEAST GULF OF MEXICO FROM MOBILE BAY, ALABAMA, TO CAPE SAN BLAS, FLORIDA

Silver Spring, Maryland
January 2021

noaa National Oceanic and Atmospheric Administration

U.S. DEPARTMENT OF COMMERCE
National Ocean Service
Coast Survey Development Laboratory

Office of Coast Survey
National Ocean Service
National Oceanic and Atmospheric Administration
U.S. Department of Commerce

The Office of Coast Survey (OCS) is the Nation's only official chartmaker. As the oldest United States scientific organization, dating from 1807, this office has a long history. Today it promotes safe navigation by managing the National Oceanic and Atmospheric Administration's (NOAA) nautical chart and oceanographic data collection and information programs.

There are four components of OCS:

The Coast Survey Development Laboratory develops new and efficient techniques to accomplish Coast Survey missions and to produce new and improved products and services for the maritime community and other coastal users.

The Marine Chart Division acquires marine navigational data to construct and maintain nautical charts, Coast Pilots, and related marine products for the United States.

The Hydrographic Surveys Division directs programs for ship and shore-based hydrographic survey units and conducts general hydrographic survey operations.

The Navigational Services Division is the focal point for Coast Survey customer service activities, concentrating predominately on charting issues, fast-response hydrographic surveys, and Coast Pilot updates.

NOAA Technical Memorandum NOS CS 45

UPDATE VDATUM FOR THE COASTAL WATERS OF TEXAS AND WESTERN LOUISIANA: MODELED TIDAL DATUMS AND THEIR ASSOCIATED SPATIAL VARYING UNCERTAINTIES

Liujuan Tang[1,2], Edward P. Myers[1], Lei Shi[1], Kurt Hess[1], Alison Carisio[3,4], Michael Michalski[3], Stephen A. White[5], and Cuong Hoang[1]

[1] NOAA/Office of Coast Survey, Coast Survey Development Laboratory
[2] Earth Resources Technology
[3] NOAA/Center for Operational Oceanographic Products and Services
[4] Lynker Technologies
[5] NOAA/National Geodetic Survey

January 2021

noaa National Oceanic and Atmospheric Administration

U. S. DEPARTMENT OF COMMERCE **Wilbur Louis Ross Jr.** **Secretary**	**National Oceanic and Atmospheric Administration** **Dr. Neil Jacobs** **Acting Under Secretary**	**National Ocean Service** **Nicole LeBoeuf** **Acting Assistant Administrator**

Office of Coast Survey **Rear Admiral Shepard M. Smith** **Director**	**Coast Survey Development Laboratory** **Dr. Shachak Peeri** **Division Chief**

NOTICE

Mention of a commercial company or product does not constitute an endorsement by NOAA. Use for publicity or advertising purposes of information from this publication concerning proprietary products or the tests of such products is not authorized.

TABLE OF CONTENTS

LIST OF TABLES vii
ABSTRACT viii
1. INTRODUCTION 1
2. METHOD 5
2.1 Hydrodynamic Modeling 5
2.2 Computing Modeled Tidal Datum Fields 5
2.3 Datum Products and Spatially Varying Uncertainty 6
2.4 VDatum Marine Grids, Bounding Polygons, and Quality Analyses 6
3. DATA AND GRID DEVELOPMENT 9
3.1 Study Area and Tidal Datum Data 9
3.2 Shoreline Data 10
3.3 Bathymetry Data 11
3.4 Grid Development 13
3.4.1 Mesh generation using size function approach 14
3.4.2 Depth compilation process 17
3.5 Model Setup 26
4. MODEL RESULTS AND DISCUSSION 27
4.1 Validation and Error Analyses 27
4.2 Final Datum Fields and Spatially Varying Uncertainty 35
4.3 Populating the VDatum Marine Grids and Quality Check 38
4.4 Lessons Learned 43
4.4.1 Sensitivity of modeled datum to offshore boundary input 43
4.4.2 Sensitivity of modeled datum to breakwaters 43
4.4.3 Sensitivity of modeled datum to water depth 45
4.4.4 Sensitivity of spatially varying uncertainty to model error 48
4.4.5 Model error at station 8761678 in the Intracoastal Waterway 48
4.4.6 Sensitivity of spatially varying uncertainty to assigned RMS 49
5. SUMMARY AND CONCLUSION 51
ACKNOWLEDGEMENTS 51
REFERENCES 52
APPENDIX A TIDE STATION DATA AND MODEL RESULTS 53
APPENDIX B TIDAL DATUMS AND SPATIALLY VARYING UNCERTAINTY IN MARINE GRIDS IN VDATUM REGION 69

LIST OF FIGURES

Figure 1 VDatum region (red box) and computational domain for the new tide model for the northeast Gulf of Mexico. Red and cyan bars represent the observed MHW at tide stations within and outside the VDatum region, respectively. As a reference, the first bar from the east represents MHW of 0.41 m. Yellow and white lines are the shoreline and open boundary of the computational domain, respectively. White box indicates the location of NEGOM. Background images are from Google Earth. 3

Figure 2 Measurement error (root mean square errors) in cm for datums at tide stations. Red dots represent 38 stations without RMSE data. The max RMSE is 3.4 cm as in the black bar. 10

Figure 3 The CUSP shoreline data available in the region. Data are downloaded from https://www.ngs.noaa.gov/CUSP/. 11

Figure 4 NOS bathymetry survey data. Data prior to 2005 (in grey) were also used in the 2008 model grid. Data in color are the newly available survey data since 2005. 12

Figure 5 Bathymetry data source overview. Data priority is based on survey date. The more recent data, the higher priority. 13

Figure 6 Mesh transition from open boundary (blue) to western mainland boundary, (a) before and (b) after manual smoothing. 15

Figure 7 Mesh details (a1-a3) before and (b1-b3) after smoothing size functions. (2) and (3) are the close-up view of the area within the two red boxes in (1). 16

Figure 8 Examples of NOS bathymetry survey data sets with (a1) simple and (b1) complex boundary polygons. Black solid line and red dashed line represent the computed and revised polygons, respectively. (a2 and b2) Mesh nodes within the polygons were assigned depth values using the dataset in (a1) and (b1), respectively. 17

Figure 9 (a) newly developed model mesh for the study area. (b) Bathymetry data sources at the mesh nodes. See Fig. 5 for the data source names. 18

Figure 10 High resolution was applied to six inlets to Bays in VDatum region. (a) Three narrow inlets with breakwaters. (b) Three nature inlets. See Figure 9a for locations. Background images are from Google Earth. 19

Figure 11 (a-j) Zoomed view of the mesh and tide stations. 23

Figure 12 Comparison of the (a) 2008 and (b) 2017 model meshes. (1-3) Histograms of node number versus depth, longitude, and latitude, respectively. 25

Figure 13 Comparison of the modeled tidal datum and observations for tide stations within the VDatum area. The dashed lines indicate the 5-cm error band. Text in blue indicates model error greater than 5 cm at the stations. 29

Figure 14 Comparison of the modeled tidal datum and observations for stations outside the VDatum area. The dashed lines indicate the 5-cm error band. Text in red and blue indicate model error greater than 10 and 5 cm, respectively. 30

Figure 15 Modeled datum error for tide stations (a) in and (b) outside the VDatum region. 32

Figure 16 Model error for (a) MHHW, (b) MLLW, (c) MHW, and (d) MLW versus observed difference in magnitude of (1) MHHW and MLLW, and (2) MHHW and MHW for the 83 tide stations in VDatum region. 33

Figure 17 Entrance to the Saint Joseph Bay. (a) Location for station 8728958. (b) Dots are NOS survey data. 34

Figure 18 (a) Modeled datums, (b) datum corrected with observations, (c) the correction applied, and (d) associated spatially varying uncertainty for the domain. Rows 1-6 are the six datums, MHHW, MHW, MLW, MLLW , MTL, and DTL, respectively. 36

Figure 19 (a) Datum products and (b) spatially varying uncertainty in the VDatum region. Rows 1-6 are for the six datum, MHHW, MHW, MLW, MLLW , MTL, and DTL, respectively. The color is in meter. The color scales are adjust to better show the details in VDatum region (e.g. not the same color scale as in Figure 18). 38

Figure 20 (a) 2012 and (b) revised bounding polygons. 39

Figure 21 (1a-5a) Datum products and (1b-5b) spatially varying uncertainty for the five marine grids in VDatum region. The color scales are the same as Figure 19. See Appendix B for details. 42

Figure 22 Sensitivity of modeled datums to offshore boundary conditions using (a) EC2001 and (b) EC2015 tidal databases. Tests were conducted using the 2008 model grid with breakwaters added to Perdido Bay. The dashed lines indicate the 5-cm error band. 43

Figure 23 (a,c) Model data comparison at 74 stations in VDatum region (b) without and (d) with breakwaters at the entrance, respectively. Tide stations inside the Perdido Bay were within the red circle. Tests were conducted using the 2008 model grid. The dashed lines indicate the 5-cm error band. 44

Figure 24 Sensitivity of modeled datum to water depth for stations outside VDatum region. (a) Two types of large model error at early stage of testing. (b) Increasing minimum water depth resolved the underestimate at MLLW(e.g. the MLLW outliers to the left of the error band in (a)). See Figure 14a for the final results. The dashed lines indicate the 5-cm error band. 45

Figure 25 Sensitivity of modeled datum to water depth at station 8728130. Tests were conducted using the 2017 model grid. 46

Figure 26 (a) A Google Earth image shows the Waikula River and the outlier station 8728171. (b) Bathymetry survey data near the station. (c) A shallow segment of the river with with expansion and contraction. 47

Figure 27 (a) Survey data segment and outlier station 8727989. (b) Aucilla River survey data. (c) Google Earth image shows the rocky segment of the river with contraction. 47

Figure 28 Sensitivity of spatially varying uncertainty to model error. (a) Before and (b) after error reduction (e.g. Figure 24a vs. Figure 14a). Tests were conducted using 144 tide stations. Unit for the color bar is in meter. 48

Figure 29 Sensitivity of spatially varying uncertainty to model error at intracoastal waterway station 8761678. (a) 8 cm and (b) 4 cm error at 8761678, Michoud substation, Intracoastal

Waterway (ICWW), Louisiana. (c) and (d) are the corresponding spatially varying uncertainty for the grids in (a) and (b) respectively. 49

Figure 30 Sensitivity of spatially varying uncertainty to assigned root mean square error. (a1) RMSE for 144 tide stations. (a2) Spatially varying uncertainty for MHW in VDatum region using the 144 tide stations in a1. (b1) Maximum rmse of 3.4 cm were assigned to the 38 stations without rmse (in red bars). (c1) Local maximum rmse were assigned. (b2 and c2) Spatially varying uncertainty for MHW as the results from (b1) and (c1), respectively. A total of 182 tide stations were used in the SVU computation for (b2) and (c2). 50

LIST OF TABLES

Table 1 Shoreline data source overview. 10
Table 2 Bathymetry data source overview..... 12
Table 3 Criteria for mesh size function..... 15
Table 4 Properties of the 2008 and 2017 meshes. 24
Table 5 Summary of averaged error for model datums at tide stations for the new grid. 28
Table 6 Model datum error at tide stations in VDatum region for the 2008 grid. Results were taken from Dhingra et al. (2008). 28
Table 7 VDatum region names, directories in the CSDL VDatum archive, and abbreviations. .. 40
Table 8 VDatum grid information for the five marine grids. 40
Table 9 Comparison of data and GTX interpolated values (Standard deviations, cm) for the five regions for tidal datums. 40
Table 10 Maximum discontinuity (cm) across the 11 interfaces (see Figure 20b)..... 41

ABSTRACT

A spatially varying uncertainty study on tidal datums was conducted for the Northeast Gulf of Mexico (NEGOF) for VDatum application. The region of interest encompasses Mobile Bay, Alabama, in the west, to Cape San Blas, Florida, in the east. We developed an updated version of the tide model for NEGOF, to incorporate the latest available National Ocean Service (NOS) bathymetry survey data, National Geodetic Survey (NGS) shoreline data, and the updated tidal datum data from the Center for Operational Oceanographic Products and Services (CO-OPS). A gridding technique based on wavelength of long waves in deep ocean was developed to improve ADCIRC model efficiency. Then we applied the spatially varying uncertainty method based on variational approach to the modeled results to produce tidal datum products and associated uncertainty. The spatially varying uncertainty results have been used to help with decision-making on placement of new tide gauges to further reduce the uncertainty in VDatum. The report also documents lessons learned from the model development and testing processes.

Key Words: tides, tidal datum, spatially varying uncertainty, ADCIRC, bathymetry, Northeast Gulf of Mexico (NEGOF), coastline

1. INTRODUCTION

The VDatum vertical datum transformation software is an outcome of the national VDatum project in the U.S., a joint effort of the tri-office VDatum team of NOAA's Office of Coast Survey (OCS), National Geodetic Survey (NGS), and Center for Operational Oceanographic Products and Services (CO-OPS) (https://vdatum.noaa.gov/). It is designed to vertically transform geospatial data among a variety of tidal, orthometric, and ellipsoid-based vertical datums. The goal is to have complete coverage of U.S. coastal waters from the landward (i.e., navigable) reaches of estuaries and charted embayments out to 75 nmi offshore. At present, VDatum includes 36 different vertical datums. It allows users to convert their data from different horizontal/vertical references into a common system and enable the fusion of diverse geospatial data in desired reference levels.

In this study, we focus on tidal datums from astronomical tides for VDatum software. VDatum includes a class of seven tidal datums: mean higher high water (MHHW), mean high water (MHW), mean low water (MLW), mean lower low water (MLLW), mean tide level (MTL), diurnal tide level (DTL), and mean sea level (MSL). CO-OPS' coastal water level stations have been providing these tidal datums data, which are derived from time series of water level data at 6 minute intervals except the MSL, which is the hourly average. A full 19-year epoch period are used for the computation of the datums at CO-OPS' long term control stations (CO-OPS, 2003). For example, MSL is computed as the arithmetic mean of hourly water observations over the National Tidal Datum Epoch (NTDE), which presently is the 1983–2001 NTDE. All other shorter period subordinate gauges rely on simultaneous comparisons between their data and the epoch control station (CO-OPS, 2003). The differences between these two stations are applied to the control station datum to acquire a 19-year's equivalent at the subordinate stations. This helps to mute out the short period meteorological and oceanographic effects which are expected to be experienced by both the control and the subordinate stations.

In general, tidal datum fields may vary over horizontal space. Tidal datums at stations are referenced to measured local water levels and should not be extended into areas of differing oceanographic characteristics. To resolve the spatially varying nature of the tidal datums in between observation locations, hydrodynamic models and spatial interpolation techniques have been employed for each VDatum application that simulate the tidal propagation characteristics in the region of interest. In order to merge all of the individual VDatum applications together to form a continuous national VDatum product, a consistent methodology for computing the tidal datums has been adopted for all region-specific VDatum applications (NOS, 2010). The approach consists of the following four major steps (Myers et al., 2005; NOS, 2010):

(1) First use the bathymetric and coastline data to develop a grid to be used by the hydrodynamic model.
(2) Next calibrate a hydrodynamic model to best simulate the observed tidal datum characteristics for the region.
(3) Then correct the model-data errors using a spatial interpolation technique.
(4) Finally provide the corrected modeled datums (i.e., datum products) on several structured grids of points to be used by the VDatum software.

Following the above methodology, 38 region-specific VDatum applications have been developed for U.S. coastal regions, among which three of them cover the Gulf of Mexico coast (Dhingra et al., 2008; Yang et al., 2010; Xu et al., 2013).

For the applications developed prior to 2016, the model-data corrections were made using the Tidal Constituent and Residual Interpolation (TCARI) tool developed by Hess et al. (1999; 2002). TCARI is a first-order deterministic spatial interpolation tool based on solution of Laplace's equation. The errors between the model results and the CO-OPS station data are interpolated throughout the domain to create an error field for each tidal datum. The error field is then used to correct the model results to create a datum field that matches the station data at those locations (Hess et al., 2005). The approach produces a single-value uncertainty estimate of the tidal datums for each model region (https://vdatum.noaa.gov/docs/est_uncertainties.html).

To provide a more accurate representation of the uncertainty in each model region, Shi and Myers (2016) developed a new statistical interpolation method, namely the spatially varying uncertainty (SVU) method, for VDatum applications. It was derived from the variational principle to calculate the corrected tidal datums by blending the model results, observations, and measurement errors together. They show that the new interpolation approach not only reduces the bias and errors, but also produces a spatially varying uncertainty. The uncertainty results can also provide important guidance for decision-making on placement of new tide gauges to further reduce the uncertainty in the VDatum products. This spatially varying uncertainty method has become the new standard for use for developing VDatum applications since then.

Here we apply Shi and Myers' method to study spatially varying uncertainty in the northeast Gulf of Mexico (NEGOF) VDatum region (Figure 1). This is part of an effort to update the three VDatum regions in the Gulf of Mexico in the next few years. The SVU study for the northwest Gulf of Mexico has been completed nearly at the same time and will be published in a separate report. The Gulf of Mexico coasts have been impacted frequently and severely by past hurricanes, resulting in changes to the coastline and nearshore bathymetry (Fearnley et al., 2009). This may induce uncertainty in the tidal datums in the area. The SVU helps to identify locations where new gauges would be beneficial in reducing uncertainty in VDatum. Once new data are collected, they will then be merged with the model to update the VDatum for this region. The same process will be used as we update other VDatum regions as well.

The northeast Gulf of Mexico VDatum region is indicated as the red box in Figure 1. It extends from Mobile Bay, Alabama, in the west to Cape San Blas, Florida, in the east. The region is featured with six bays and relatively flat coastline at the open coast. The bathymetry slope is gentle from shoreline to 40 m water depth and then drops sharply to more than 2000 m deep. The tidal pattern in the region is dominated by diurnal tides (Gill and Schultz, 2001). The first version of the tidal model for the region was developed by Dhingra et al. (2008). We refer it as the 2008 tidal model in this report. Since then, new observations on tidal datums and bathymetry survey data have become available. Given the amount of new data, we have redeveloped the tide model to reflect the new information and coverage as best possible. Tang et al. (2018) describes the major results and findings while more details are provided in this report.

The rest of this technical report is organized as follows: Section 2 briefly describes the method; Section 3 presents the data, grid development, and model setup of the tide model; Section 4

discusses the modeling results, including datum validation, associated spatially varying uncertainty, applications, and lessons learned; summary and conclusion are provided in Section 5

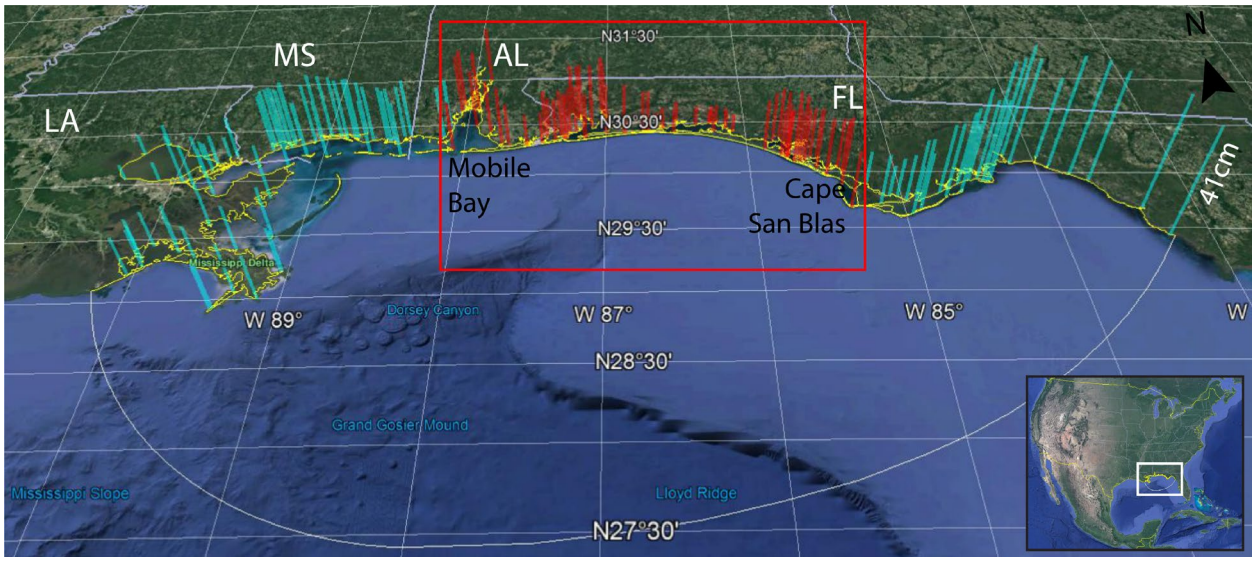

Figure 1 VDatum region (red box) and computational domain for the new tide model for the northeast Gulf of Mexico. Red and cyan bars represent the observed MHW at tide stations within and outside the VDatum region, respectively. As a reference, the first bar from the east represents MHW of 0.41 m. Yellow and white lines are the shoreline and open boundary of the computational domain, respectively. White box indicates the location of NEGOM. Background images are from Google Earth.

2. METHOD

2.1 Hydrodynamic Modeling

The hydrodynamic model used for this study is the two-dimensional, depth-integrated version of the Advanced Circulation (ADCIRC) model (Luettich et al., 1992; Luettich and Westerink, 2004). It utilizes the fully nonlinear shallow water equations with hydrostatic pressure and Boussinesq approximations. It solves the continuity and the non-conservative momentum equations for free surface elevation and the depth-averaged velocity components. The equations are discretized: horizontally in space using the finite element method with three-node linear triangles; and in time using the finite difference method, the implicit Crank–Nicolson approximation with second order accuracy. The non-linear terms are evaluated explicitly. The ADCIRC code allows a variety of users specified input parameters. Here we used the fully nonlinear form of the equations, which includes non-linear bottom friction, finite amplitude, and convection terms. The ADCIRC model has been parallelized using domain decomposition, a conjugate gradient solver, and Message Passing Interface (MPI) based message passing. This parallel version of the code was compiled and run on NOAA's Jet high performance computing system in Boulder, Colorado. The ADCIRC model has been used in previous VDatum areas (Hess et al., 2005; Spargo and Woolard, 2005), taking advantage of highly flexible, irregularly spaced grids. Numerous studies have shown this model to be robust throughout the Eastern North Atlantic and Gulf of Mexico regions (Luettich and Westerink, 1995; Mukai et al., 2002), and the West Coast (Spargo, 2004).

2.2 Computing Modeled Tidal Datum Fields

The modeled water level time series are then used to tabulate the higher-high, lower-high, higher-low, and lower-low waters, from which the datums could be computed. The method to extract the highs and lows is based on the approach used by CO-OPS (Gill and Schultz, 2001), which is for analysis of water level measurements at tide stations. It is coded in the C language in the CO-OPS Data Processing and Analysis System (DPAS). The modeled water surface elevation is in general less noisy comparing to the measurements at tide stations. For the VDatum effort the new Fortran program levels.f (or lv8j.f) was written to duplicate the CO-OPS methodology (NOS, 2010; Hess and White, 2004). The program is based on the original C language computer program and related texts, and discussions with various members of CO-OPS. More details can be found in NOS (2010).

Seven tidal datums (MHHW, MHW, MSL, MTL, DTL, MLW, and MLLW) are computed based on the highs and lows. The analysis starts with the identification of all the tidal extrema (highs and lows) in the modeled time series of water surface elevation. It continues with the selection (within a 25-hour time period) of the higher of the two highs and the lower of the two lows. If only one high water is present in the time period, it is categorized as a higher high. Thus, for high water (for example), each day has either a lower high and a higher high, or a single higher high. The average of all the highs and the higher highs is called the Mean High Water (MHW), and the average of just the higher highs is called the Mean Higher High Water (MHHW). The process for producing MLW and MLLW from the low waters is similar. The average of the MHW and the MLW is called the Mean Tide Level (MTL) and the average of the MHHW and the MLLW is called the Diurnal Tidal Level (DTL). Mean Sea Level (MSL) is the average of the hourly water levels. For further information on tidal datums, see Gill and Schultz (2001).

The analysis is repeated for time series of water surface elevation at every node in the ADCIRC mesh and then we have the modeled tidal datum fields.

2.3 Datum Products and Spatially Varying Uncertainty

The VDatum's vertical datum transformations require that the values returned by the VDatum software need to be equivalent to values determined through observations at tide gauge locations. Therefore, the modeled tidal datum fields need to be corrected with tide station data. Here we refer to the corrected model datum fields as the datum products.

In the past, this was achieved by deterministic interpolation method (Hess and Gill, 2003; NOS, 2010). It spatially interpolated the error between the model and the station data to allow the final datum fields to match the station data at those locations. This was through a prediction and correction procedure, the latter of which uses a deterministic spatial interpolation method. A solver based on Laplace's equation was used for the spatial interpolation of modeled tidal datum and observed tidal datum discrepancies over the water.

As VDatum currently provides single-value uncertainty estimates in the tidal datums for each regional application, the next goal is to provide a spatially varying uncertainty field for each tidal datum to improve the uncertainty estimates. Therefore in this study, we apply Shi and Myers' (2016) statistical method to blend the modeled and the observed tidal datums, as well as to compute the associated spatially varying uncertainty for the entire domain.

Here we give a brief introduction to the method. More details can be found at Shi and Myers (2016). The method is derived from the variational principle in data assimilation to obtain analysis solution by minimizing a cost function. The construction of the cost function is such that the discrepancy between the analysis solution and observations satisfies the constraint prescribed by the user. The constraint that the VDatum technical team adopted for statistical interpolation is that the discrepancy between the analysis field and the observations at all tide stations should be equal to or less than 1 cm or the CO-OPS' error value, whichever is less. This is achieved by introducing a diagonal weight matrix that regulates not only the weight of the model error for a particular station in the cost function but also the analysis results.

2.4 VDatum Marine Grids, Bounding Polygons, and Quality Analyses

The VDatum software requires regularly spaced grids called "marine grids" that contain the datum information at the water nodes and null information at the land nodes (NOS, 2010). The datum product and associated spatially varying uncertainty from section 2.3 are based on the unstructured grid. Therefore, they need to be populated in to the marine grids to be used by the software.

We use the grid generating software (vgridder21.f) to generate the VDatum marine grid for a specific region, which consists of points with uniform spacing in the longitude and latitude directions. Digitized coastline data are used to determine which points in this marine grid are water and which are land. Points located within water, or within a distance of approximately one-half a marine grid element size of water, are set to water. The water points of the VDatum marine grid are then populated with the tidal datum and uncertainty information, which are interpolated from

the corrected model datums using the program vpop28.f. The output will then be saved in GTX format for use by the VDatum software.

The final tidal datum products as represented on the VDatum marine grid in the GTX format must be checked in several ways, including (1) validation test at station locations, (2) continuity test at common boundaries, (3) overlapping test, and (4) polygon test (NOS, 2010). For the validation test, the GTX files are checked against observations to confirm that the datums approximately match at the tide stations. The error at each station should be no greater than 1 or 2 cm. When there are adjacent tidal datum grids, there must be a check for continuity of values across the common boundaries (e.g., continuity test). This is done with program test_cont15.f. In some regions, the tidal marine grids can actually overlap, resulting in ambiguity in the selection of the correct grid (NOS, 2010). Therefore, the use of a bounding polygon is necessary. Given a latitude-longitude point in the overlap region, a check is made of whether the point falls within a specific bounding polygon; if so, the marine grid for that region can be used. If not, additional polygons are checked. The overlapping test is to ensure that the bounding polygons do not overlap with each other. We use test_ovlp8.f to check and make sure that there is no overlapping between the adjacent bounding polygons. The polygon test is to check the bounding polygon to ensure it is completely inside the marine grid (NOS, 2010). The test_poly4.f is used to check and ensure bounding polygon is completely inside the marine grid.

3. DATA AND GRID DEVELOPMENT

3.1 Study Area and Tidal Datum Data

The VDatum region extended from Mobile Bay, Alabama, in the west to Cape San Blas, Florida, in the east (from -88.0857ºE to -85.2811ºE). There are 83 NOAA CO-OPS tide stations in the region. Figure 1 shows the station locations (the red bars). The height of each bar represents the MHW at the station. As will be discussed in Section 4, stations in the VDatum region show three group patterns, which are correlated to their geographical locations. Stations in Group 1 are located either on open coast or less protected bays. This group has the greatest tidal datum in the VDatum region, with MHW around 0.18-0.25 m. Group 2 are the six stations inside Perdido Bay, with MHW around 0.12 m. The third group are the eight stations inside the Choctawahatchee Bay, which have the smallest MHW, around 0.08 m.

To reduce the boundary effect, we expand the model domain boundary away from the center of the VDatum region. Figure 1 shows that the computational domain is extended approximately five-sixths of the width of the VDatum coverage area to both the east and to the west. This introduces 99 additional NOAA tide stations in the computational domain, which are plotted as the cyan bars in Figure 1. The stations located near the east land boundary in Florida have the greatest tidal datum in the domain, with MHW around 0.50 m. The tidal datums at the stations to the west are similar to those of Group 1 in the VDatum area except the four stations located inside Lake Pontchartrain, with a smaller MHW around 0.08 m.

Altogether there are 182 tide stations in the computational domain. Figure 2 shows the datum measurement error in root mean square error, which are available for 144 stations. The maximum error are 2.9 cm and 3.4 cm within and outside VDatum region, respectively. Error data are not available for 38 stations indicated as red dots in Figure 2, due to insufficient data in CO-OPS' database. Those measurements were mainly from the early 1970s and predated the database (personal communications with CO-OPS' M.Michalski, 2017). For details on how the RMSE for tidal datums were computed for CO-OPS tide stations, please see Bondar (1981).

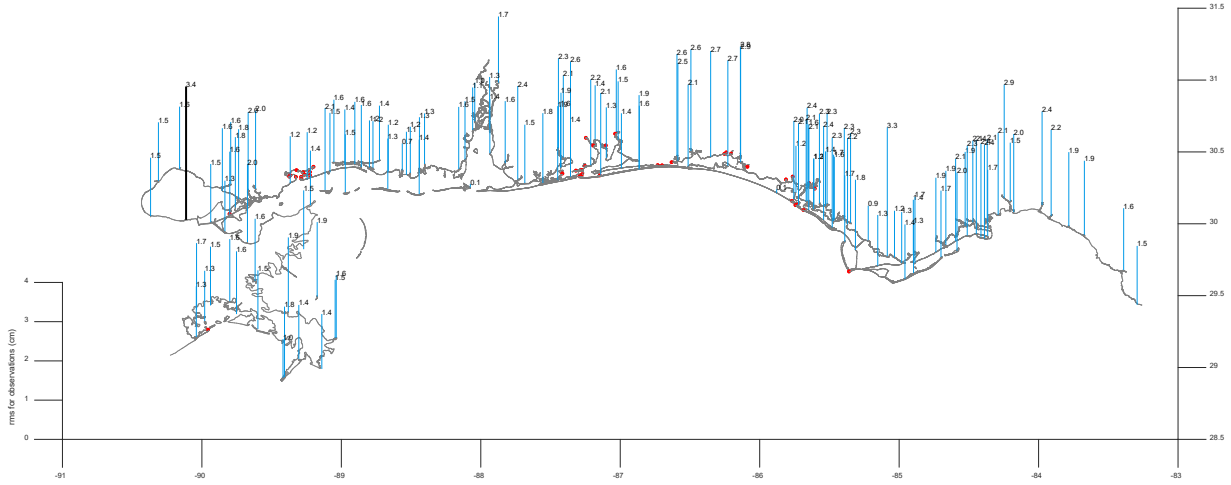

Figure 2 Measurement error (root mean square errors) in cm for datums at tide stations. Red dots represent 38 stations without RMSE data. The max rmse is 3.4 cm as in the black bar.

3.2 Shoreline Data

The MHW coastline is used as the land boundary for creating the unstructured grid for the tidal model. It also defines the extent of the VDatum marine grid. Table 1 summarizes the shoreline data sources used.

Table 1 Shoreline data source overview.

Data Sources	Year	Vertical Datum	Horizontal Datum
NOAA Continually updated shoreline product (CUSP) data	2016	MHW	NAD83
NGS Vector shoreline	2017	MHW	NAD83
MHW shoreline (Dhingra el al., 2008)	2008	MHW	NAD83
Google Earth Satellite Image	2017		NAD83

The MHW shoreline from NOAA's Continually Updated Shoreline Product (CUSP) data are the considered the most recent and accurate shoreline data available (https://www.ngs.noaa.gov/CUSP/). Figure 3 shows the CUSP data available for the region at the time of development. The Horizontal Datum is North American Datum of 1983 (NAD83). The data have scales between 1:1,000 – 1:24,000. Individual national shoreline projects and high-resolution LiDAR-derived shoreline were merged to form the framework of the CUSP data.

In this study, the MHW shorelines have been updated with all available CUSP data except for the Louisiana coast to the west of VDatum region, where simplifications are made to the marsh land coast based on the shoreline used by the 2008 VDatum model and the tide model for Eastern Louisiana and Mississippi (Yang et al., 2010). For locations where the CUSP data are unavailable, the MHW shoreline from the NGS Vector Shoreline Data are used. All data were compared with Google Earth Satellite image. Corrections were made to certain area where shoreline appears to be incomplete or inaccurate. The final coastline used for model development is illustrated as the grey line in Figure 2.

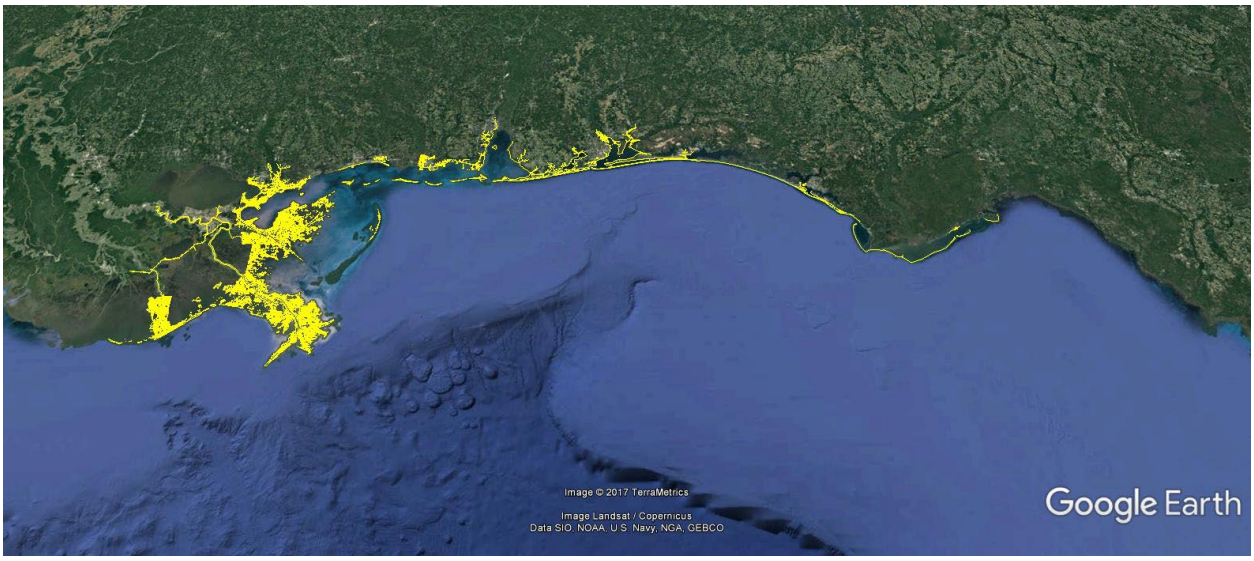

Figure 3 The CUSP shoreline data available in the region. Data are downloaded from https://www.ngs.noaa.gov/CUSP/.

3.3 Bathymetry Data

Table 2 summarizes the bathymetry data used to compile the model grid. In general, the new data sources superseded the old sources when they overlapped. Figures 4 and 5 show the spatial extent of each data source.

Data are from several primary sources/agencies. NOAA's NOS bathymetry survey and ENC data, National Centers for Environmental Information's (NCEI) Digital Elevation Models (DEMs), and the U.S. Army Corps of Engineers (USACE) survey data.

Table 2 Bathymetry data source overview.

Data Sources	Year	Datum Vertical	Horizontal
NOS Bathymetry Survey	1872–2016	MLLW/MLW	NAD83
ENC	2005	MLLW	NAD83
NCEI Mobile Bay 1/3" DEM	2011	MHW	NAD83
NCEI New Orleans 1/3" DEM	2011	MHW	NAD83
NCEI Southern Louisiana 1/3" DEM	2010	MHW	NAD83
NCEI Biloxi 1/3" DEM	2008	MHW	WGS84
NCEI Panama City 1/3" DEM	2008	MHW	WGS84
USGS Grand Bay 10 m DEM	2015	MLLW	NAD83
NCEI Northern Gulf 1" DEM		MHW	NAD83
USACE Escambia River Survey	2015	MLLW	FL State Plane
[1] Aucilla River Survey	2014	NAVD88	NAD83 903 North
[1] Econfina River Survey	2014	NAVD88	NAD83 903 North
[2] Wakulla River Segment Survey	2015	Unknown	WGS84

1: Data provided by Land & Sea Surveying Concepts, Inc. and Suwannee River District Management District.
2: Data provided by Howard T. Odum Florida Springs Institute.

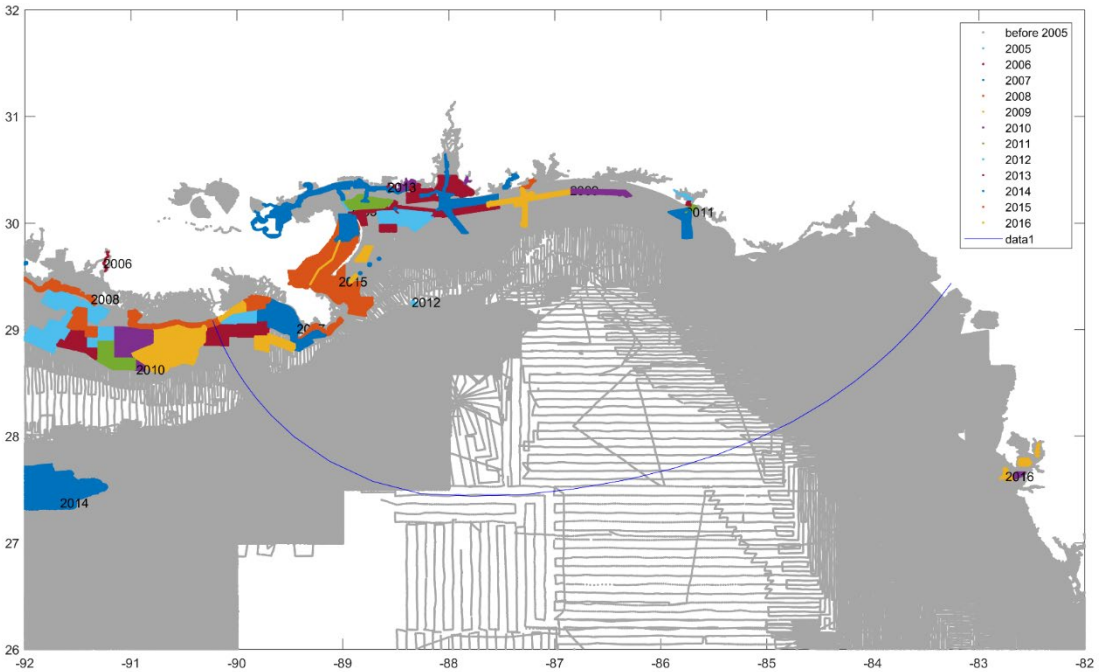

Figure 4 NOS bathymetry survey data. Data prior to 2005 (in grey) were also used in the 2008 model grid. Data in color are the survey data since 2005.

The NOS sounding data possess the most coverage in the domain. It includes surveys conducted between 1885 and 2016. The datums are referenced to either MLW or MLLW, depending on the years of data collection. Figure 4 shows the NOS bathymetry survey data. Data in colors represent the newly available survey since the development of the previous model grid, whereas data in grey are prior to 2005.

Five high resolution DEMs (1/3 arc sec) from NCEI are available for the region as shown in Figure 5 (Taylor et al., 2008a; Love et al., 2010a,b, 2011; Amante et al., 2011) . The Biloxi and Panama City DEMs were developed in 2008 while the Mobile Bay and New Orleans DEMs were released in 2011. The Southern Louisiana DEM was developed in 2010. These DEMs contains some LiDAR bathymetry and USACE survey data for some of the rivers or intracoastal waterways that are not included in the NOS data. The USGS 10m Grand Bay DEM based on MLLW developed in 2015 were also used in the study (DeWitt et al., 2015).

The bathymetry data priority for the grid development is illustrated in Figure 5: the more recent data, the higher the priority. Data values were converted, when necessary, to the NAD83 horizontal datum and Mean Sea Level vertical datum using VDatum software.

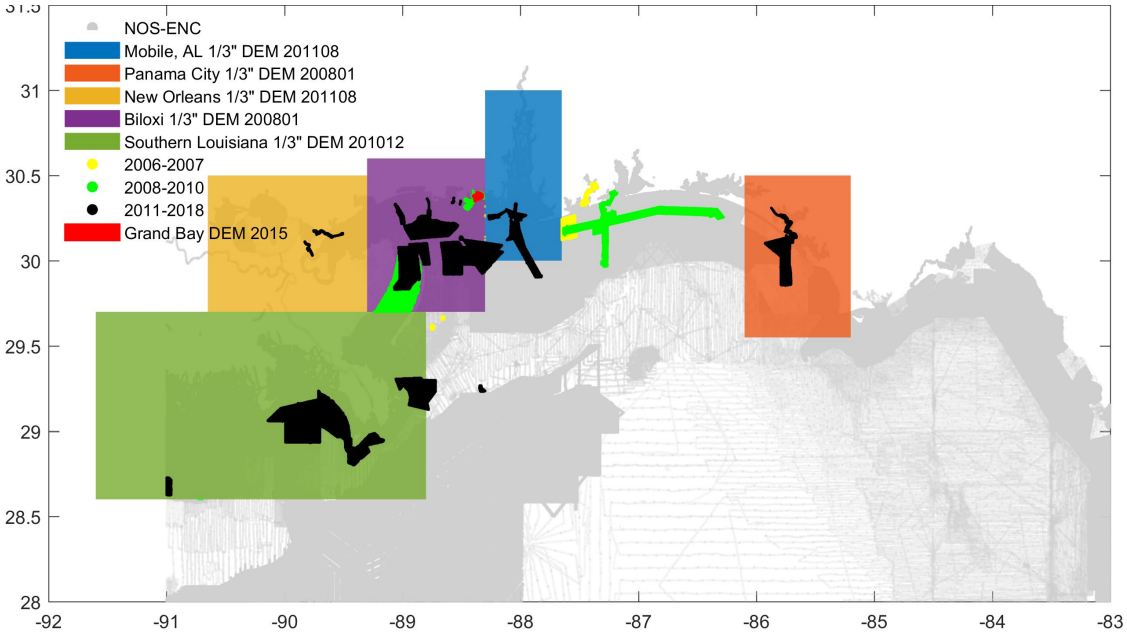

Figure 5 Bathymetry data source overview. Data priority is based on survey date. The more recent data, the higher priority.

3.4 Grid Development

As illustrated in Figure 1, the mesh domain were defined by the coastline (i.e., as the land boundary) and offshore open boundary. The VDatum region (from -88.0857ºE to -85.2811ºE) was centered

in the domain. The mainland boundary to the west was similar to the 2008 VDatum mesh while the eastern boundary was extended further east to reduce the boundary effect to the VDatum region.

The grid development includes two main processes, (1) mesh generation and (2) water depth interpolating based on data priority.

3.4.1 Mesh generation using size function approach

The mesh was generated by using the Surface-water Modeling System (SMS) software (https://www.aquaveo.com/) with the size function approach. A size function is simply a collection of scatter points (in a scatter data set) that define element resolutions in different portions of the domain. It is an effective approach since it can assign high resolution only to areas that are needed, such as very shallow areas (to better resolve the nonlinear wave dynamics), and coastline with high curvatures or area with sudden change in depth (to give a better representation of local geometry and bathymetry).

Table 3 summarizes the criteria used to define the size function. In the deep ocean, the dynamics of long waves are essentially governed by the shallow water approximations. That is to say, the propagation speed of tides can be approximated by $\sqrt{gd}$, where d is the water depth and g is the acceleration due to gravity. In the study, we used two parameters, wave length (L) and distance to shoreline (D), to control the size function (s). The initial resolution s_0 was set to 10 points per wave length:

$$s_0 = \frac{L}{10} = \frac{T\sqrt{gd}}{10} \qquad (1)$$

where T is the wave period. Here we use 3 hours for T to be on the conservative side, comparing to the typical semidiurnal tidal periods of 12 hours or longer.

Next we adjust the resolution based on distance to shore in the form of the ratio of D to a reference distance D_{ref}:

$$s = r s_0 = \frac{D}{D_{ref}} s_o \qquad (2)$$

In this way, for two points at the same water depth, the one closer to shore has a higher resolution. The reference distance D_{ref} can vary for different ocean depth. We used maximum offshore distances as D_{ref} for various depth contours. Here we give an example on how to generate the size function along the 1000 m depth contour. First we developed a DEM on a rectangular grid based on the bathymetry data. Next we extract the points along 1000m contour line, compute D for all points along the contour, and use D_{ref} =max(D) at d=1000m. Repeating the process for different depth contours to obtain the size functions in deep ocean.

For the shallow area and along the coastline, higher resolutions were assigned manually using SMS. We applied 60 m (or approximately 2-arc-sec) resolution for narrow breakwater entrances,

100-200 m for natural bay entrances as well as coastline inside bays within the VDatum region, 400 m for the relatively straight open coastline within or near the VDatum region, and 800 m for coastline far away from the VDatum region. Table 3 summarizes the criteria.

Table 3 Criteria for mesh size function.

Area type	Parameters/Criteria for resolution
Deep water offshore	a. Wave length (3 hours, 10 points per wave length, upper limit: 40-50 km) b. Distance to shore (ratio scale)
Shallow water Nearshore Depth<10 or 20m	a. Breakwater entrances : 60m b. Very narrow channels and rivers: 60 m c. Natural entrance: 100 m d. Entrance to Mobile Bay: 200 m e. Water way: higher resolution
Shoreline Depth~=0	a. Breakwater entrances: 60 m b. Inside bay: 100 -200m c. Open coast: 400 m d. Outside VDatum region: far, 800 m; close, 400m.

In order to provide good transition from deep ocean to coastline, the size function needs to be smoothed so the values (resolutions) do not change too quickly. SMS provides a toolbox to perform the smoothing task. However, some areas still need manually smoothing first. Such areas include locations where the open boundary connects to the mainland boundary and narrow entrances to bays or rivers. Figure 6 illustrates how smoothing can enhance the poor transition from the open boundary to the mainland boundary. Figure 7 shows more examples of mesh details before (a1-a3) and after (b1-b3) the smoothing. The mesh quality in panels b1-b3 were improved compared with those in panels a1-a3.

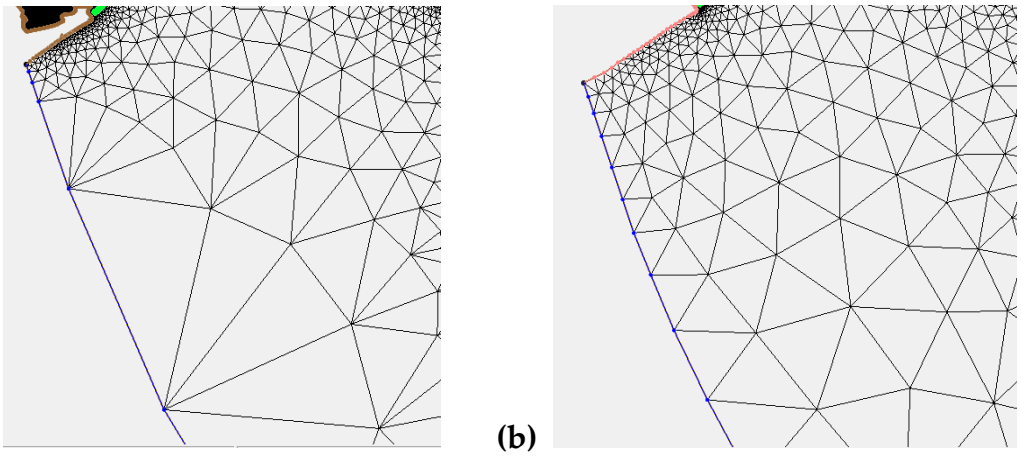

Figure 6 Mesh transition from open boundary (blue) to western mainland boundary, (a) before and (b) after manual smoothing.

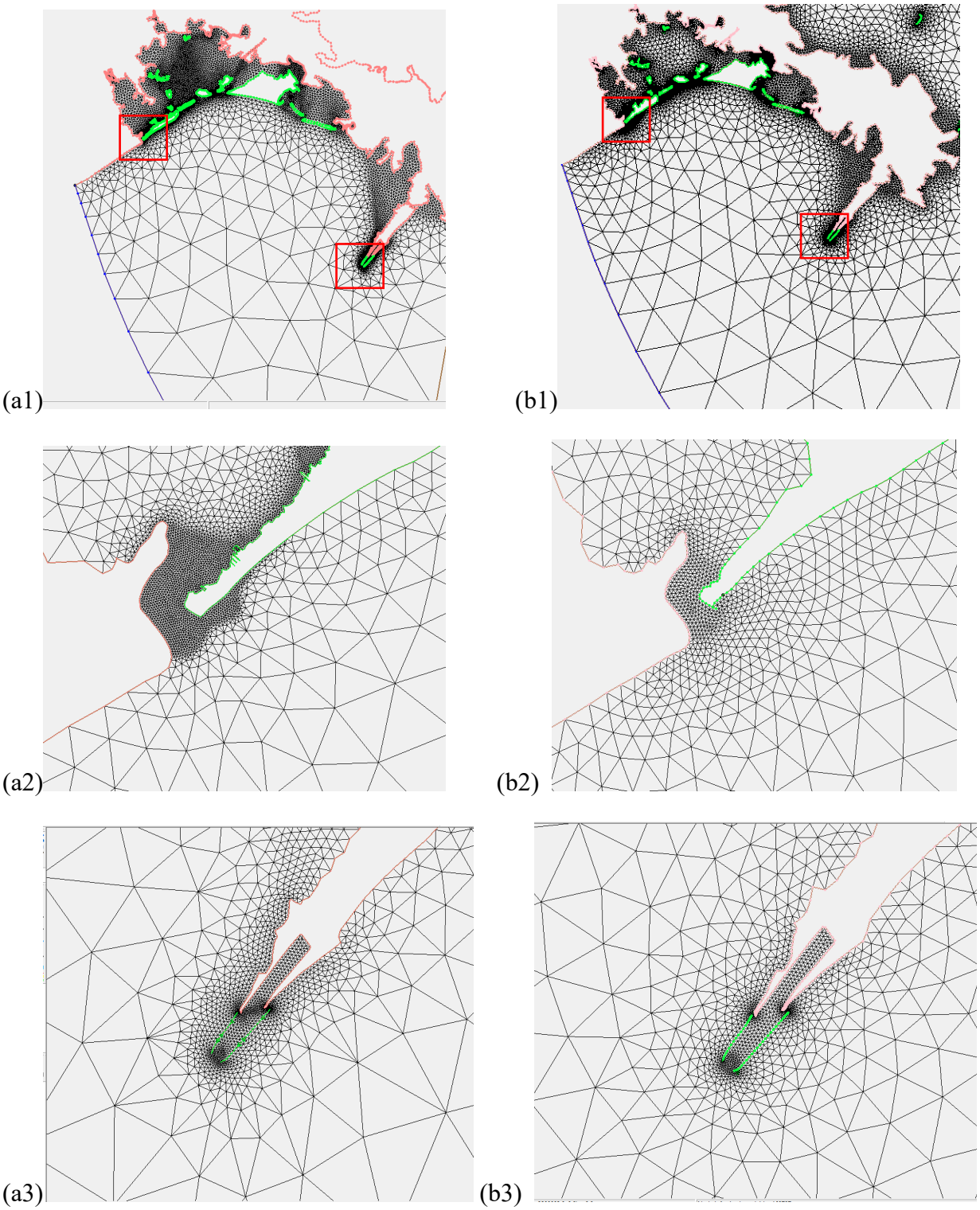

Figure 7 Mesh details (a1-a3) before and (b1-b3) after smoothing size functions. (a2) and (a3) are the close-up view of the area within the two red boxes in (a1).

3.4.2 Depth compilation process

To compile multiple data sources into a single grid, subsets of the source data were created. Panels a1 and b1 in Figure 8 show two examples of NOS survey data subsets with simple and complex boundaries, respectively. A boundary polygon was then found for each subset by using Matlab function boundary.m. Boundary polygon for dataset (b1) needs additional adjustment since the Matlab function was unable to find the correct boundary for locations with sharp curvature (Figure 8 b1).

The mesh nodes within the boundary polygon were then assigned a water depth value using the nearest data point from the dataset (Figure 8 panels a2 and b2). The nearest point selection can avoid using points inside the bay for selecting depth for nodes outside the bay where the boundary polygon is of a complex shape (Figure 8 b2).

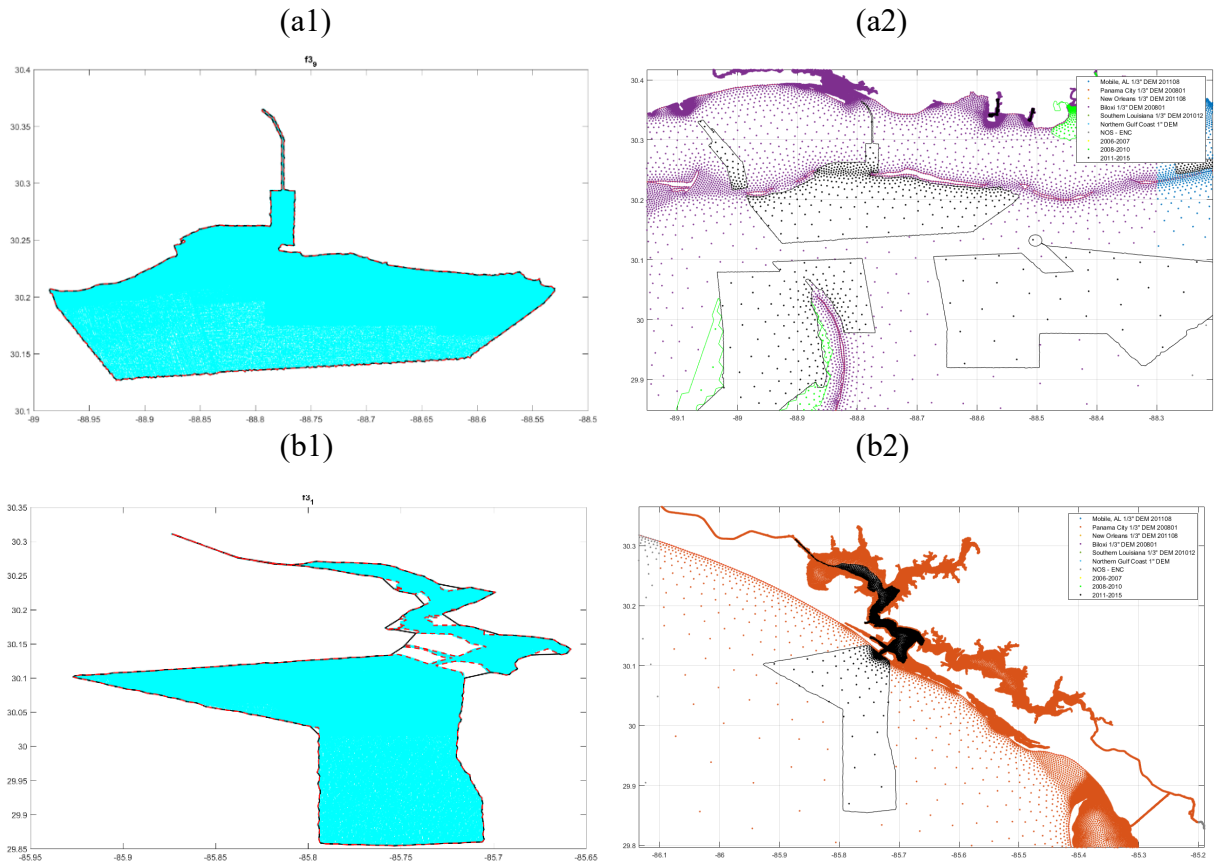

Figure 8 Examples of NOS bathymetry survey data sets with (a1) simple and (b1) complex boundary polygons. Black solid line and red dashed line represent the computed and revised polygons, respectively. (a2 and b2) Mesh nodes within the polygons were assigned depth values using the dataset in (a1) and (b1), respectively.

Data priority was based on survey date. In general, the more recent data superseded the previous data when they overlapped. Figure 9a illustrates the final model grid overlapped on Google Earth whereas Figure 9b displays the data sources for the mesh nodes. The resolution ranges from 46 km

at the open ocean boundary down to 9 m in sections of narrow rivers. The grid has 216,155 nodes and 374,318 elements. Figure 10 shows high resolution applied to six inlets to the bays in VDatum region. Figure 11 panels a-j shows the mesh details.

(a)

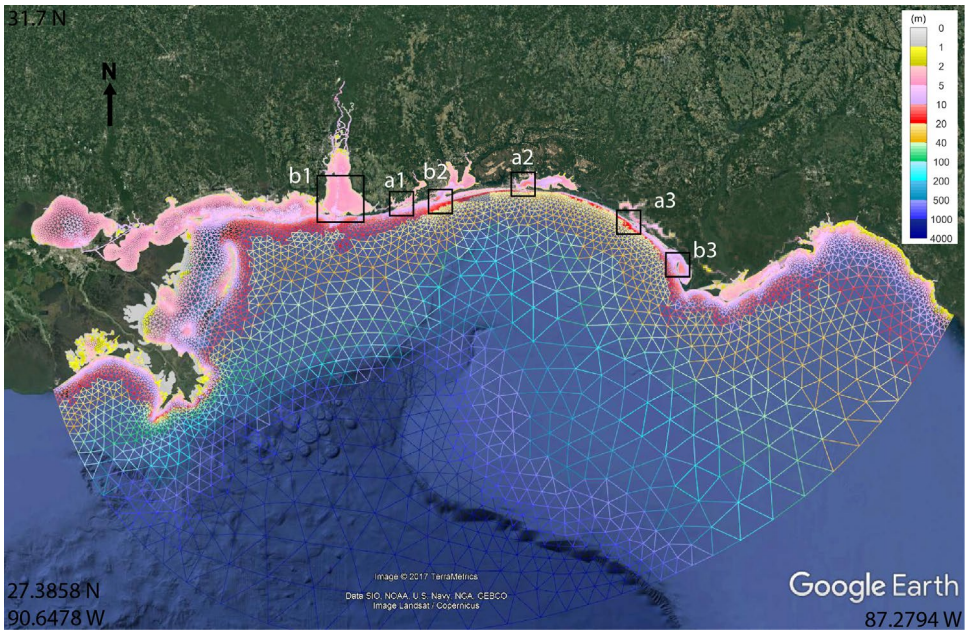

(b)

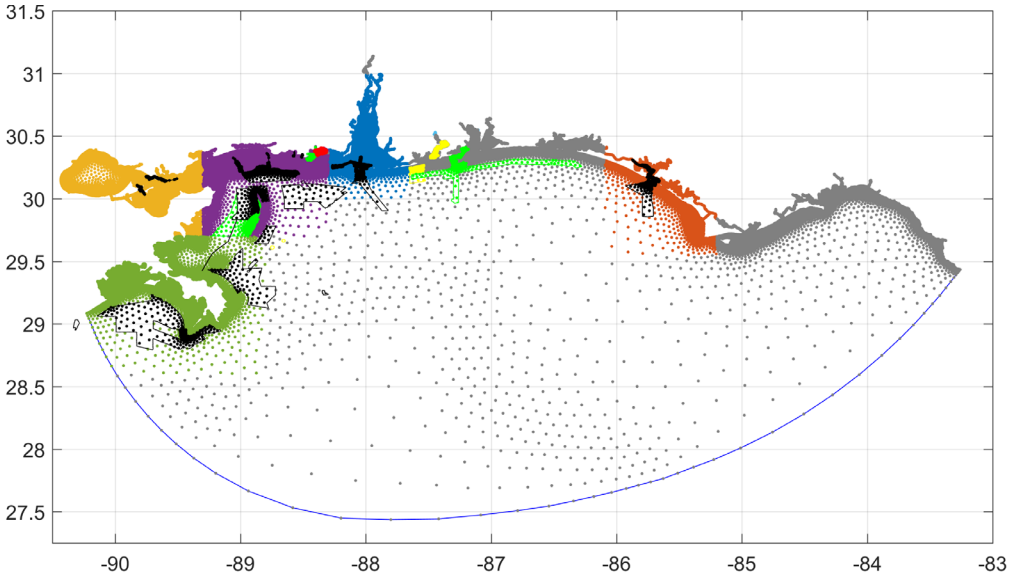

Figure 9 (a) newly developed model mesh for the study area. (b) Bathymetry data sources at the mesh nodes. See Fig. 5 for the data source names.

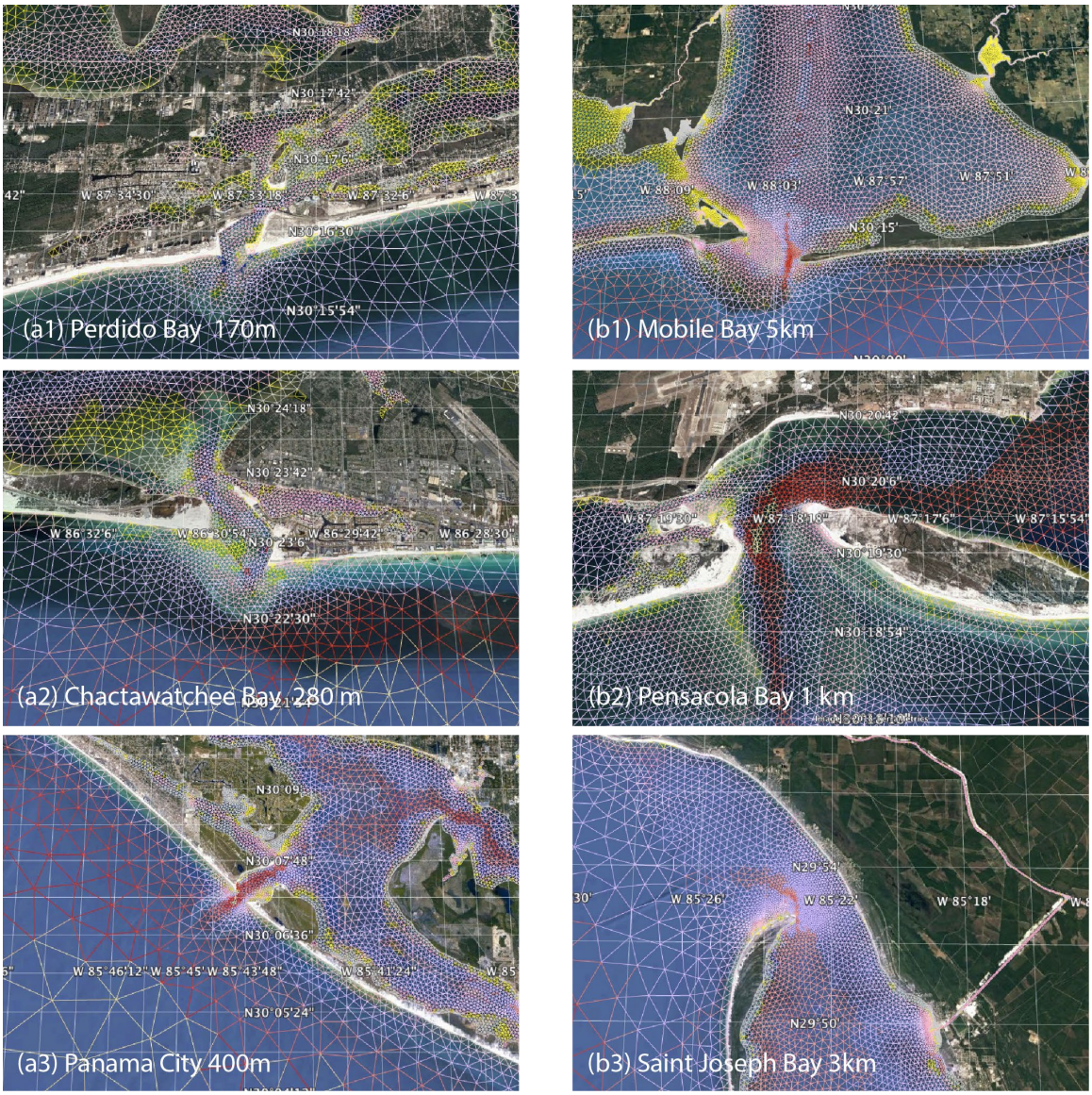

Figure 10 High resolution was applied to six inlets to Bays in VDatum region. (a) Three narrow inlets with breakwaters. (b) Three nature inlets. See Figure 9a for locations. Background images are from Google Earth.

(a)

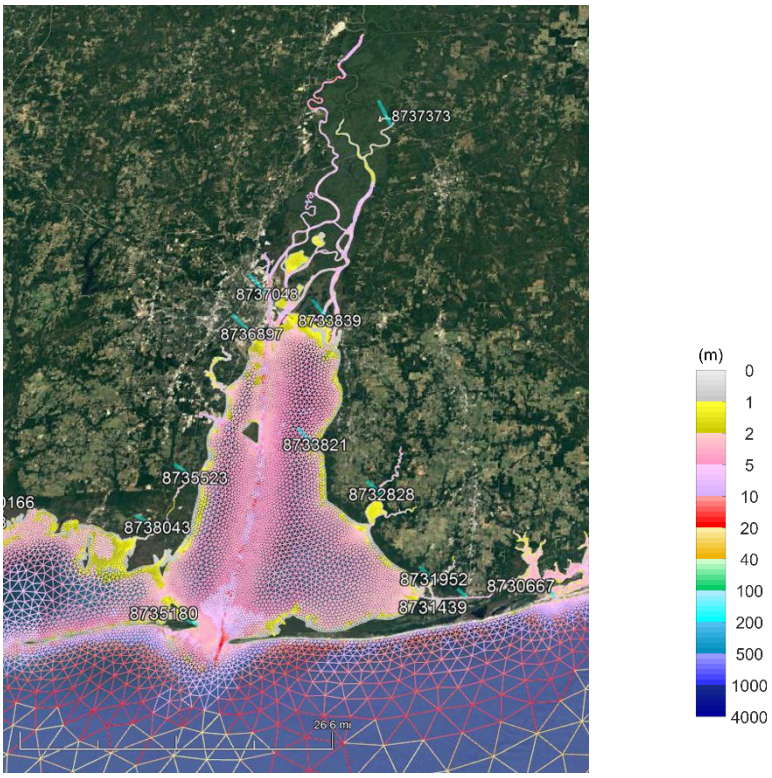
8737373
8737048
8733839
8736897
8733821
8735523
8732828
8738043
8731952
8730667
8731439
8735180
26.6 mi
(m)
0
1
2
5
10
20
40
100
200
500
1000
4000

(b)

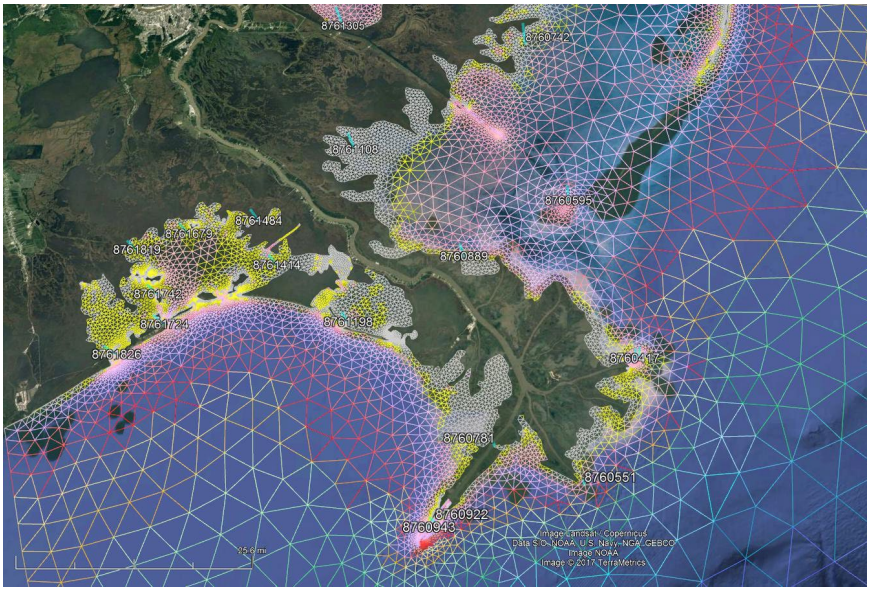
8761305
8760742
8761108
8760595
8764484
8761619
8760889
8761414
8761724
8761198
8760478
8760781
8760551
8760922
8760948
25.6 mi

(c)

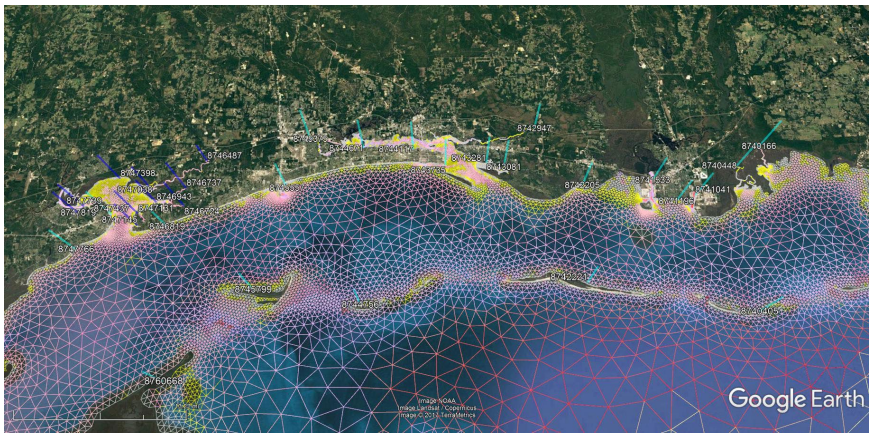
8742947
8746487
8747398
8746737
8746943
8740166
8740448
8741041
8760668
Google Earth

(d)

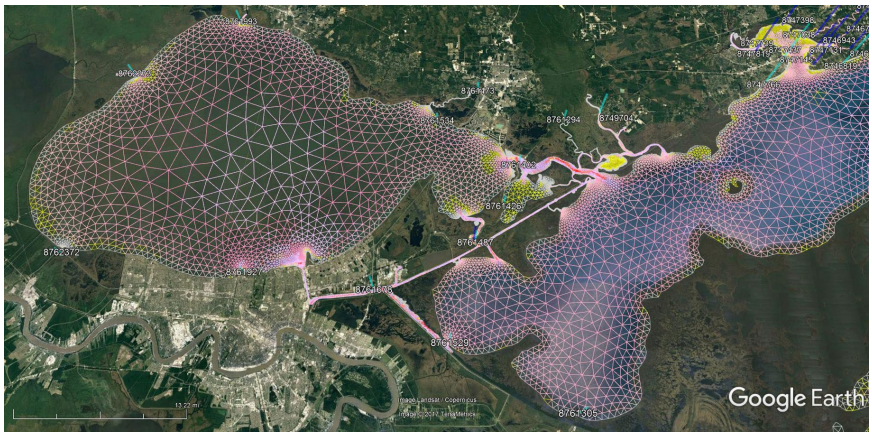
8762372
8764227
8764314
8764486
8764587
8761305
Google Earth

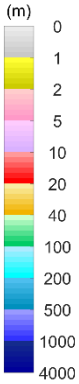
(m)
0
1
2
5
10
20
40
100
200
500
1000
4000

(e)

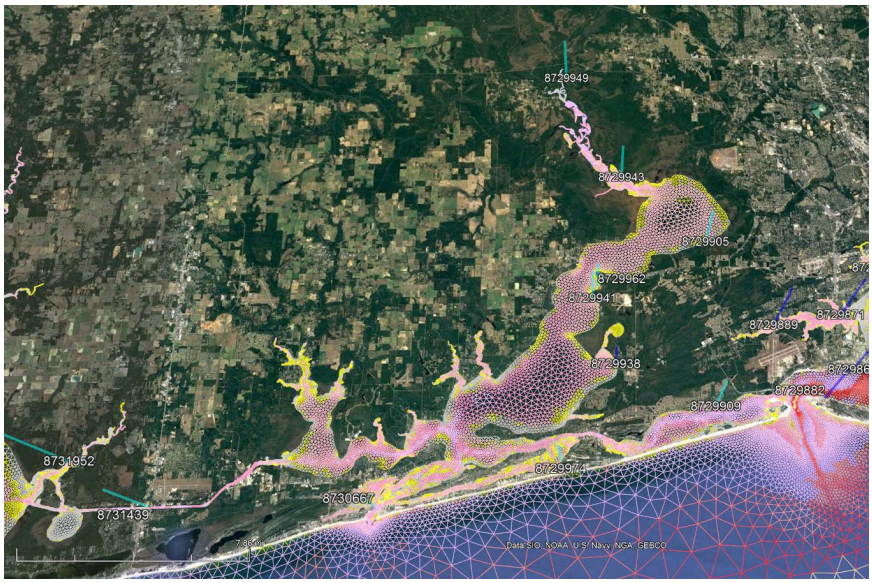
8729949
8729943
8729905
8729962
8729941
8729889
8729938
8729882
8729909
8731952
8729977
8731439
8730667
Data SIO, NOAA, U.S. Navy, NGA, GEBCO

(f)

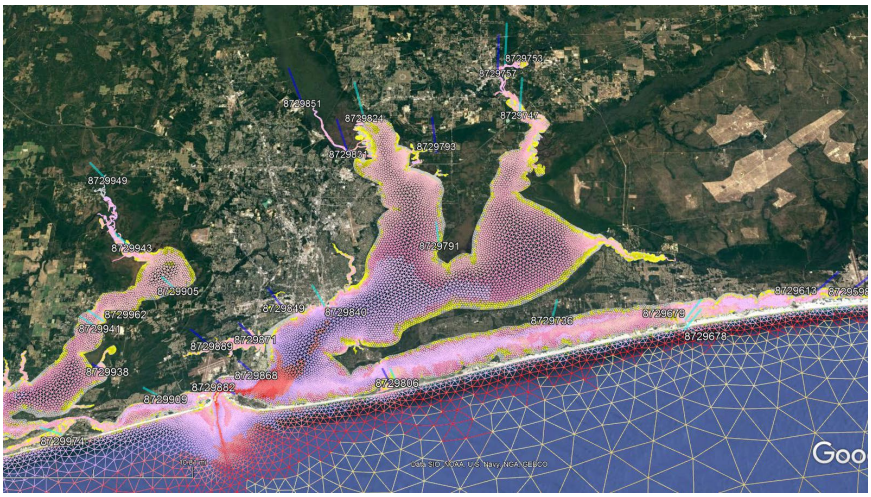
8729851
8729824
8729793
8729949
8729943
8729791
8729905
8729962
8729941
8729889
8729938
8729882
8729678
8729906
8729974

(g)

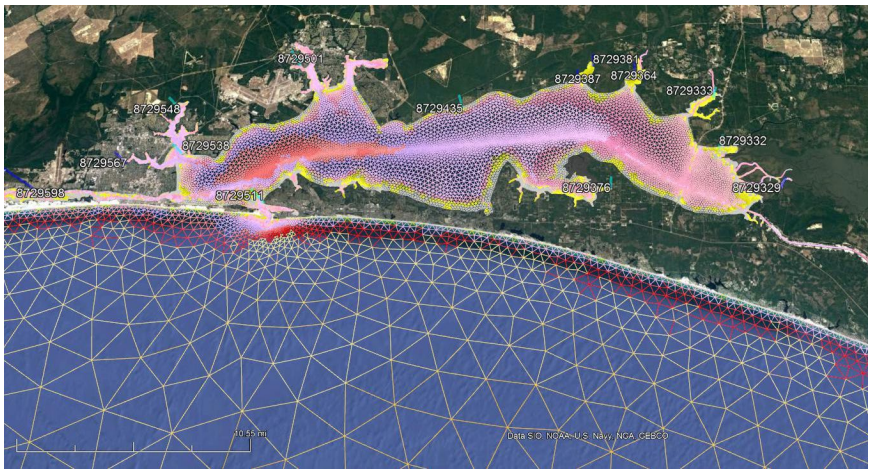
8729561
8729381
8729387
8729364
8729333
8729548
8729435
8729538
8729332
8729567
8729598
8729511
8729376
8729329
10.55 mi
Data SIO, NOAA, U.S. Navy, NCA, CEBCO

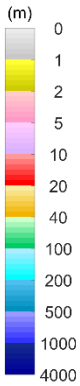
(m)
0
1
2
5
10
20
40
100
200
500
1000
4000

(h)

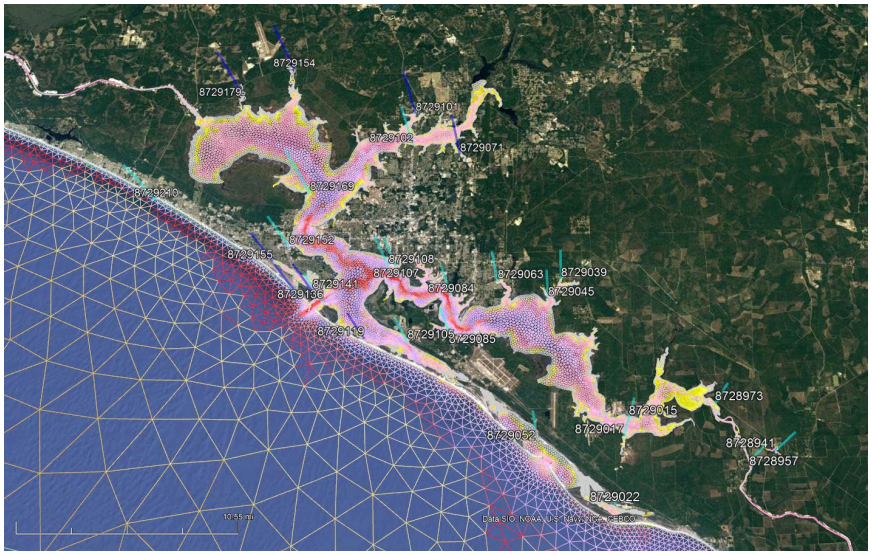
8729154
8729179
8729101
8729102
8729071
8729109
8729210
8729132
8729155
8729108
8729107
8729063
8729039
8729141
8729084
8729045
8729136
8729119
8729105
8729085
8728973
8729015
8729017
8729052
8728941
8728957
8729022
10.55 mi
Data SIO, NOAA, U.S. Navy, NCA, CEBCO

(i)

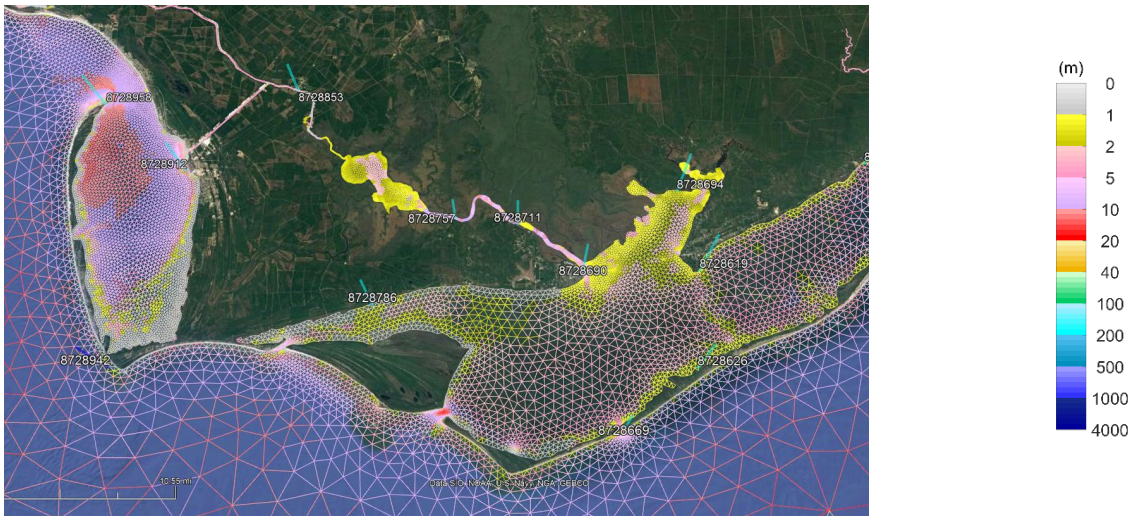

(j)

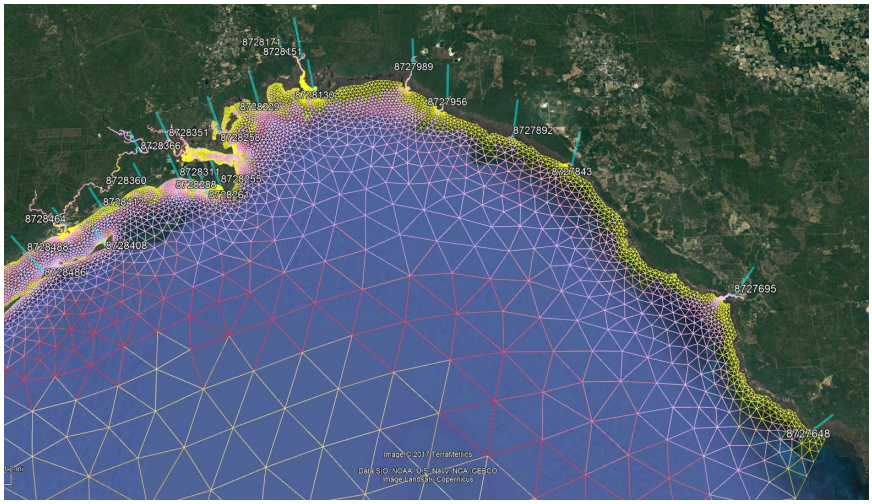

Figure 11 (a-j) Zoomed view of the mesh and tide stations.

Table 4 summarize the mesh properties. The new (2017) mesh increases 88% and 73% in coverages on shoreline length and computational domain, respectively. However, the total node number increases by only 12%. This was partially due to the decrease in the number of deep water nodes. Figure 12 compares the mesh and histograms for the 2008 and 2017 models. The 2008 mesh has a relatively uniform distribution in shallow water (Figure 12 a1). The 2017 mesh increases nodes with decreasing water depth (Figure 12 b1). In this way it can better represent the shallow bathymetry features. Note the nodes in deep water account only for 0.8% of the total nodes (Table 4). That is to say, we put 99.2% of the nodes in shallow water to better resolve the wave dynamics in nearshore areas.

Table 4 Properties of the 2008 and 2017 meshes.

Mesh properties	2008 mesh	New mesh	Increase in %
Shoreline length (km)	3979	7482	88%
Area (km^2)	79,474	137,751	73%
Element number	367,019	374,318	2%
Node number	192,889	216,155	12%
Node number w/depth >20 m (percentage to total nodes)	40,545 (21%)	1777 (0.8%)	−96%
Node number w/depth 10–20 m	28,312	9721	−66%
Node number w/depth <10 m (percentage to total nodes)	124,091 (64%)	205,095 (95%)	65%

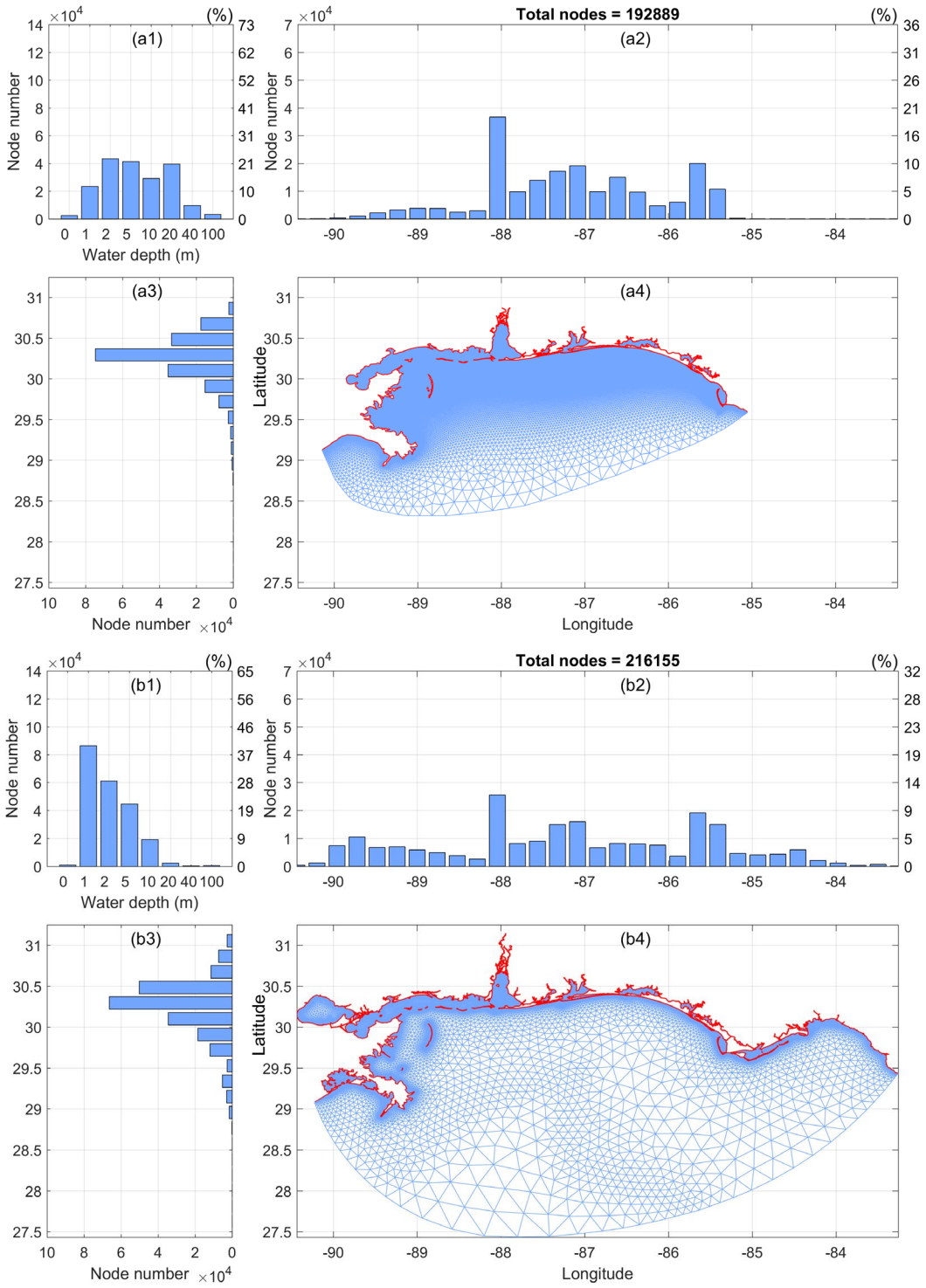

Figure 12 Comparison of the (a) 2008 and (b) 2017 model meshes. (1-3) Histograms of node number versus depth, longitude, and latitude, respectively.

3.5 Model Setup

The open boundary of the model grid, located in the Gulf of Mexico, was forced with a synthetic tide that was generated using the amplitude and phase of six tidal constituents (K1, O1, Q1, M2, S2, and N2), which were extracted from the East Coast 2015 (or EC2015) tidal constituent database (Szpilka et al., 2016). Similar to Dhingra et al. (2008), the model runs began with a smooth, hyperbolic tangent, time ramp function, which was applied to the boundary forcing tide for the first 5 days. The node factors and equilibrium arguments were set to the values from the middle of 1992 (which is in the middle of the 1983-2001 NTDE). A no flow boundary was set for all land segments. The lateral eddy viscosity coefficient was set to 5 m^2/s, which was the lowest number tested that did not produce numerical instabilities. The user-specified bottom friction coefficient C_f value was set to a standard value of 0.003.

The model was run for 40 days with a 3-second time step. The small time step was due to the Courant number limitation imposed by the small element sizes. The water surface elevation was output at every node in the grid every 6 minutes for the last 33 days of the 40-day model run as fort.63.nc. The file size is 12.8 GB. We found that this huge file size became the bottleneck of the computation. Once the file size exceeds certain limit, the writing speed decreases significantly with increasing file size. A single run could not be completed within the eight hour wall time limit of the Jet system.

Two methods can be used to resolve this issue: one is to use ADCIRC hot start setup and the other is to split the output file, fort.63.nc, into two parts by two single runs. Here we chose the latter due to its high efficiency. It took only a total of 3 wall-clock hours to complete the 40-day run utilizing 256 processors. For test runs where only time series at tide stations are needed (e.g., output fort.61.nc of 11.7 MB instead of fort.63.nc), no file split is needed. Then it takes approximately 47 wall-clock minutes for a run. In this way, it not only saves computational resources but also improves the test efficiency.

4. MODEL RESULTS AND DISCUSSION

4.1 Validation and Error Analyses

Figures 13 and 14 compare the modeled datums to observations at tide stations within and outside the VDatum region, respectively. Appendix A lists the detailed model results and observations at each station. Table 5 summarizes the model error. The CO-OPS's value of the datum at a station is obs_i and the modeled datum is $model_i$. The model error (err_i), percentage error, average error (err_{avg}), and root mean square error (rmse) are calculated as follows:

$$err_i = model_i - obs_i$$

$$\text{percentage } err_i = (model_i - obs_i)/obs_i \times 100$$

$$err_{avg} = \frac{1}{N}\sum_{i=1}^{N}|err_i|$$

$$rmse = \sqrt{\frac{1}{N}\sum_{i=1}^{N} err_i{}^2}$$

where i is the i^{th} station, and N is the number of stations used. Within the VDatum region, there are 83 tide stations (N=83), while N=99 in the outside region. The total number of stations in the computational domain is 182.

For the 83 tide stations within the VDatum region, the average error over the four datums is 0.012m or 7.9% (Table 5). This is an improvement in accuracy compared with the 0.018 m (11.0%) average error for the 2008 tide model (Table 6 and Dhingra et al., 2008). As will be discussed in Section 4.4.1, the update in offshore input boundary conditions from EC2015 tidal database (Szpilka et al., 2016) contributes to this overall improvement. The greatest improvement is in MLLW: the average error is reduced from 0.022 m (12.33%) to 0.013m (7.2 %). Since MLLW is most sensitive to the shallow water depth among the datums, this indicates the new tide model has more accurate representation of shallow water depth in coastal area.

The above results also point to another important conclusion: the gridding technique, i.e., the size function approach based on wave length in deep ocean, enabled efficiency of ADCIRC model. For example, the 2017 mesh has only 1777 nodes at water depth greater than 20m, which represent 96% reduction of the 40,545 nodes in deep ocean for the 2008 mesh (Table 4).

Table 5 Summary of averaged error for model datums at tide stations for the new grid.

Tide Stations	Error	MHHW (m)	MHW (m)	MLW (m)	MLLW (m)	Four datums (m)
83 stations in VDatum region	avg. error	0.010	0.014	0.013	0.013	0.012
	%	6.0%	9.3%	8.9%	7.2%	7.9%
	RMSE	0.013	0.017	0.017	0.016	0.016
99 stations outside	avg. error	0.028	0.020	0.020	0.032	0.025
	%	14.0%	12.6%	12.8%	14.2%	13.4%
	RMSE	0.035	0.029	0.025	0.038	0.032
All 182 tide stations	avg. error	0.020	0.017	0.017	0.023	0.019
	%	10.4%	11.1%	11.0%	11.0%	10.9%
	RMSE	0.028	0.024	0.022	0.030	0.026

Table 6 Model datum error at tide stations in VDatum region for the 2008 grid. Results were taken from Dhingra et al. (2008).

Tide Stations	Error	MHHW (m)	MHW (m)	MLW (m)	MLLW (m)	Four datums (m)
74 stations in VDatum region	avg. error	0.0186	0.0155	0.156	0.0219	0.0179
	%	10.44%	10.87%	10.9%	12.33%	10.97%

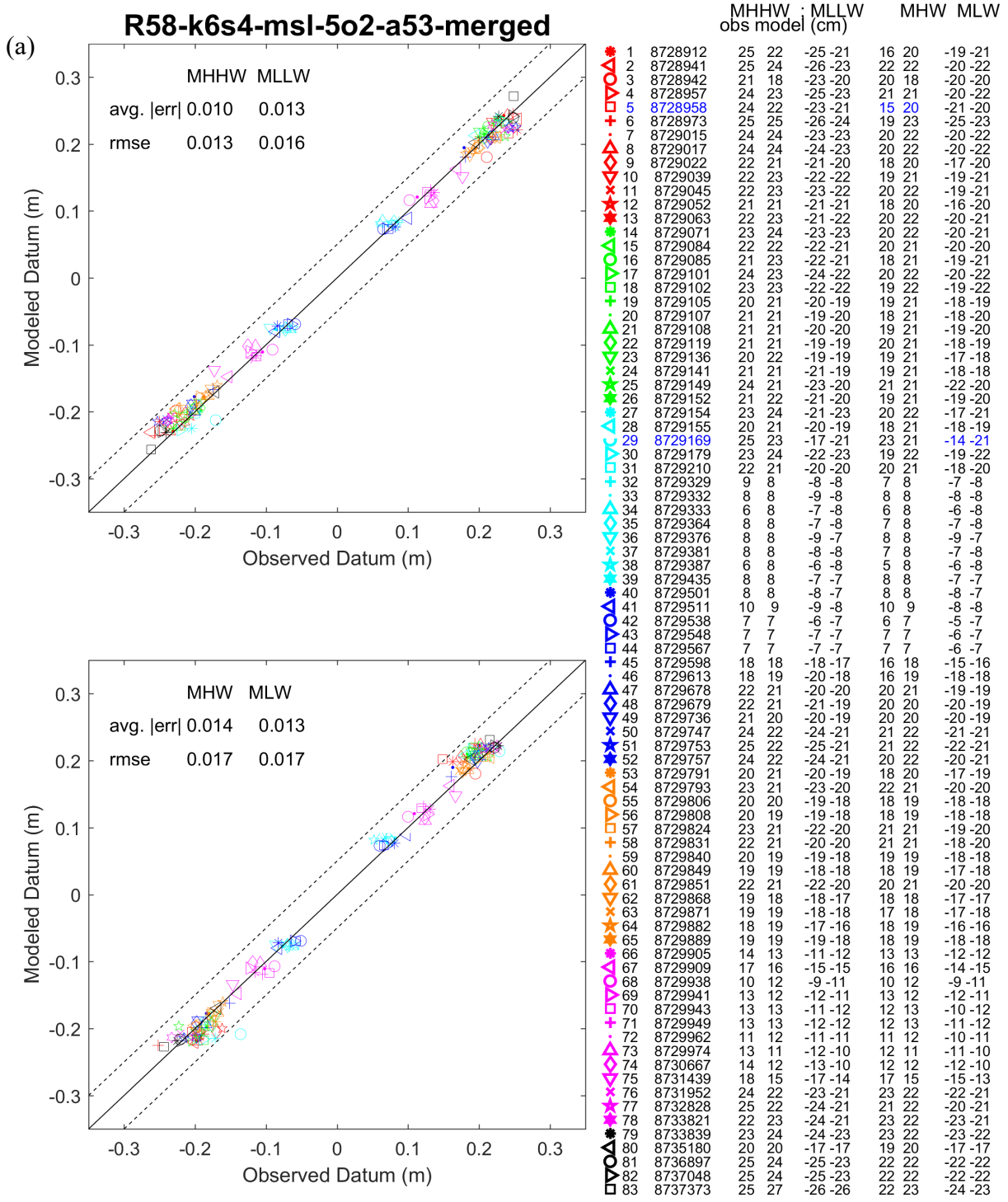

Figure 13 Comparison of the modeled tidal datum and observations for tide stations within the VDatum area. The dashed lines indicate the 5-cm error band. Text in blue indicates model error greater than 5 cm at the stations.

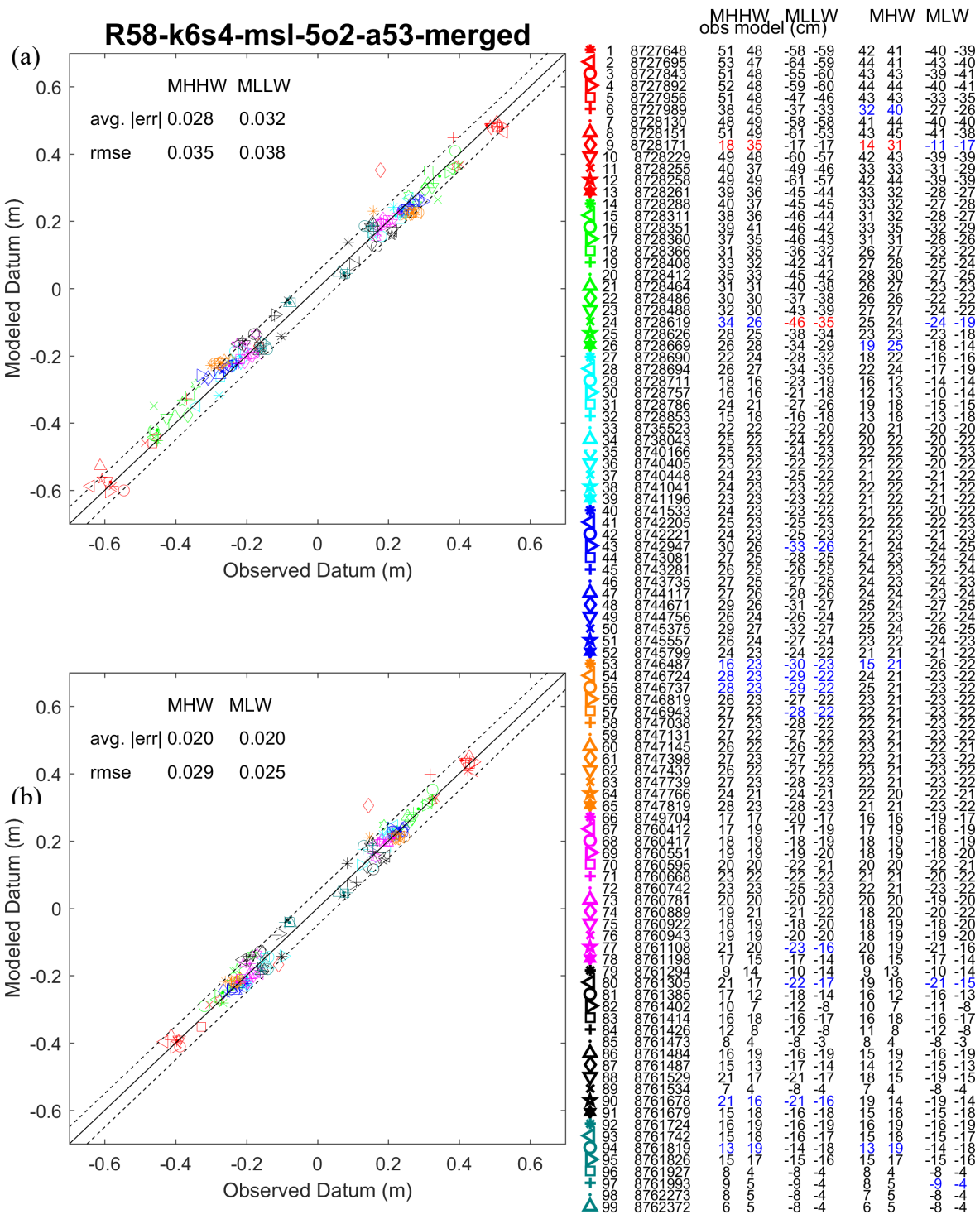

Figure 14 Comparison of the modeled tidal datum and observations for stations outside the VDatum area. The dashed lines indicate the 5-cm error band. Text in red and blue indicate model error greater than 10 and 5 cm, respectively.

The model error in the VDatum region are smaller than those outside the region. Figure 15 clearly illustrates this trend. Each bar represents 2 cm in width along the x axis. In the VDatum region, 95.5% modeled datums have error within ±3 cm, while only 65.9% for outside region. The outside region is mainly used to serve as land boundary condition for the model. Its coarser resolution may contribute to the larger model error.

The maximum error in the VDatum region are 0.033, 0.042, 0.054 and 0.073 m for MHHW, MLLW, MHW, and MLW, respectively. Two of them, MHW and MLW, exceeded the 5 cm error band as shown in Figure 13. To explore what factors may contribute to the maximum error, we plot error against the observed difference in datum magnitude, i.e. (1) MHHW- |MLLW| and (2) MHHW-MHW, in Figures 16.1 and 16.2, respectively. The result indicates:

(1) The maximum error for MLW and MHW are relatively independent. That is to say, largest error in MLW/MLLW do not correspond with largest error in MHW/MHHW, and vice versa. This indicates different maximum error mechanisms between MLW and MHW.

(2) The maximum error for MLW and MLLW are highly dependent. Both are from the same station, 8729169. This indicates similar maximum error mechanism between MLW and MLLW. This is also held for the large MHW and MHHW error at stations 8728958 and 8728912.

(3) The maximum error for MLW/MLLW occurs when the difference in the observed MHHW and |MLLW| is the largest. Figure 16.1b indicates that there is one such outlier station 8729169. While MHHW-|MLLW| for all other stations are less than 0.027 m, station 8729169 shows 0.076 m difference, more than double of the other stations. As will discussed in section 4.4, shallow water depth can decrease |MLLW| more effectively than MHHW, due to the greater friction effect on MLLW. The model and bathymetry data might not well reflect the shallow water depth around station 8729169.

(4) The maximum error for MHW/MHHW occurs when the difference in the observed MHHW and MHW is the largest. Figure 16 panels 2a and 2c indicate two such outlier stations: 8728958 and 8728912. Both are inside the Saint Joseph Bay. Station 8728958 is very close to the entrance of the Bay near the jetty area (Figure17a). Figure 17b shows there is discrepancy between NOS survey data in 1985 and 2017 shoreline. Some survey points with depth fall on to the land area. This indicates the bathymetry data for the jetty area might not reflect current shoreline and depth.

For large model error outside VDatum region, we will have a discussion in Section 4.4, since they are not the focus of this study.

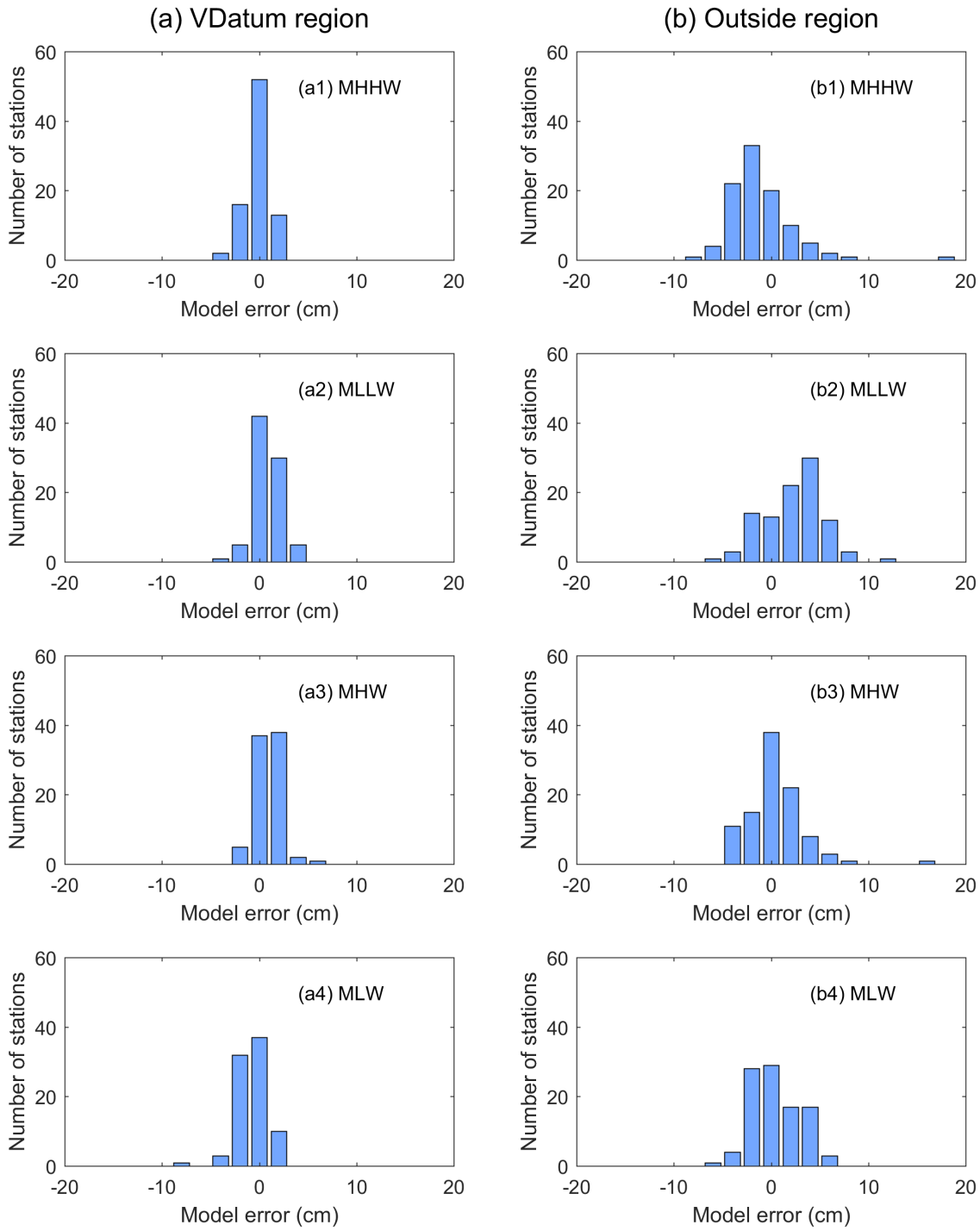

Figure 15 Modeled datum error for tide stations (a) in and (b) outside the VDatum region.

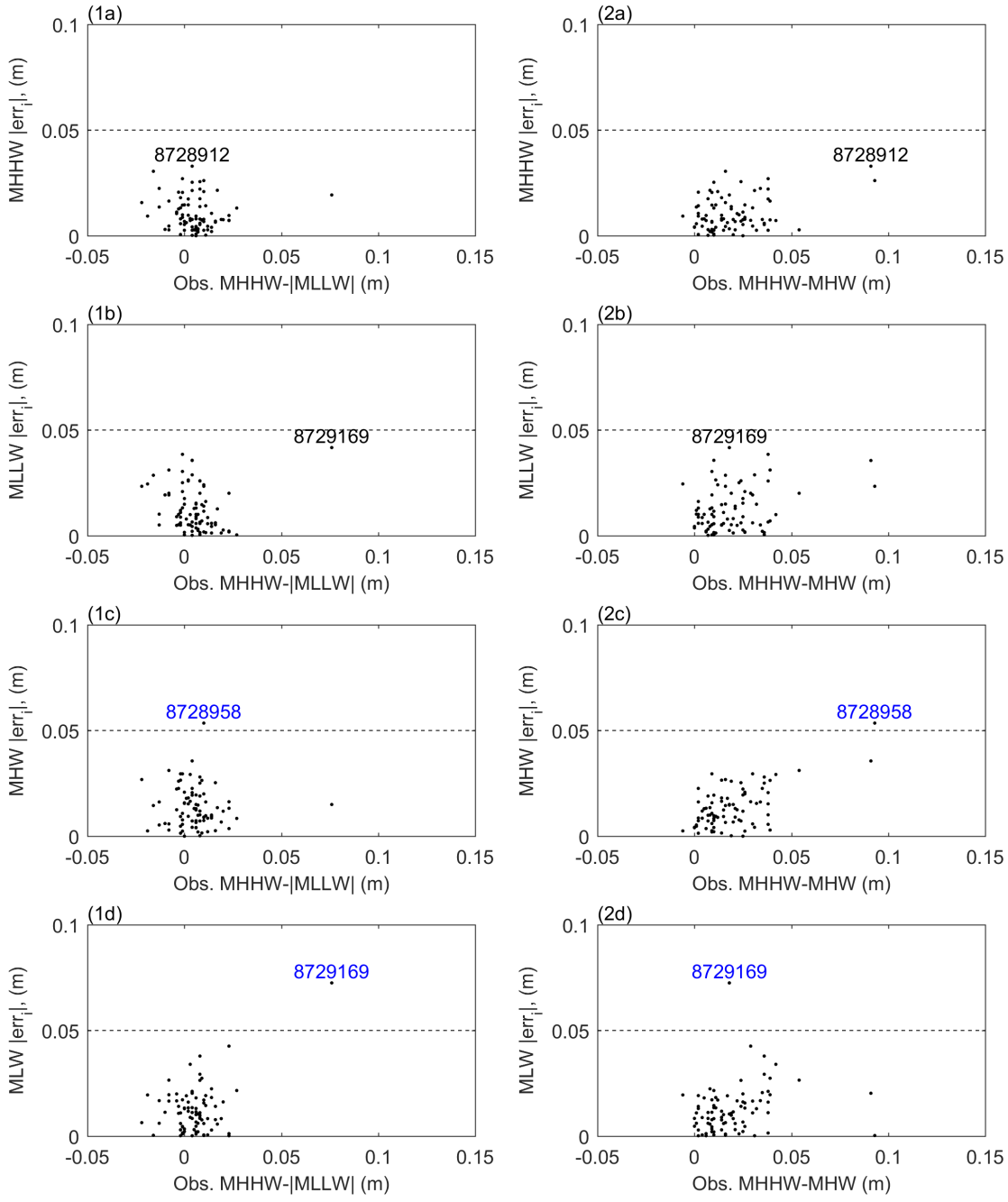

Figure 16 Model error for (a) MHHW, (b) MLLW, (c) MHW, and (d) MLW versus observed difference in magnitude of (1) MHHW and MLLW, and (2) MHHW and MHW for the 83 tide stations in VDatum region.

(a)

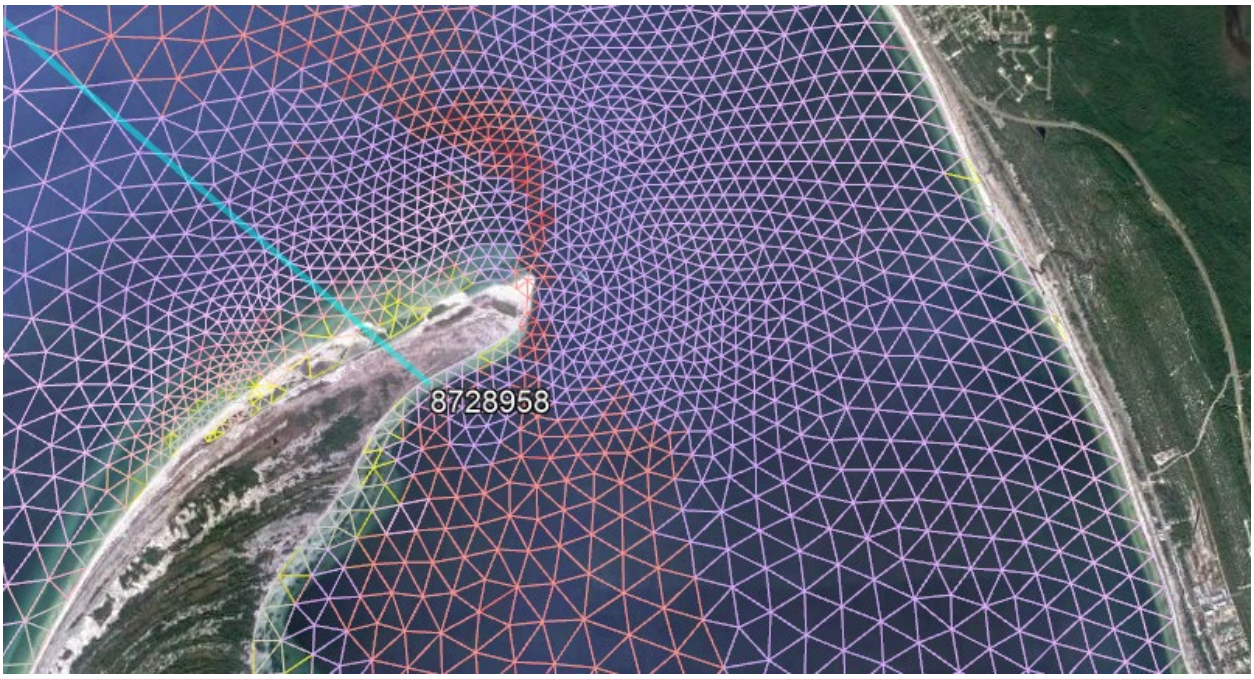

(b)

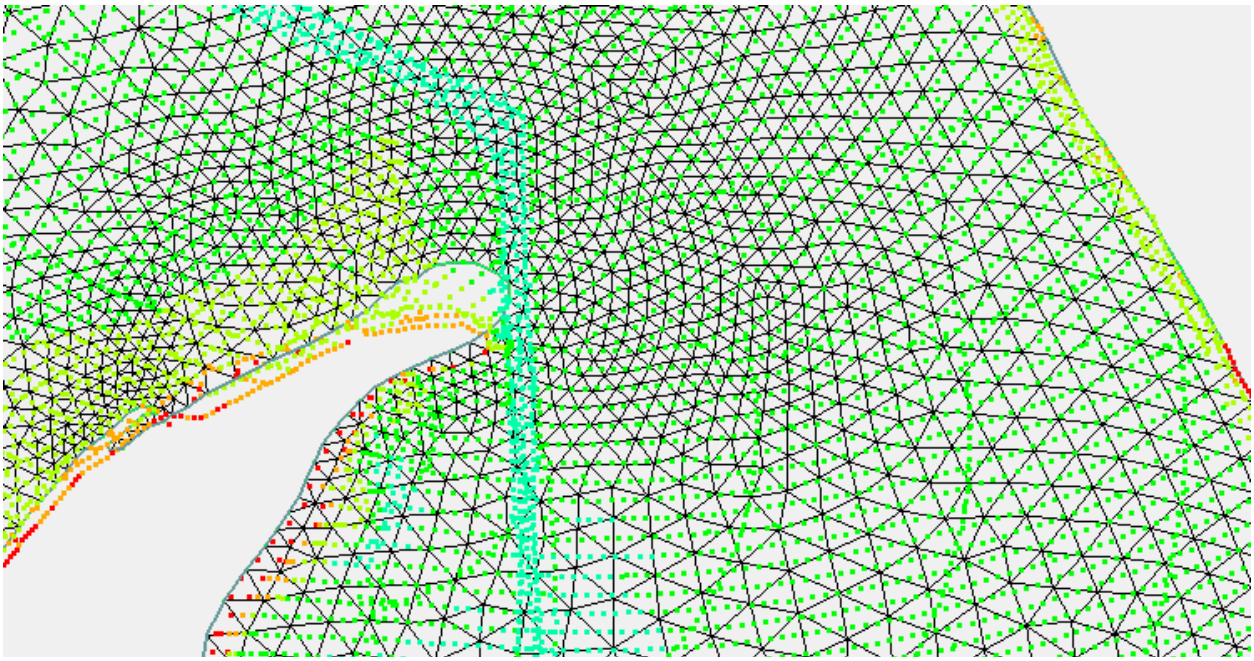

Figure 17 Entrance to the Saint Joseph Bay. (a) Location for station 8728958 (Image from Google Earth) and (b) Dots are NOS survey data.

4.2 Final Datum Fields and Spatially Varying Uncertainty

Columns a-d in Figure 18 show the (a) modeled datums, (b) datum product adjusted with observations, (c) the adjustment applied, and (d) associated spatially varying uncertainty for the entire model domain. Rows 1-6 are for the six datums, MHHW, MHW, MLW, MLLW, MTL, and DTL, respectively. Columns 1-3 use the same color map ranging from -0.4 to 0.4 m. The color map for Column 4 ranges from 0 to 0.05 m.

The adjusted datums (Figure 18b) are the sum of the original model output (column a), and the adjustment (column c). The interpolation adjusts the background model values (column a) over the whole domain. It corrects discrepancies between observations (e.g., Figure 1) and model results for the datums (e.g., column a) at the observation locations by statistically blending the observations and model results. In this way, the final set of tidal datum fields match (within a 1-cm limit) the observations at stations (the 182 tide stations in this case). Column c in Figure 18 indicates that the adjustments are in general very small for majority of the domain.

The statistical interpolation also produces spatially-varying uncertainty estimates (Figure 18d). The background model uncertainty had been improved at and around tide stations, and to a lesser extent in the offshore area. The maximum uncertainty is 3 cm in the middle of the offshore boundary for MHHW (Figure 18 column d row 1). This is the farthest location from any tide stations. The uncertainty of MTL and DTL are smaller due to the small magnitude for these two datums.

Figure 19 shows the adjusted datum products and spatially varying uncertainty in the VDatum region. The color scales were redesigned to show the local details. More details can be found in Figure 21 and Appendix B. These results indicate:

(1) Along the coasts, large uncertainty can be seen in the southern portion of Saint Joseph Bay, Florida, for both MHHW and MLLW (Figure 19 panels 1b and 4b). The maximum uncertainty is 1.6 cm for MHHW. This is also the location that has the maximum MHHW and |MLLW|. Note that the MHHW-MHW and |MLLW-MLW| are also the greatest among the stations in the VDatum region.

(2) For other bays, relative large uncertainty are found locally in the Choctawahatchee Bay, Florida. The maximum uncertainty ranges from 1.8 to 2.0 cm.

(3) Some large uncertainties are due to lack of measurement. Such examples include the upper stream of the Mobile River, Ala. (1.9 cm maximum uncertainty, Fig. 21 2b), the Deer Point Lake, Fla., to the northern most of the Saint Andrew Bay (1.8 cm maximum uncertainty for MLLW, Figure 21 1b).

(4) Large uncertainty can also be caused by the relatively large model error. One example is the 1.9 cm maximum uncertainty and 4 cm model error for MLW at station 8728973 at Wetappo Creek, East Bay, Florida (Figure 21 panel 1b3).

(a)Model output (b) Product (c) Correction (d) SVU

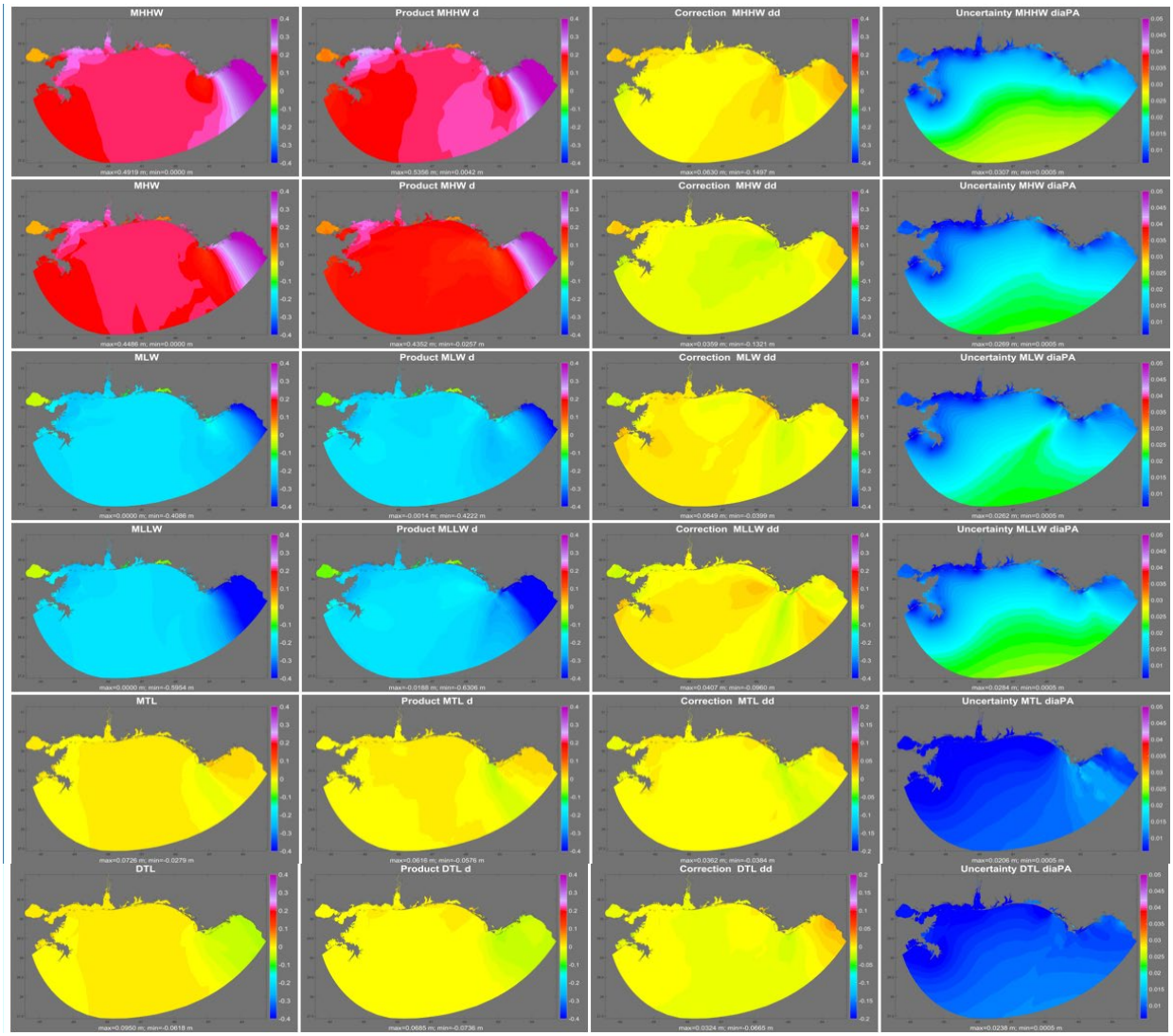

Figure 18 (a) Modeled datums, (b) datum corrected with observations, (c) the correction applied, and (d) associated spatially varying uncertainty for the domain. Rows 1-6 are the six datums, MHHW, MHW, MLW, MLLW , MTL, and DTL, respectively.

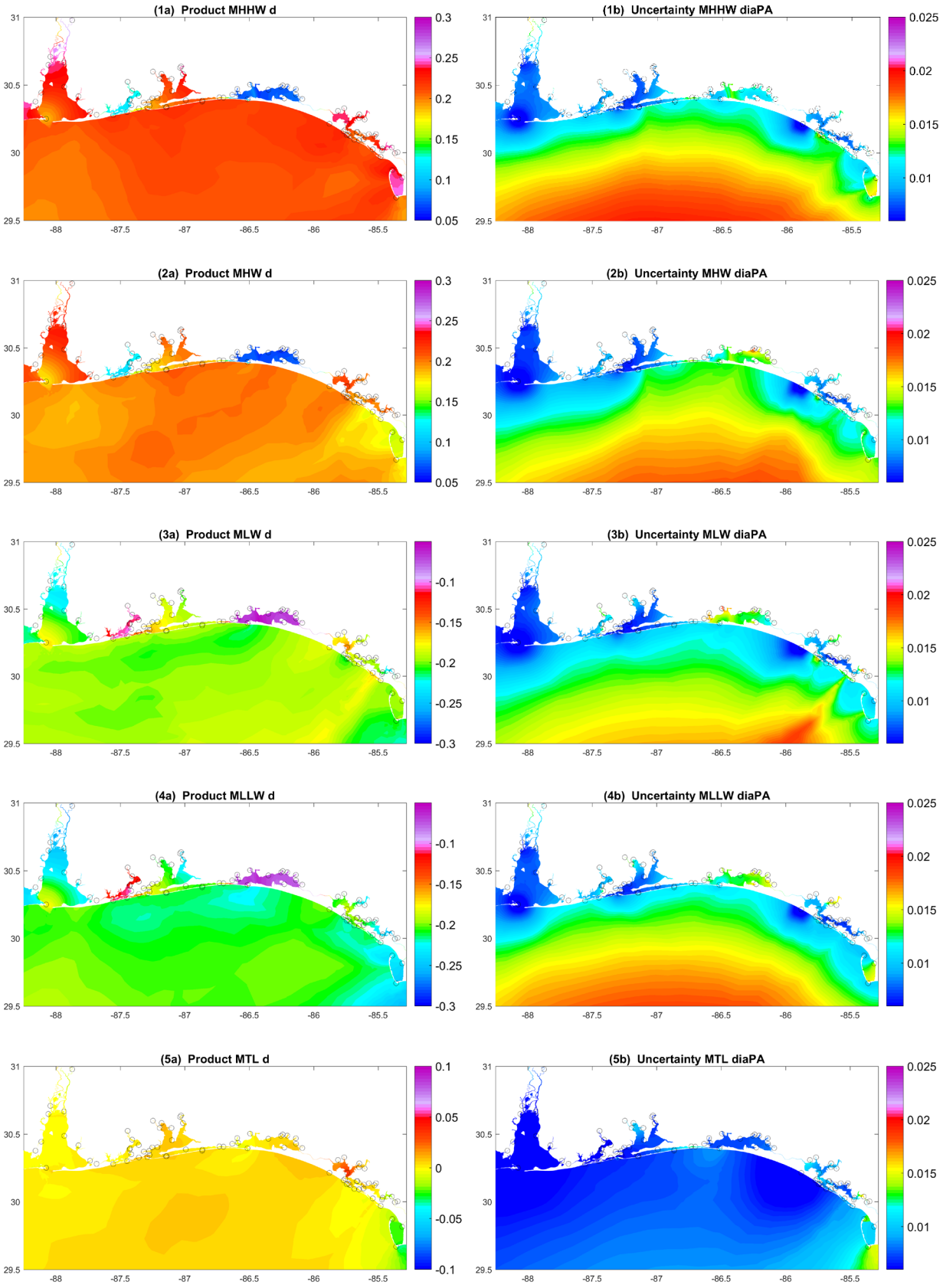
(1a) Product MHHW d
(1b) Uncertainty MHHW diaPA
(2a) Product MHW d
(2b) Uncertainty MHW diaPA
(3a) Product MLW d
(3b) Uncertainty MLW diaPA
(4a) Product MLLW d
(4b) Uncertainty MLLW diaPA
(5a) Product MTL d
(5b) Uncertainty MTL diaPA
31
30.5
30
29.5
-88
-87.5
-87
-86.5
-86
-85.5
0.3
0.25
0.2
0.15
0.1
0.05
-0.1
-0.15
-0.2
-0.25
-0.3
0.025
0.02
0.015
0.01
0
-0.05

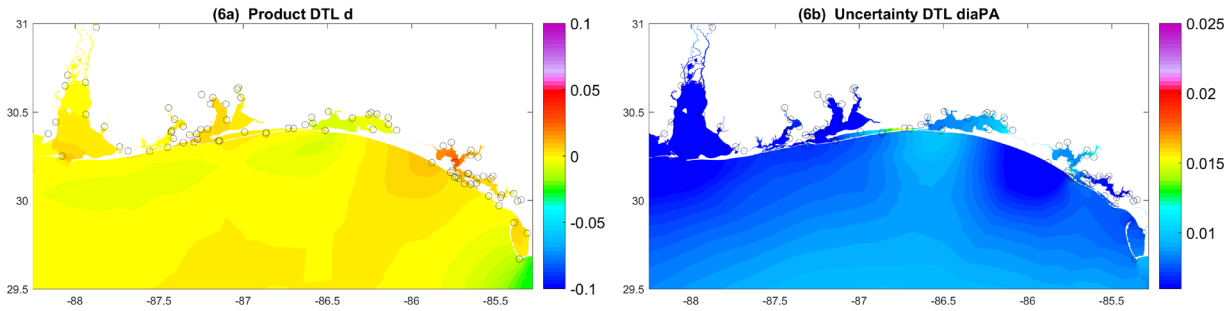

Figure 19 (a) Datum products and (b) spatially varying uncertainty in the VDatum region. Rows 1-6 are for the six datum, MHHW, MHW, MLW, MLLW , MTL, and DTL, respectively. The color is in meter. The color scales are adjust to better show the details in VDatum region (e.g. not the same color scale as in Figure 18).

4.3 Populating the VDatum Marine Grids and Quality Check

Figure 20a shows the five previous bounding polygons in VDatum region (Hess, 2012). In this study, they were reconfigured as shown in Figure 20b, to cover all the tide stations in the region as well as the newly-added intra-costal waterways. In addition the bounding polygon for northwest Florida was also modified. For convenience, we have used the designations and abbreviations for the VDatum regions as in Table 7. The new polygons share the common interfaces with the adjacent polygons whenever possible, e.g., no overlaps between the polygons.

Using the new polygons, new marine grids were generated for the five areas. Table 8 shows the information for the five marine grids. Then the datums and spatially varying uncertainty were populated into the new marine grids and saved as GTX files. Figure 21 shows an overview of the 60 GTX files. Plot for each GTX file can be found in Appendix B.

A comparison of the VDatum values in the GTX files to the observations at the tide stations is shown in the Table 9. The standard deviations range from 0.07 to 0.83 cm. The maximum error is about 1 cm.

Continuity of values across interfaces was then checked. There are 11 interfaces: (1) New Orleans-NEGOM, (2) New Orleans-Mobile Bay, (3) Mobile Bay-NEGOM, (4) Mobile Bay-Pensacola Bay, (5) Pensacola Bay-NEGOM, (6) Pensacola Bay-St Andrews Bay, (7) St Andrews Bay-NEGOM, (8) St Joseph Bay-NEGOM, (9) Cedar Key-NEGOM, (10) St Joseph Bay-Cedar Key , and (11) St Andrews Bay-St Joseph Bay. The interfaces are shown in Figure 20b. The final results for the continuity tests are shown in Table 10.

In the NEGOM-Cedar Key VDatum boundary, where these was a maximum of 2.8-cm difference in MLW across the interface. The difference is due to the differing values produced by the ADCIRC models for the NE Gulf of Mexico and for the Florida shelf. Similar difference was also noted from previous version of the tidal model (Hess, 2012).

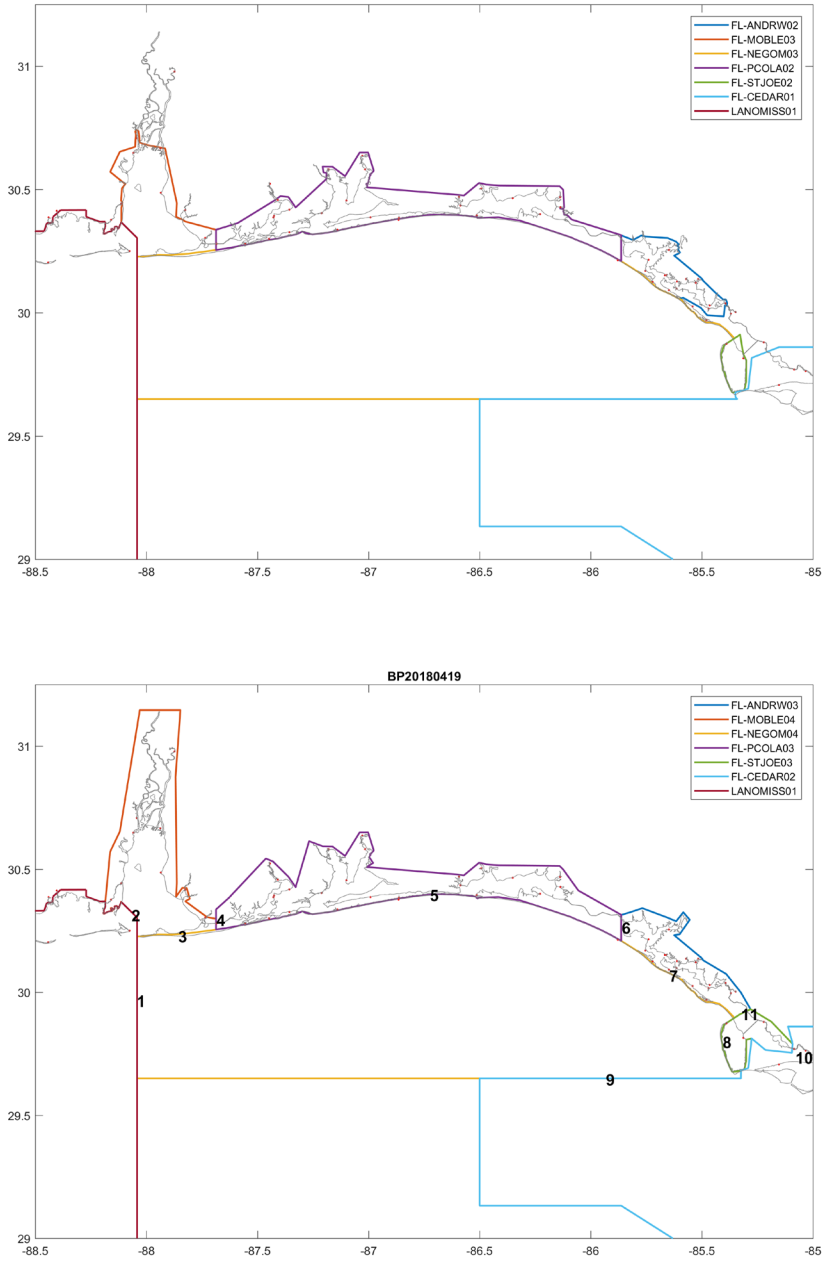

Figure 20 (a) 2012 and (b) revised bounding polygons.

Table 7 VDatum region names, directories in the CSDL VDatum archive, and abbreviations.

REGION	ORIGINAL DIRECTORY	REVISED DIRECTORY in 2012	REVISED DIRECTORY in 2018	Abbreviation
St Joseph Bay, FL	FL_stjoe01	FL_stjoe02	FL_stjoe03	STJOE
St Andrews Bay, FL	FL_andrw01	FL_andrw02	FL_andrw03	ANDRW
Pensacola Bay, FL	FL_pcola01	FL_pcola02	FL_pcola03	PCOLA
Mobile Bay, AL	FL_moble02	FL_moble03	FL_moble04	MOBLE
NE Gulf of Mexico	FL_negom02	FL_negom03	FL_negom04	NEGOM
Louisiana, New Orleans, and Mississippi	LAnomiss01	(unchanged)	(unchanged)	LAMIS
Cedar Key, FL	FL_cedar01	(unchanged)	FL_cedar02	CEDAR

Table 8 VDatum grid information for the five marine grids.

VDatum **REGION**	Southwestern **Limit**	Northeastern **Limit**	Vertical Spacing **Deg**	Horizontal Spacing **Deg (m)**	No.of Vert. **Nodes**	**No. of Hori. Nodes**	**Size of one GTX file (MB)**
FL_andrw03	29.895497 274.135812	30.343097 274.720212	0.0006	0.0006	746	974	6
FL_moble04	30.226638 271.805180	31.148238 272.31518	0.0006	0.0006	1536	850	11
FL_negom04	29.649000 271.956800	30.401 274.6778	0.001	0.001	752	2721	17
FL_pcola03	30.208376 272.312585	30.651776 274.137785	0.0006	0.0006	739	3042	19
FL_stjoe03	29.676251 274.585691	29.933051 274.910291	0.0006	0.0006	428	541	2

Table 9 Comparison of data and GTX interpolated values (Standard deviations, cm) for the five regions for tidal datums.

REGION	No. of Tide Stations	MHHW	MHW	DTL	MTL	MLW	MLLW
FL_andrw03	26	0.61	0.67	0.46	0.69	0.67	0.66
FL_moble04	7	0.6	0.43	0.31	0.39	0.83	0.61
FL_negom04	4	0.42	0.57	0.36	0.5	0.75	0.65
FL_pcola03	43	0.65	0.65	0.44	0.55	0.68	0.62
FL_stjoe03	3	0.76	0.39	0.07	0.83	0.59	0.66

Table 10 Maximum discontinuity (cm) across the 11 interfaces (see Figure 20b).

N	MHHW	MHW	DTL	MTL	MLW	MLLW
1	0.67	0.69	0.82	0.36	0.99	0.72
2	2.12	1.44	0.53	0.35	0.86	0.58
3	0.17	0.17	0.07	0.13	0.11	0.07
4	0.56	0.55	0.17	0.17	1.01	1.02
5	1.35	1.18	0.3	0.35	0.7	0.89
6	0.17	0.16	0.02	0.04	0.25	0.27
7	0.39	0.35	0.11	0.1	0.93	0.29
8	0.06	0.03	0.02	0.03	0.04	0.02
9	1.88	1.57	1.05	2.35	2.78	1.03
10	0.21	0.83	0.6	2.39	1.1	1.1
11	0.03	0.03	0	0.01	0.03	0.02

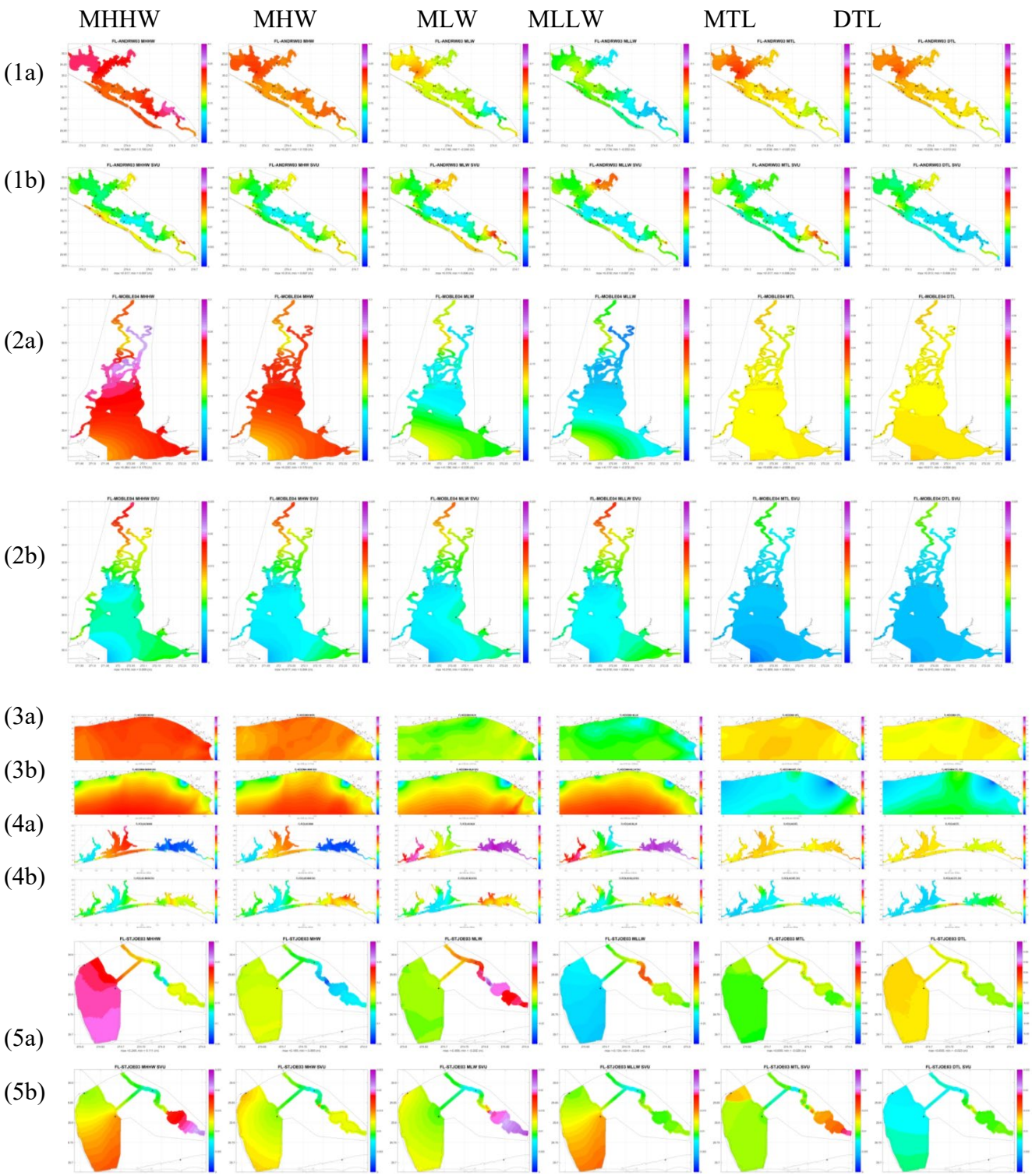

Figure 21 (1a-5a) Datum products and (1b-5b) spatially varying uncertainty for the five marine grids in VDatum region. The color scales are the same as Figure 19. See Appendix B for details.

4.4 Lessons Learned

In this section, we document the lessons learned during the development and testing processes.

4.4.1 Sensitivity of modeled datum to offshore boundary input

Figure 22 compares the modeled datums using the (a) EC2001 and (b) EC2015 tidal databases (Mukai et al., 2002; Szpilka et al., 2016). The two tests were conducted using the same 2008 mode grid. The EC2015 tidal database reduced error for both MHHW and MLLW, from 2.01 and 2.5 cm to 1.18 and 1.43 cm, respectively. These represent more than 40% reduction from the original error.

The EC2015 tidal database has incorporated the bathymetry data from the VDatum tide models developed for U.S. East Coast (Szpilka et al., 2016). Therefore, it likely has more accurate representation of the bathymetry data, particularly in shallow coastal region.

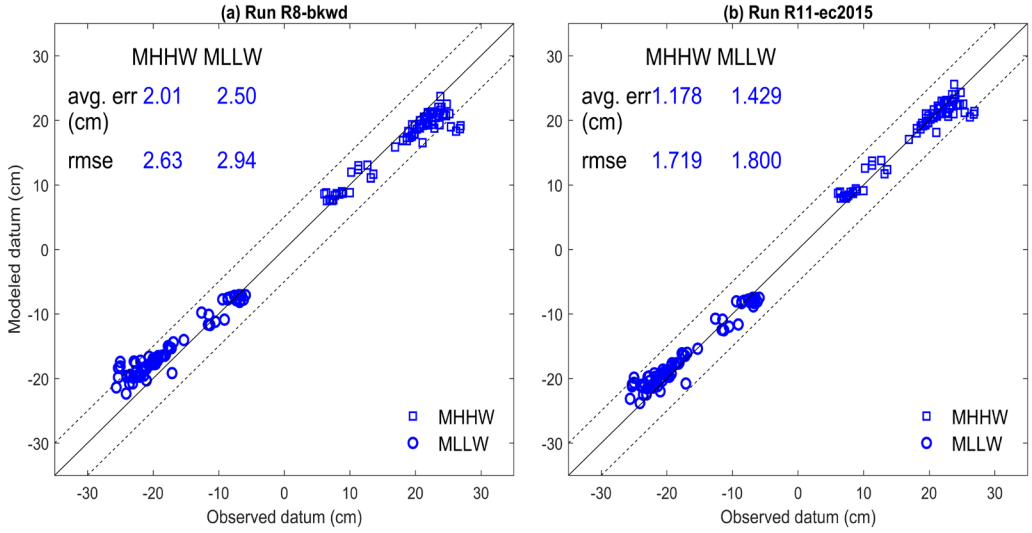

Figure 22 Sensitivity of modeled datums to offshore boundary conditions using (a) EC2001 and (b) EC2015 tidal databases. Tests were conducted using the 2008 model grid with breakwaters added to Perdido Bay. The dashed lines indicate the 5-cm error band.

4.4.2 Sensitivity of modeled datum to breakwaters

Dhingra et al. (2008) found an over-prediction trend inside the Perdido Bay, Fla., which resulted the highest error in the Bay area. Several changes were incorporated, including extended domain to include the Perdido River, added a radiation boundary condition to the upstream end of the river, and refined the intracostal water way that connects Perdido Bay to Pensacola Bay, Florida etc. However, no major changes in the datums resulted (Dhingra et al., 2008).

When we conducted the first test run using the original 2008 model grid and input files, we got the same overestimate for stations inside the Perdio Bay (Figure 23a). By overlapping the model grid on Google Earth, we found that the two breakwaters at the entrance of Perdido Bay were missing

from the 2008 model grid (Figure 23b). The next test we did was to pick up 9 nodes (red circles in Figure 23b), aligned them with the breakwaters as in Figure 23d, and assigned a land value of -1m. Figure 23c shows the updated model results: the Perdido Bay stations now are nicely distributing on both side of the solid line, e.g., no bias as in Figure 23a. The averaged model error are also reduced.

The above results point to the importance of the breakwaters at Perdido Bay entrance for model accuracy. The narrow entrance formed by the breakwaters can limit the total amount of tidal wave energy that can propagate into the Bay, thus affecting the tidal range. The model grid must accurately resolve such sudden change in bathymetry and coastal geometry.

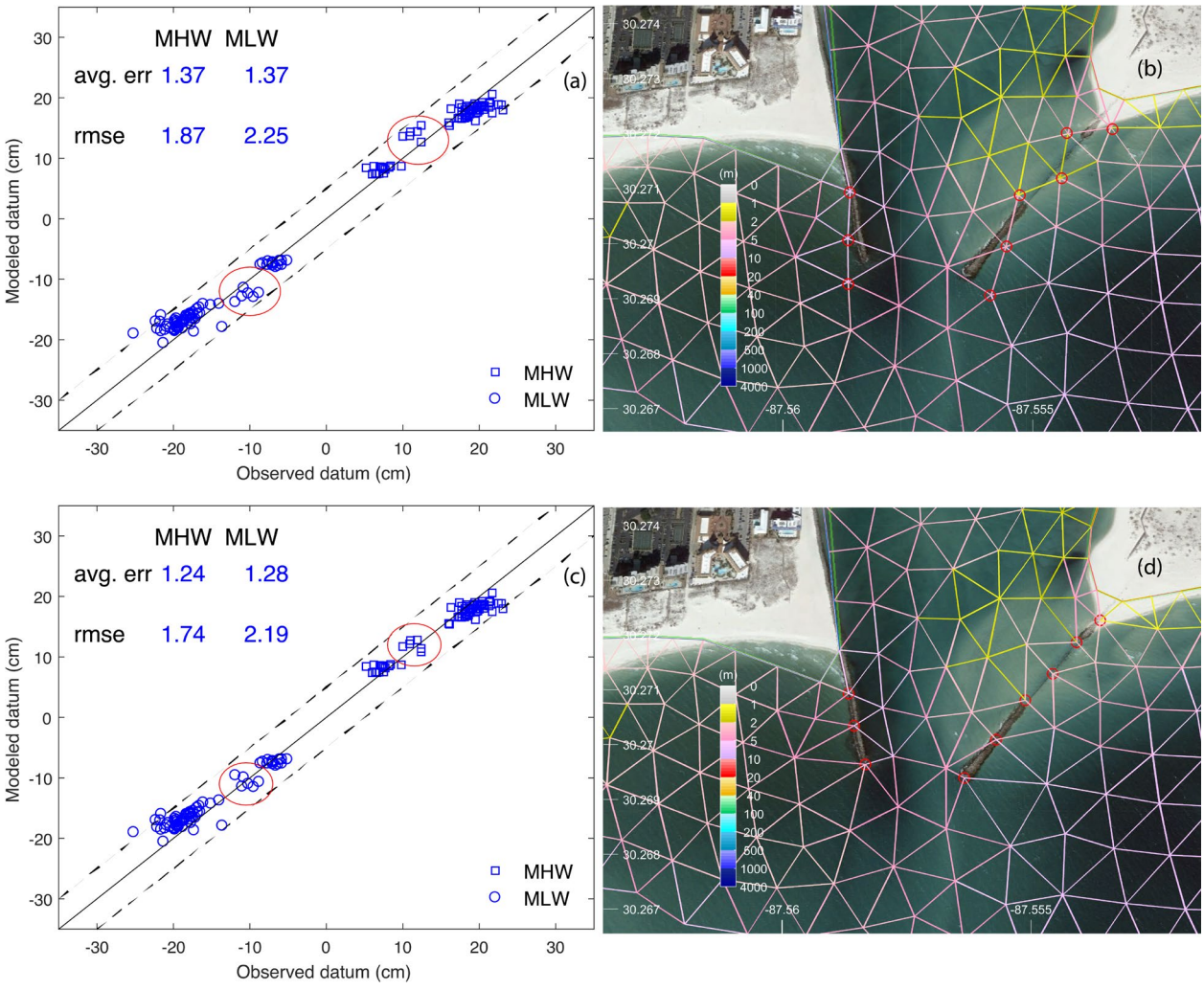

Figure 23 (a,c) Model data comparison at 74 stations in VDatum region (b) without and (d) with breakwaters at the entrance, respectively. Tide stations inside the Perdido Bay were within the red circle. Tests were conducted using the 2008 model grid. The dashed lines indicate the 5-cm error band.

4.4.3 Sensitivity of modeled datum to water depth

In this study, we found that water depth in coastal area plays an important role on model accuracy. Two types of very large model error (>10 cm) were found due to inaccurate water depth: (1) an underestimate when water depth is not deep enough and (2) an overestimate when water depth is too deep. Underestimate refers to the magnitude of the modeled datum smaller than the observation, while overestimate means the magnitude of the modeled datum greater than the observation. Figure 24a show these two types of error at an early stage of testing for stations outside the VDatum region.

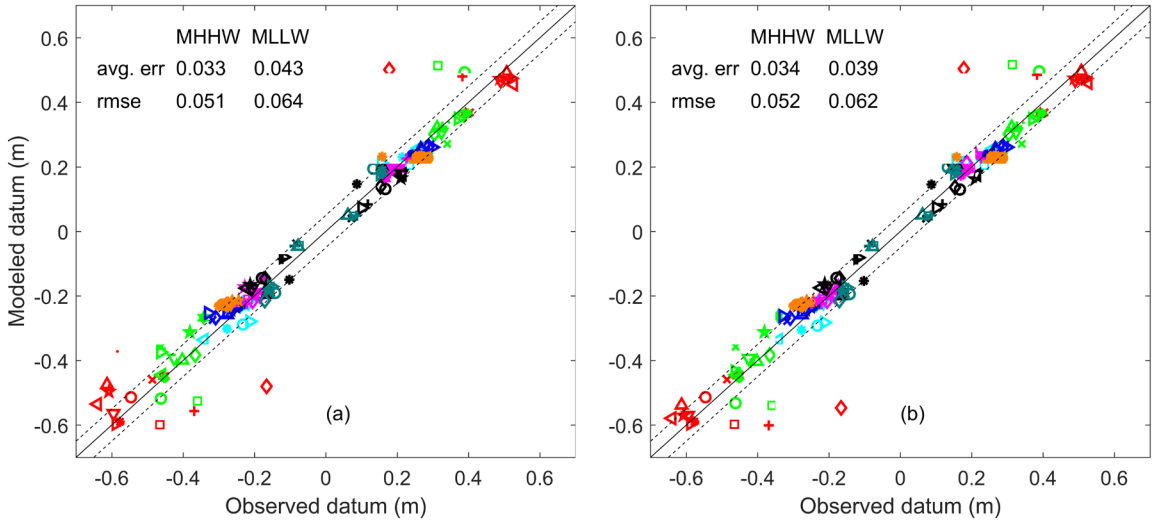

Figure 24 Sensitivity of modeled datum to water depth for stations outside VDatum region. (a) Two types of large model error at early stage of testing. (b) Increasing minimum water depth resolved the underestimate at MLLW (e.g. the MLLW outliers to the left of the error band in (a)). See Figure 14a for the final results. The dashed lines indicate the 5-cm error band.

(a)

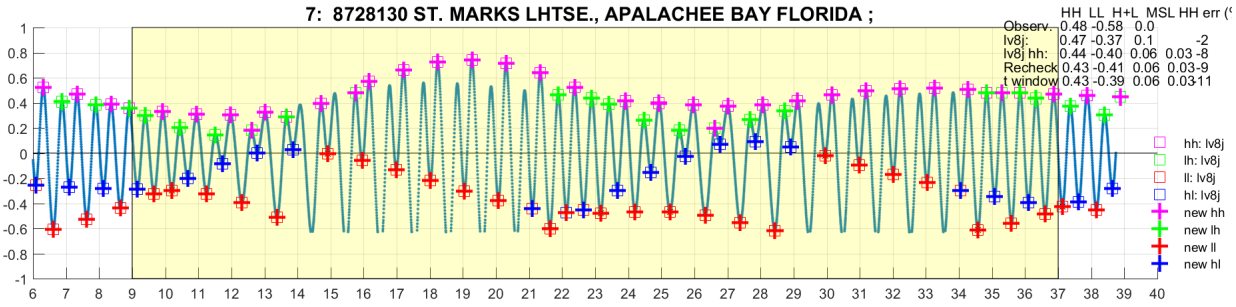

(b)

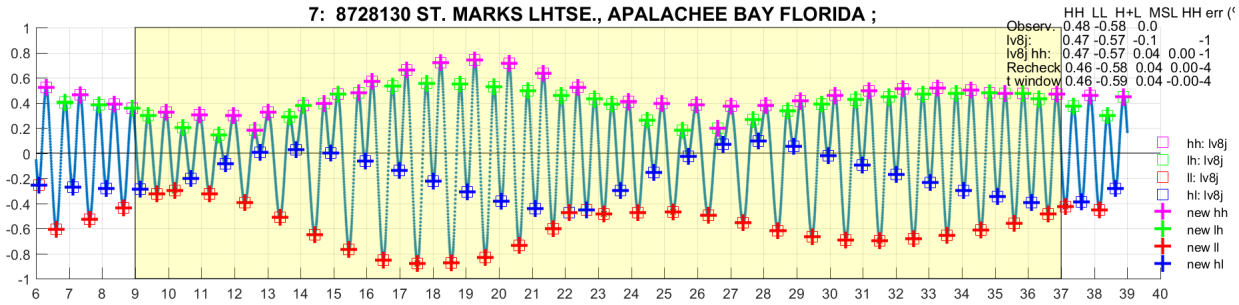

Figure 25 Sensitivity of modeled datum to water depth at station 8728130. Tests were conducted using the 2017 model grid.

The first type of error (large underestimate) usually happens to |MLLW|. For example, Figure 24a shows that MLLW has greater average model error than MHHW. This is due to the underestimate for some stations at MLLW only (those stations above the 5cm error band at MLLW in Figure 24a). An examination on the model time series at station 8728130 reveals that at low water, the model outputs a non-value due to the exposure of the shallow bottom (Figure 25a). Such being the case, the tidal datum computing software lv8j.f was unable to find the correct lows (Figure 25a). Due to lack of high resolution bathemetry data near the stations, an alternative solution is to adjust the water depth around the stations, making them slightly deeper to avoid the bottom exposure at MLLW. This tentatively solved the problem as illustrated in Figures 25b. The MLLW error for station 8728130 reduced from 21 cm underestimate to 1 cm.

The second type of error (large overestimate) can be found at both |MLLW| and MHHW. This usually occurs at some river stations that are not only relatively far away from the open coast but also have very shallow and narrow segments (e.g., Figures 26 and 27). The outliers in Figure 24b are corresponding to five such river tide stations.

The MHHW at station 8728171 in Wakulla River, Fla., is 18 cm, which is 23 cm smaller than the nearby station 8728151 (Figure 26a). This is due to the shallow depth and narrow segments in the river branch to station 8728171. Figure 26b show survey data for a segment of the river. It confirms the very shallow water depth (less than 0.5 m) near the station (Figure 26b). Figure 26c shows another shallow segment in the river, with expansion and then contraction of the river width.

The MHHW at station 8727989 in Aucilla River, Florida is 38 cm, which is approximately 13 cm smaller than the nearby stations at open coast. Figure 27 a and b show the survey data for the river. We can see the line survey data did not capture the full picture of the rock section in Figure 27c.

The difficulty in modeling such outlier river stations is the lack of complete, high resolution bathymetry data that can accurately represent the change of depth along the river as well as on cross section. For such stations, special adjustments were applied to the river depth to reduce the error as much as possible. It is based the modeler's best judgment, using available information from observation and bathymetry data, and Google Earth satellite imagery. Note that such adjustments are at locations within the model grid but far away from the VDatum region.

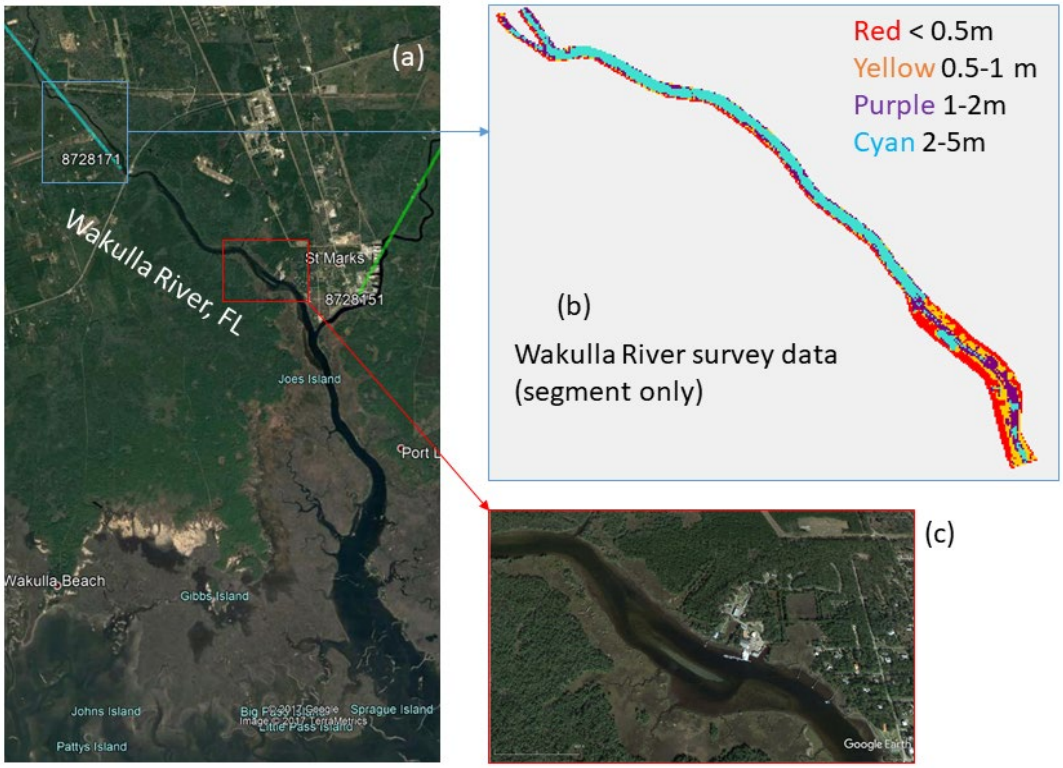

Figure 26 (a) A Google Earth image shows the Waikula River and the outlier station 8728171. (b) Bathymetry survey data near the station. (c) A shallow segment of the river with expansion and contraction.

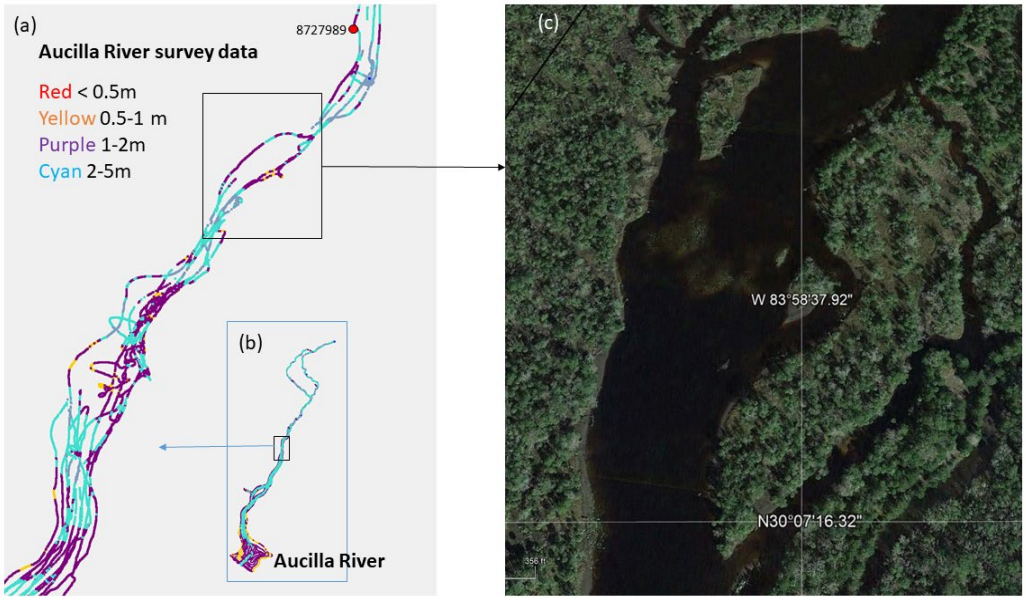

Figure 27 (a) Survey data segment and outlier station 8727989. (b) Aucilla River survey data. (c) Google Earth image shows the rocky segment of the river with contraction.

4.4.4 Sensitivity of spatially varying uncertainty to model error

Large model error from tide stations can propagate as background uncertainty during spatially varying uncertainty computation. Figure 28a shows the spatially varying uncertainty for MLLW using the preliminary results with large model error presented as in Figure 24a. As the model error being reduced in the final results shown in Figure 14a, the spatially varying uncertainty is also reduced as in Figure 28b. The tests were conducted using the 144 tide stations with root mean squared error data.

The above result point to the importance of improving model accuracy in order to reduce the spatially varying uncertainty.

(a) (b)

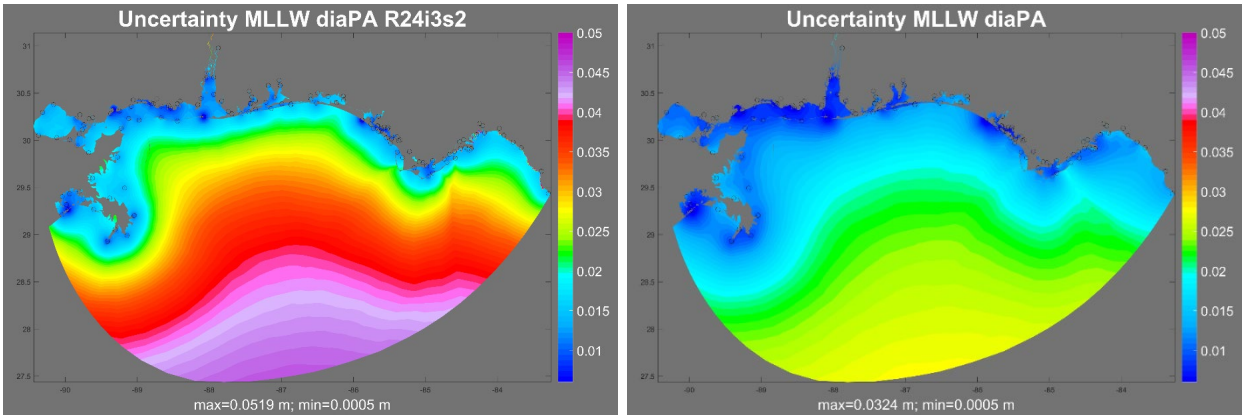

Figure 28 Sensitivity of spatially varying uncertainty to model error. (a) Before and (b) after error reduction (e.g. Figure 24a vs. Figure 14a). Tests were conducted using 144 tide stations. Unit for the color bar is in meter.

4.4.5 Model error at station 8761678 in the Intracoastal Waterway

For tide stations located in the Intracoastal Waterway (ICWW), additional attention needs to be paid to the multi-connecting channels. Such an example is station 8761678, Michoud substation, ICWW, Louisiana (Figure 29 a). The observed MHHW and MLLW are 21 cm at the station. Figure 29 a1 shows an early testing version of the mesh around the station. It produces -8cm error in both MHHW and |MLLW|. This is near double the -3 to -4 cm error magnitude at the four nearby tide stations. After connecting the channel to Lake Borgne through station 8761529 (Figure 29 b), the model error reduces to -4 cm for MHHW. This is consistent with the error for the nearby tide stations. Note that this reduction in error also improves the spatially varying uncertainty in the area from Figure 29 c to d.

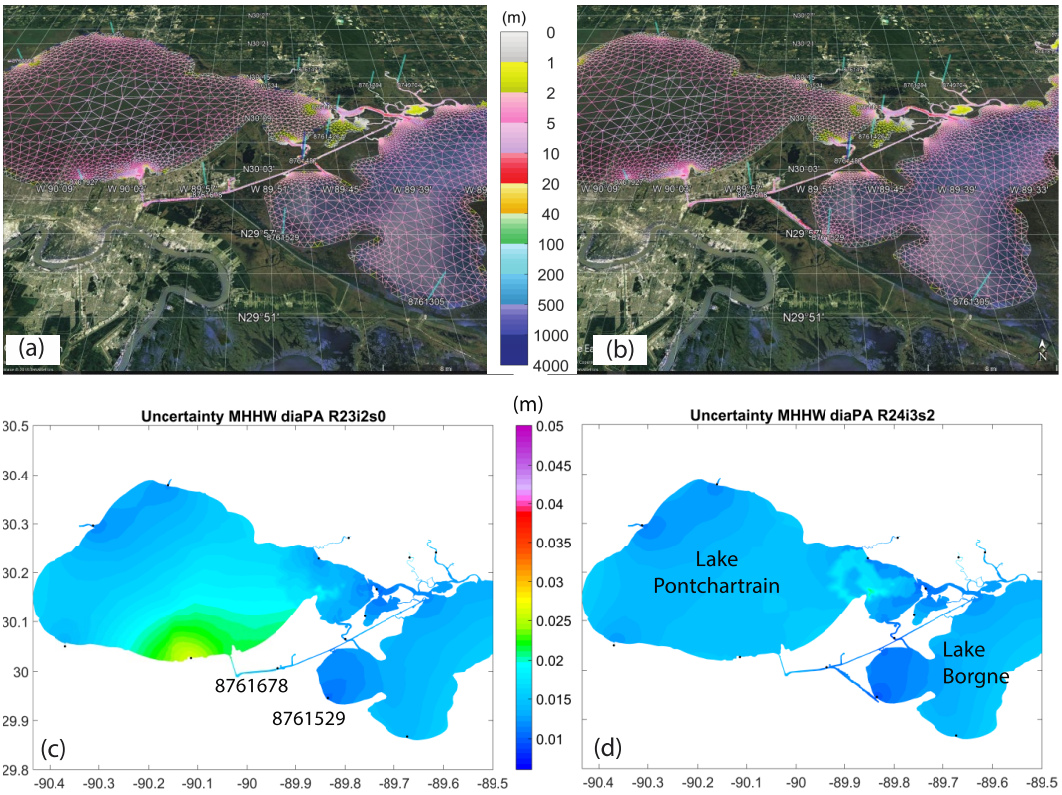

Figure 29 Sensitivity of spatially varying uncertainty to model error at intracoastal waterway station 8761678. (a) 8 cm and (b) 4 cm error at 8761678, Michoud substation, Intracoastal Waterway (ICWW), Louisiana. (c) and (d) are the corresponding spatially varying uncertainty for the grids in (a) and (b) respectively.

4.4.6 Sensitivity of spatially varying uncertainty to assigned RMS

As mentioned in section 3.1, 38 of the 182 tide stations in the model domain have no computed root mean square error (rmse) data for the observations. However, the observations from the stations still need to be used to correct the model datums. To solve this problem, reasonable rmse values need to be assigned to the stations so they can be incorporated in the spatially varying uncertainty computation. A set of sensitivity tests were conducted to evaluate the effect of rmse on uncertainty. The first test is to assign the maximum rmse (3.4 cm) among the 144 stations to the 38 stations (Figure 30.b1). This test is on the conservative side. The resulting spatially varying uncertainty is shown in Figure 30.b2. We can see in the VDatum region, this large rmse introduces large local uncertainty near some tide stations, especially 8728942 on the southern tip of the Cape San Blas.

Figure 30.c1 shows local maximum error were assigned to the 38 stations, e.g., the maximum root mean square error among the nearest three stations. It assumes the rmse for the nearby stations should be similar due to the relatively similar bathymetry and tidal range. In this way, the error pattern falls nicely along the trend as shown in Figure 30.c1, instead of introducing intrusions as

shown in Figure 30.b1. The resulting spatially varying uncertainty for MHW is shown in Figure 30.c2. We apply this method to produce the final datum products and spatially varying uncertainty here. Note that rmse also depends on the length of the observed time series. For a short time series, the datum will be related to a local long-term station, which may be different from the three nearest stations.

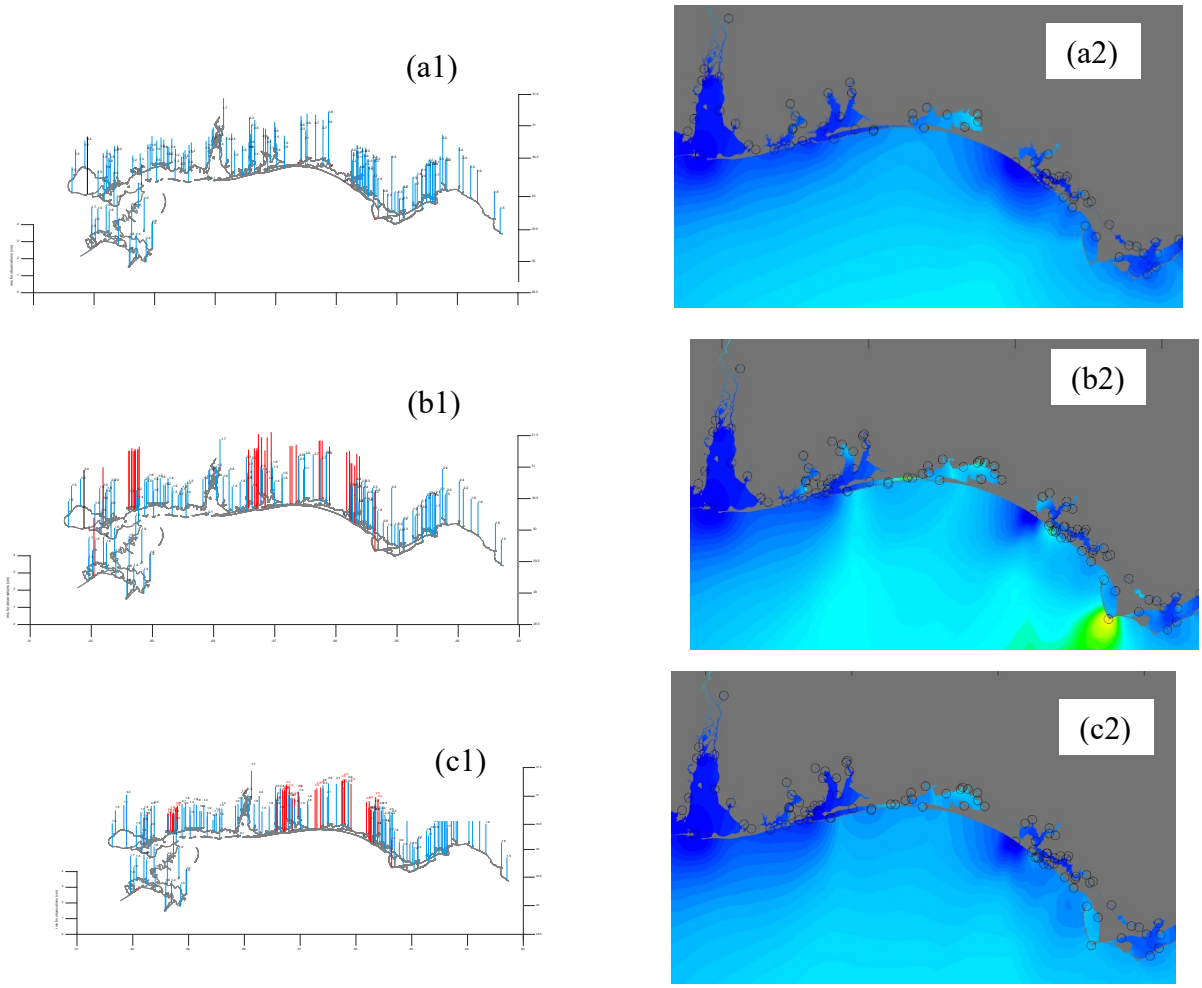

Figure 30 Sensitivity of spatially varying uncertainty to assigned Root mean square error. (a1) Root mean square error for 144 tide stations. (a2) Spatially varying uncertainty for MHW in VDatum region using the 144 tide stations in a1. (b1) Maximum rmse of 3.4 cm were assigned to the 38 stations without rmse (in red bars). (c1) Local maximum rmse were assigned. (b2 and c2) Spatially varying uncertainty for MHW as the results from (b1) and (c1), respectively. A total of 182 tide stations were used in the SVU computation for (b2) and (c2).

5. SUMMARY AND CONCLUSION

In this report, we highlight the creation of the tidal datum fields and associated spatially varying uncertainty for VDatum. From west to east, the region of interest encompasses Mobile Bay, Perdido Bay (Alabama and Florida), Pensocola Bay, Choctawatchee Bay, St. Andrew Bay, St. Joseph Bay, and Cape San Blas, Florida. We present the development, testing of the numerical model of tides in north-eastern Gulf of Mexico, and lessons learned.

In the VDatum region, the average model error is 1.2 cm (or 7.9%) for the four datums for the 83 tide stations, among which 95.5% of the modeled datums have errors within 3 cm. After applying the spatially varying uncertainty method, the maximum absolute error in the datum products at station locations is 1 cm and the maximum uncertainty in the VDatum region is 2.5 cm. Compared to the single value uncertainty for a region, the spatially varying uncertainty provides more accurate representation of the uncertainty for the datum products.

The study points out that large model errors, measurement errors, and lack of observations can contribute to large spatially varying uncertainty. Accurate water depth data with high resolution in coastal areas is essential for improving model accuracy. This is especially important for shallow and narrow rivers. The tide model also needs to resolve the narrow entrances with breakwaters for bays well. For tide stations located in the intracoastal waterway, additional attention needs to be made to the multi-connecting channels. As we extend VDatum coverage to rivers and intracoastal waterways, high-quality river bathymetry data such as river LiDAR mapping data are needed.

The spatially varying uncertainty have been provided to the tri-office Vdatum teamfor decision-making on placement of new tide gauges of high precision. New tide gauge data can be used to address the issues of lack of observations and large measurement errors and, therefore, to further reduce the uncertainty in the VDatum products in the future.

ACKNOWLEDGEMENTS

We thank CSDL's Zizang Yang for his detail reviews, many thoughtful discussions, comments, and editing of the report; Hongqiang Zhou for discussions. Kurt Nelson at CSDL, Chris Libeau at Marine Chart Division, Juliet Kinney at NOAA/UNH Joint Hydrographic Center, Tim Carlile at Land and Sea Surveying Inc, Emily Taylor at Howard T. Odum Florida Springs Institute, and George Cole at Aucilla Research Institute for bathymetry data and discussion; CSDL's IT group for their supports. Liujuan Tang thanks Chang Zhao and Karen Ferebee at ERT, Julia Powell and Neeraj Saraf at CSDL for their administrative support; and Pacific Hydrographic Branch and Olivia Hauser for providing office accommodation and support to the project.

REFERENCES

Amante, C.J., M.R. Love, L.A. Taylor, and B.W. Eakins, 2011. Digital Elevation Models of Mobile, Alabama: Procedures, Data Sources and Analysis. U.S. Department of Commerce, National Oceanic and Atmospheric Administration, National Geophysical Data Center, Boulder, Colorado, **NOAA Technical Memorandum** NESDIS NGDC-44, 43pp.

Bodnar, A. N., 1981. Estimating Accuracies of Tidal Datums from Short Term Observations. National Oceanic and Atmospheric Administration, Center for Operational Oceanographic Products and Services**:** 32. Silver Spring, Maryland.

CO-OPS, 2003. Computational Techniques for Tidal Datum Handbook; **NOAA Special Publication** NOS-OPS 2: Silver Spring, Maryland, p. 98.

DeWitt, N.C., C.A. Stalk, C.G. Smith , S.D. Locker, J. Fredericks , T.A. McCloskey, and C. Wheaton, 2015. Single beam bathymetry data collected in 2015 from Grand Bay, Mississippi/Alabama. https://doi.org/10.5066/F7NP22M2

Dhingra, E. A., K. W. Hess, and S. A. White, 2008. VDatum for the Northeast Gulf of Mexico from Mobile Bay, Alabama, to Cap San Blas, Florida: Tidal Datum Modeling and Population of the marine Grids., **NOAA Technical Memorandum** NOS CS 14, 64 pp. National Oceanic and Atmospheric Administration, National Ocean Service, Office of Coast Survey, Coast Survey Development Laboratory, Silver Spring, Maryland.

Gill, S. K. and J. R. Schultz, 2001. Tidal Datums and Their Applications. NOAA Special Publication NOS CO-OPS 1, 111p. + appendix. Silver Spring, Maryland.

Hess, K. W., R.A. Schmalz, C. Zervas, and W.C. Collier, 1999. Tidal constituent and residual interpolation (TCARI): A new method for the tidal correction of bathymetric data**:** 99.

Hess, K. W., 2002. Spatial interpolation of tidal data in irregularly-shaped coastal regions by numerical solution of laplace's equation. **Estuarine, Coastal and Shelf Science** 54: 175-192.

Hess, W.K. and S.K. Grill, 2003. Puget Sound Tidal Datum by Spatial Interpolation. In Proceedings of the American Meteorological Society Fifth Conference on Coastal Atmospheric and Oceanic Prediction and Processes, Seattle, WA.

Hess, K. W. and S. A. White, 2004: VDatum for Puget Sound: Generation of the Grid and Population with Tidal Datums and Sea Surface Topography. **NOAA Technical Memorandum** NOS CS 4, 27 pp. National Oceanic and Atmospheric Administration, National Ocean Service, Office of Coast Survey, Coast Survey Development Laboratory, Silver Spring, Maryland.

Hess, K. W. S., E. Anne; A.M. Wong, S.A. White, and S.K. Gill, 2005. VDatum for central coastal North Carolina : tidal datums, marine grids, and sea surface topography. **NOAA technical report** NOS CS 21. National Oceanic and Atmospheric Administration, National Ocean Service, Office of Coast Survey, Coast Survey Development Laboratory, Silver Spring, Maryland.

Hess, K. W., 2012. REVISED VDATUM FOR THE NORTHEAST GULF OF MEXICO. Unpublished document, 7 pp.

Love, M.R., R.J. Caldwell, K.S. Carignan, B.W. Eakins and L.A. Taylor, 2010a. Digital Elevation Models of Southern Louisiana: Procedures, Data Sources and Analysis. U.S. Department of Commerce, National Oceanic and Atmospheric Administration, National Geophysical Data Center, Boulder, Colorado, 22pp.

Love, M.R., C.J. Amante, K.S. Carignan, B.W. Eakins, and L.A. Taylor, 2010b. Digital Elevation Models of the Northern Gulf of Coast: Procedures, Data Sources and Analysis. National Oceanic and Atmospheric Administration, National Geophysical Data Center, Boulder, Colorado, 38pp.

Love, M.R., C.J. Amante, L.A. Taylor and B.W. Eakins, 2011. Digital Elevation Models of New Orleans, Louisiana: Procedures, Data Sources and Analysis. **NOAA Technical Memorandum** NESDIS NGDC-49, 46pp. National Oceanic and Atmospheric Administration, National Geophysical Data Center, Boulder, Colorado,

Luettich, R.A., J.J. Westerink, and N.W. Scheffner, 1992. ADCIRC: An Advanced Three-Dimensional Circulation Model of Shelves, Coasts, and Estuaries, Report 1: theory and methodology of ADCIRC-2DDI and ADCIRC-3DL. *U.S. Department of the Army, Technical* Report DRP-92-6.

Luettich, R. A. J., Westerink, and J.J, Ed. (1995). Continental shelf scale convergence studies with a barotropic tidal model. Quantitative Skill Assessment for Coastal Ocean Models, American Geophysical Union press.

Luettich, R.A. and J.J. Westerink, 2004. Formulation and Numerical Implementation of the 2D/3D ADCIRC Finite Element Model version 44.XX. http://www.unc.edu/ims/adcirc/publications/2004/2004_Luettich.pdf.

Mukai A.Y., J.J. Westerink, R.A. Luettich Jr., and D. Mark, 2002. East coast 2001, a tidal constituent database for the western North Atlantic, Gulf of Mexico and Caribbean Sea, US Army Engineer Research and Development Center, Coastal and Hydraulics Laboratory, Technical Report, ERDC/CHL TR-02-24, September 2002, 201p.

Myers, E.P.; A. Wong, K. Hess, S. White, E. Spargo, J. Feyen, Z. Yang, P. Richardson, C. Auer, J. Sellars, et al. Development of a national VDatum, and its application to sea level rise in North Carolina. In Proceedings of the U. S. Hydrographic Conference, San Diego, CA, USA, 29–31 March 2005.

NOS, 2010. Standard Procedures to Develop and Support NOAA's Vertical Datum Transformation Tool, VDATUM, version 2010.08.03, 120p.

Shi, L., and E.P. Myers, 2016. Statistical Interpolation of Tidal Datums and Computation of Its Associated Spatially Varying Uncertainty. **J. Mar. Sci. Eng.** 4(4): 64.

Spargo, E., J.J. Westerink, R.A. Luettich, and D. Mark, 2004. Developing a Tidal Constituent Database for the Eastern North Pacific Ocean, Estuarine and Coastal Modeling VIII, M. Spaulding et al. [eds], ASCE, p.217-235.

Spargo, E. A. and J.W. Woolard, 2005. VDatum for the Calcasieu River from Lake Charles to the Gulf of Mexico, Louisiana: tidal datum modeling and population of the grid. **NOAA Technical Report** NOSCS 19, 25p. National Oceanic and Atmospheric Administration, National Ocean Service, Office of Coast Survey, Coast Survey Development Laboratory, Silver Spring, Maryland.

Szpilka, C, K. Dresback., R. Kolar, J. Feyen, and J. Wang, 2016: Improvements for the Western North Atlantic, Caribbean and Gulf of Mexico ADCIRC Tidal Database (EC2015). **J. Mar. Sci. Eng**., 4(4), 72; doi:10.3390/jmse4040072.

Tang, L., E. Myers, L. Shi, K. Hess, A. Carisio, M. Michalski, S. White, and C. Hoang, 2018. Tidal Datums with Spatially Varying Uncertainty in North-East Gulf of Mexico for VDatum Application. **J. Mar. Sci. Eng**. 2018, 6(4), 114; doi:10.3390/jmse6040114

Taylor, L.A., B.W. Eakins, K.S. Carignan, R.R. Warneken, T. Sazonova, D.C. Schoollcraft, and G.F. Sharman, 2008a. Digital Elevation Model of Panama City, Florida, 2008. Procedures, Data Sources and Analysis. **NOAA Technical Memorandum** NESDIS NGDC-8, 27pp. National Oceanic and Atmospheric Administration, National Geophysical Data Center, Boulder, Colorado,

Taylor, L.A., B.W. Eakins, K.S. Carignan, R.R. Warneken, T. Sazonova, and D.C. Schoollcraft, 2008: Digital Elevation Model of Biloxi, Mississippi, 2008b: Procedures, Data Sources and Analysis. **NOAA Technical Memorandum** NESDIS NGDC-9, 32pp. National Oceanic and Atmospheric Administration, National Geophysical Data Center, Boulder, Colorado.

Xu, J., E.P. Myers, I. Jeong, and S.A. White, 2013. VDatum for the coastal waters of Texas and western Louisiana : tidal DAtums and topography of the sea surface. **NOAA Technical Memorandum** NOS CS 29, 48 pp. National Oceanic and Atmospheric Administration, National Ocean Service, Office of Coast Survey, Coast Survey Development Laboratory, Silver Spring, Maryland.

Yang, E. P. Myers, A. M. Wong, and S. A. White, 2010. VDatum for Eastern Louisiana and Mississippi Coastal Waters: Tidal Datums, Marine Grids, and Sea Surface Topography. **NOAA Technical Memorandum** NOS CS 19, 56 pp. National Oceanic and Atmospheric Administration, National Ocean Service, Office of Coast Survey, Coast Survey Development Laboratory, Silver Spring, Maryland.

Yang, Z.Y., E. P. Myers, I. Jeong, and S. A. White, 2012. VDatum for the Coastal Waters from the Florida Shelf to the South Atlantic Bight: Tidal Datums, Marine Grids, and Sea Surface Topography. **NOAA Technical Memorandum** NOS CS 27, 97 pp. National Oceanic and Atmospheric Administration, National Ocean Service, Office of Coast Survey, Coast Survey Development Laboratory, Silver Spring, Maryland.

APPENDIX A TIDE STATION DATA AND MODEL RESULTS

TABLE A1 TIDE STATION DATA AND MODEL RESULTS

No.	Station	Location	Longitude	Obs		Model			Source
	ID	Name	Latitude	rms	MHHW	MHW	MLW	MLLW	ID
1	8727648	HORSESHOE POINT FLORIDA	-83.293333 29.436667	0.01	0.51 0.48 -0.04 -7%	0.42 0.41 -0.02 -4%	-0.40 -0.39 0.00 -1%	-0.58 -0.59 -0.01 2%	obs model diff error
2	8727695	STEINHATCHEE FLORIDA	-83.390000 29.671667	0.02	0.53 0.47 -0.06 -11%	0.44 0.41 -0.03 -7%	-0.43 -0.40 0.04 -8%	-0.64 -0.59 0.05 -8%	obs model diff error
3	8727843	SPRING WARRIOR CREEK FLORIDA	-83.671667 29.920000	0.02	0.51 0.48 -0.03 -5%	0.43 0.43 0.00 0%	-0.39 -0.41 -0.02 6%	-0.55 -0.60 -0.05 10%	obs model diff error
4	8727892	FENHOLLOWAY RIVER FLORIDA	-83.783333 29.980000	0.02	0.52 0.48 -0.04 -7%	0.44 0.44 -0.01 -1%	-0.40 -0.41 -0.01 2%	-0.59 -0.60 -0.02 3%	obs model diff error
5	8727956	ECONFINA RIVER, INSIDE FLORIDA	-83.910000 30.053333	0.02	0.51 0.48 -0.03 -6%	0.43 0.43 -0.00 -0%	-0.33 -0.35 -0.03 8%	-0.47 -0.46 0.00 -1%	obs model diff error
6	8727989	AUCILLA RIVER FLORIDA	-83.975000 30.126667	0.02	0.38 0.45 0.06 17%	0.32 0.40 0.08 25%	-0.27 -0.26 0.01 -2%	-0.37 -0.33 0.04 -11%	obs model diff error
7	8728130	ST. MARKS LHTSE., APALACHEE BAY FLORIDA	-84.178333 30.078333	0.02	0.48 0.49 0.01 1%	0.41 0.44 0.03 8%	-0.40 -0.40 0.00 -0%	-0.58 -0.58 0.01 -1%	obs model diff error
8	8728151	ST. MARKS CITY FLORIDA	-84.203333 30.155000	0.01	0.51 0.49 -0.01 -2%	0.43 0.45 0.02 5%	-0.41 -0.38 0.03 -8%	-0.61 -0.53 0.08 -14%	obs model diff error
9	8728171	WAKULLA RIVER FLORIDA	-84.246667 30.176667	0.03	0.18 0.35 0.17 98%	0.14 0.31 0.16 112%	-0.11 -0.17 -0.06 53%	-0.17 -0.17 -0.00 3%	obs model diff error
10	8728229	SHELL POINT FLORIDA	-84.290000 30.060000	0.02	0.49 0.48 -0.01 -2%	0.42 0.43 0.02 4%	-0.39 -0.39 -0.00 0%	-0.59 -0.57 0.02 -4%	obs model diff error
11	8728255	ALLIGATOR HARBOR FLORIDA	-84.365000 29.911667	0.02	0.40 0.37 -0.04 -9%	0.33 0.33 -0.01 -2%	-0.30 -0.29 0.02 -6%	-0.49 -0.46 0.03 -6%	obs model diff error
12	8728258	FIDDLERS POINT FLORIDA	-84.368333 30.015000	0.02	0.49 0.49 -0.00 -0%	0.42 0.44 0.02 5%	-0.39 -0.39 0.00 -1%	-0.61 -0.57 0.04 -7%	obs model diff error
13	8728261	ALLIGATOR POINT, SW CAPE FLORIDA	-84.388333 29.895000	0.02	0.39 0.36 -0.03 -8%	0.33 0.32 -0.01 -2%	-0.28 -0.27 0.00 -1%	-0.45 -0.44 0.01 -2%	obs model diff error

No.	Station	Location	Longitude	Obs		Model			Source
	ID	Name	Latitude	rms	MHHW	MHW	MLW	MLLW	ID
14	8728288	ALLIGATOR POINT FLORIDA	-84.413333 29.903333	0.02	0.40 0.37 -0.03 -8%	0.33 0.32 -0.00 -0%	-0.27 -0.28 -0.01 6%	-0.45 -0.45 -0.00 0%	obs model diff error
15	8728311	ST. TERESA BEACH FLORIDA	-84.446667 29.928333	0.02	0.38 0.36 -0.02 -5%	0.31 0.32 0.00 1%	-0.28 -0.27 0.01 -4%	-0.46 -0.44 0.02 -4%	obs model diff error
16	8728351	OCHLOCKONEE RIVER STATE PARK FLORIDA	-84.471667 30.005000	0.02	0.39 0.41 0.02 5%	0.33 0.35 0.03 9%	-0.32 -0.29 0.03 -9%	-0.46 -0.42 0.04 -9%	obs model diff error
17	8728360	TURKEY POINT FLORIDA	-84.511667 29.915000	0.02	0.37 0.35 -0.02 -7%	0.31 0.31 -0.00 -0%	-0.28 -0.26 0.02 -6%	-0.46 -0.43 0.03 -7%	obs model diff error
18	8728366	MCINTYRE, OCHLOCKONEE RIVER FLORIDA	-84.526667 29.981667	0.02	0.31 0.35 0.04 11%	0.26 0.27 0.01 4%	-0.23 -0.22 0.02 -7%	-0.36 -0.32 0.04 -12%	obs model diff error
19	8728408	DOG ISLAND, EAST END FLORIDA	-84.585000 29.810000	0.02	0.33 0.32 -0.01 -2%	0.27 0.28 0.01 5%	-0.25 -0.24 0.01 -2%	-0.42 -0.41 0.01 -3%	obs model diff error
20	8728412	LANARK, ST. GEORGES SOUND FLORIDA	-84.595000 29.878333	0.02	0.34 0.33 -0.01 -3%	0.28 0.30 0.01 4%	-0.27 -0.25 0.02 -6%	-0.45 -0.42 0.03 -7%	obs model diff error
21	8728464	CARRABELLE RIVER, ST. GEORGE SOUND FLORIDA	-84.665000 29.850000	0.02	0.31 0.31 -0.00 -1%	0.26 0.27 0.02 7%	-0.23 -0.23 0.00 -2%	-0.40 -0.38 0.02 -6%	obs model diff error
22	8728486	NE END, ST. GEORGE ISLAND FLORIDA	-84.700000 29.766667	0.02	0.30 0.30 -0.01 -3%	0.26 0.26 -0.00 -0%	-0.21 -0.22 -0.00 0%	-0.37 -0.38 -0.01 3%	obs model diff error
23	8728488	SOUTH CARRABELLE BEACH FLORIDA	-84.736667 29.801667	0.02	0.32 0.30 -0.02 -7%	0.27 0.27 -0.00 -0%	-0.24 -0.22 0.01 -6%	-0.42 -0.39 0.04 -9%	obs model diff error
24	8728619	CAT POINT, APALACHICOLA BAY FLORIDA	-84.886667 29.723333	0.02	0.34 0.26 -0.08 -22%	0.25 0.24 -0.01 -3%	-0.24 -0.19 0.05 -21%	-0.46 -0.35 0.11 -24%	obs model diff error
25	8728626	ST. GEORGE ISLAND, BAYSIDE FLORIDA	-84.896667 29.653333	0.01	0.28 0.25 -0.03 -10%	0.23 0.23 0.01 2%	-0.23 -0.18 0.05 -21%	-0.38 -0.34 0.04 -12%	obs model diff error
26	8728669	SIKES CUT,ST.GEORGE ISLAND FLORIDA	-84.958333 29.613333	0.01	0.26 0.28 0.02 8%	0.19 0.25 0.06 32%	-0.18 -0.14 0.05 -25%	-0.34 -0.29 0.06 -17%	obs model diff error

No.	Station	Location	Longitude	Obs		Model			Source
	ID	Name	Latitude	rms	MHHW	MHW	MLW	MLLW	ID
27	8728690	APALACHICOLA, APALACHICOLA RIVER FLORIDA	-84.981667 29.726667	0.01	0.21 0.24 0.03 13%	0.18 0.22 0.04 20%	-0.15 -0.16 -0.01 4%	-0.28 -0.32 -0.04 15%	obs model diff error
28	8728694	WHITE BEACH, EAST BAY FLORIDA	-84.898333 29.785000	0.01	0.26 0.27 0.01 3%	0.22 0.24 0.03 13%	-0.17 -0.19 -0.02 9%	-0.34 -0.35 -0.01 2%	obs model diff error
29	8728711	APALACHICOLA RIVER FLORIDA	-85.033333 29.763333	0.01	0.18 0.16 -0.02 -14%	0.15 0.12 -0.03 -20%	-0.14 -0.14 -0.01 5%	-0.23 -0.19 0.05 -19%	obs model diff error
30	8728757	HUCKLEBERRY LANDING, JACKSON RIVER FLORIDA	-85.085000 29.770000	0.03	0.16 0.16 0.01 3%	0.12 0.13 0.01 4%	-0.10 -0.14 -0.05 49%	-0.21 -0.18 0.03 -15%	obs model diff error
31	8728786	ELEVEN MILE, ST. VINCENT SOUND FLORIDA	-85.153333 29.706667	0.01	0.23 0.21 -0.03 -12%	0.19 0.18 -0.01 -7%	-0.15 -0.15 0.00 -0%	-0.27 -0.26 0.01 -4%	obs model diff error
32	8728853	WHITE CITY, INTERCOASTAL WATER WAY, FL FLORID	-85.221667 29.880000	0.01	0.15 0.18 0.03 23%	0.13 0.17 0.04 35%	-0.13 -0.18 -0.05 35%	-0.16 -0.18 -0.02 14%	obs model diff error
33	8728912	PORT ST. JOE FLORIDA	-85.313333 29.815000	0.02	0.25 0.22 -0.03 -13%	0.16 0.20 0.04 22%	-0.19 -0.21 -0.02 11%	-0.25 -0.21 0.04 -14%	obs model diff error
34	8728941	NORTH PRONG, WETAPPO CREEK FLORIDA	-85.348333 30.003333	0.02	0.25 0.24 -0.02 -6%	0.21 0.22 0.00 1%	-0.20 -0.22 -0.02 10%	-0.26 -0.23 0.03 -12%	obs model diff error
35	8728942	CAPE SAN BLAS FLORIDA	-85.360000 29.668333	n/a	0.21 0.18 -0.03 -14%	0.20 0.18 -0.01 -7%	-0.20 -0.20 -0.00 0%	-0.23 -0.20 0.03 -13%	obs model diff error
36	8728957	OVERSTREET FLORIDA	-85.370000 29.996667	0.02	0.24 0.23 -0.00 -2%	0.21 0.21 0.01 3%	-0.20 -0.22 -0.02 8%	-0.24 -0.23 0.02 -8%	obs model diff error
37	8728958	ST. JOSEPH POINT, ST. JOSEPH BAY FLORIDA	-85.390000 29.873333	0.02	0.24 0.22 -0.03 -11%	0.15 0.20 0.05 36%	-0.20 -0.20 0.00 -0%	-0.23 -0.21 0.02 -10%	obs model diff error
38	8728973	WETAPPO CREEK, EAST BAY FLORIDA	-85.393333 30.038333	0.02	0.25 0.25 -0.00 -1%	0.19 0.23 0.03 16%	-0.25 -0.23 0.03 -11%	-0.26 -0.24 0.02 -8%	obs model diff error
39	8729015	ALLANTON, EAST BAY FLORIDA	-85.465000 30.030000	0.02	0.23 0.24 0.01 3%	0.20 0.22 0.02 11%	-0.20 -0.22 -0.02 10%	-0.23 -0.23 0.00 -1%	obs model diff error

No.	Station	Location	Longitude	Obs		Model			Source
	ID	Name	Latitude	rms	MHHW	MHW	MLW	MLLW	ID
40	8729017	FARMDALE, EAST BAY, ST. ANDREW BAY FLORIDA	-85.470000 30.016667	0.02	0.24 0.24 0.00 1%	0.20 0.22 0.02 10%	-0.20 -0.22 -0.02 11%	-0.24 -0.23 0.01 -3%	obs model diff error
41	8729022	ST. ANDREW SOUND, EAST END FLORIDA	-85.480000 29.970000	0.02	0.22 0.21 -0.01 -3%	0.17 0.20 0.03 17%	-0.17 -0.20 -0.03 20%	-0.21 -0.20 0.01 -5%	obs model diff error
42	8729039	PARKER BRANCH, LAIRD BAYOU, EAST BAY FLORIDA	-85.516667 30.136667	0.02	0.22 0.23 0.01 7%	0.19 0.21 0.02 11%	-0.19 -0.21 -0.01 7%	-0.22 -0.22 0.00 -1%	obs model diff error
43	8729045	LAIRD BAYOU, EAST BAY FLORIDA	-85.528333 30.121667	0.01	0.22 0.23 0.01 5%	0.20 0.22 0.02 11%	-0.19 -0.21 -0.02 10%	-0.23 -0.22 0.01 -4%	obs model diff error
44	8729052	ST ANDREW SOUND FLORIDA	-85.541667 30.025000	0.02	0.21 0.21 -0.01 -2%	0.18 0.20 0.03 14%	-0.16 -0.20 -0.04 23%	-0.21 -0.21 -0.00 0%	obs model diff error
45	8729063	CALLAWAY BAYOU EAST BAY FLORIDA	-85.571667 30.136667	0.02	0.22 0.23 0.01 3%	0.20 0.22 0.02 10%	-0.20 -0.21 -0.02 8%	-0.21 -0.22 -0.00 1%	obs model diff error
46	8729071	MILL BAYOU, NORTH BAY FLORIDA	-85.605000 30.245000	n/a	0.23 0.24 0.01 5%	0.20 0.22 0.01 6%	-0.20 -0.21 -0.02 8%	-0.23 -0.23 0.00 -2%	obs model diff error
47	8729084	PARKER, EAST BAY FLORIDA	-85.611667 30.126667	0.01	0.21 0.22 0.01 4%	0.20 0.21 0.01 5%	-0.20 -0.20 -0.01 3%	-0.22 -0.21 0.01 -5%	obs model diff error
48	8729085	PEARL BAYOU, EAST BAY FLORIDA	-85.613333 30.098333	0.01	0.21 0.23 0.01 6%	0.18 0.21 0.03 16%	-0.19 -0.20 -0.01 6%	-0.21 -0.21 0.01 -3%	obs model diff error
49	8729101	SOUTHPORT, NORTH BAY FLORIDA	-85.646667 30.283333	n/a	0.24 0.23 -0.00 -1%	0.20 0.22 0.02 8%	-0.20 -0.22 -0.01 6%	-0.24 -0.22 0.01 -6%	obs model diff error
50	8729102	LYNN HAVEN, NORTH BAY FLORIDA	-85.648333 30.255000	0.02	0.23 0.23 0.01 3%	0.19 0.22 0.03 15%	-0.19 -0.22 -0.03 16%	-0.22 -0.22 -0.00 1%	obs model diff error
51	8729105	BEACON BEACH, ST ANDREW BAY FLORIDA	-85.648333 30.091667	0.02	0.20 0.21 0.01 5%	0.19 0.21 0.02 10%	-0.18 -0.19 -0.01 6%	-0.20 -0.19 0.01 -3%	obs model diff error
52	8729107	MASSALINA BAYOU, ST. ANDREW BAY FLORIDA	-85.660000 30.151667	0.02	0.21 0.21 0.01 3%	0.18 0.21 0.03 14%	-0.18 -0.20 -0.01 8%	-0.19 -0.20 -0.01 3%	obs model diff error

No.	Station	Location	Longitude	Obs		Model			Source
	ID	Name	Latitude	rms	MHHW	MHW	MLW	MLLW	ID
53	8729108	PANAMA CITY, ST. ANDREW BAY FLORIDA	-85.666667 30.151667	0.02	0.21 0.21 0.01 4%	0.19 0.21 0.02 9%	-0.19 -0.20 -0.01 5%	-0.20 -0.20 0.01 -3%	obs model diff error
54	8729119	SHELL ISLAND, ST. ANDREW B. FLORIDA	-85.685000 30.095000	n/a	0.21 0.21 0.00 2%	0.20 0.21 0.01 5%	-0.18 -0.19 -0.02 10%	-0.19 -0.19 -0.00 1%	obs model diff error
55	8729136	NEW ENTRANCE CHANNEL, ST. ANDREW BAY FLORIDA	-85.721667 30.125000	0.02	0.20 0.22 0.02 9%	0.19 0.21 0.02 10%	-0.17 -0.18 -0.01 5%	-0.19 -0.19 0.01 -3%	obs model diff error
56	8729141	ST ANDREW STATE PARK GR LAGOON FLORIDA	-85.731667 30.133333	n/a	0.21 0.21 0.00 0%	0.19 0.21 0.02 10%	-0.18 -0.18 -0.01 4%	-0.21 -0.19 0.02 -7%	obs model diff error
57	8729149	ST. ANDREW STATE PARK FLORIDA	-85.743333 30.130000	n/a	0.24 0.21 -0.03 -11%	0.21 0.21 -0.01 -3%	-0.22 -0.20 0.03 -12%	-0.23 -0.20 0.03 -11%	obs model diff error
58	8729152	ALLIGATOR BAYOU, PANAMA CITY FLORIDA	-85.755000 30.170000	0.02	0.21 0.22 0.01 6%	0.19 0.21 0.03 14%	-0.19 -0.20 -0.01 6%	-0.21 -0.20 0.01 -2%	obs model diff error
59	8729154	BURNT MILL CREEK, WEST BAY FLORIDA	-85.763333 30.328333	n/a	0.23 0.24 0.01 3%	0.20 0.22 0.02 8%	-0.17 -0.21 -0.04 25%	-0.20 -0.23 -0.02 10%	obs model diff error
60	8729155	GRAND LAGOON, WEST END FLORIDA	-85.768333 30.158333	n/a	0.20 0.21 0.02 9%	0.18 0.21 0.03 15%	-0.18 -0.19 -0.00 2%	-0.20 -0.19 0.01 -3%	obs model diff error
61	8729169	SHELL POINT, WEST BAY FLORIDA	-85.740000 30.215000	0.01	0.25 0.23 -0.02 -8%	0.23 0.21 -0.02 -7%	-0.14 -0.21 -0.07 53%	-0.17 -0.21 -0.04 24%	obs model diff error
62	8729179	CROOKED CREEK, WEST BAY FLORIDA	-85.811667 30.308333	n/a	0.23 0.24 0.01 3%	0.19 0.22 0.03 14%	-0.19 -0.22 -0.03 14%	-0.22 -0.23 -0.01 3%	obs model diff error
63	8729210	PANAMA CITY BEACH, GULF OF MEXICO FLORIDA	-85.878333 30.213333	0.00	0.22 0.21 -0.01 -3%	0.20 0.21 0.01 6%	-0.18 -0.20 -0.02 9%	-0.20 -0.20 -0.00 1%	obs model diff error
64	8729329	CHOCTAWHATCHEE RIVER FLORIDA	-86.088333 30.396667	n/a	0.09 0.08 -0.00 -4%	0.07 0.08 0.01 21%	-0.07 -0.08 -0.01 16%	-0.08 -0.08 0.00 -3%	obs model diff error
65	8729332	JOLLY BAY, CHOCTAWHATCHEE BAY FLORIDA	-86.136667 30.428333	0.03	0.08 0.08 -0.00 -1%	0.08 0.08 0.00 2%	-0.08 -0.08 -0.00 0%	-0.09 -0.08 0.01 -10%	obs model diff error

No.	Station	Location	Longitude	Obs		Model			Source
	ID	Name	Latitude	rms	MHHW	MHW	MLW	MLLW	ID
66	8729333	LA GRANGE BAYOU FLORIDA	-86.138333 30.468333	0.03	0.06 0.08 0.02 32%	0.06 0.08 0.02 36%	-0.06 -0.08 -0.01 22%	-0.07 -0.08 -0.01 15%	obs model diff error
67	8729364	ALLAQUAY BAYOU FLORIDA	-86.205000 30.488333	n/a	0.08 0.08 0.00 4%	0.07 0.08 0.01 14%	-0.07 -0.08 -0.01 9%	-0.07 -0.08 -0.00 4%	obs model diff error
68	8729376	SANTA ROSA HOGTOWN BAYOU FLORIDA	-86.228333 30.400000	0.03	0.08 0.08 -0.00 -4%	0.07 0.08 0.01 8%	-0.09 -0.07 0.01 -13%	-0.09 -0.07 0.02 -21%	obs model diff error
69	8729381	BASIN CREEK FLORIDA	-86.240000 30.496667	n/a	0.07 0.08 0.01 9%	0.07 0.08 0.02 24%	-0.07 -0.08 -0.00 5%	-0.07 -0.08 -0.00 1%	obs model diff error
70	8729387	BASIN BAYOU, CHOCTAWHATCHEE BAY FLORIDA	-86.253333 30.486667	n/a	0.06 0.08 0.02 34%	0.05 0.08 0.03 57%	-0.06 -0.08 -0.02 30%	-0.06 -0.08 -0.01 21%	obs model diff error
71	8729435	BIG HAMMOCK PT, CHOCTAWHATCHEE BAY FLORIDA	-86.351667 30.465000	0.03	0.08 0.08 0.00 5%	0.08 0.08 0.00 5%	-0.07 -0.07 -0.00 7%	-0.07 -0.07 -0.00 5%	obs model diff error
72	8729501	VALPARISO, BOGGY BAYOU FLORIDA	-86.493333 30.503333	0.03	0.08 0.08 -0.01 -7%	0.08 0.08 -0.00 -6%	-0.08 -0.07 0.01 -13%	-0.08 -0.07 0.01 -14%	obs model diff error
73	8729511	DESTIN, EAST PASS FLORIDA	-86.513333 30.395000	0.02	0.10 0.09 -0.01 -11%	0.10 0.09 -0.01 -9%	-0.08 -0.08 0.00 -3%	-0.09 -0.08 0.01 -7%	obs model diff error
74	8729538	GARNIER BAYOU, SHALIMAR FLORIDA	-86.586667 30.435000	0.03	0.07 0.07 0.01 12%	0.06 0.07 0.01 22%	-0.05 -0.07 -0.02 35%	-0.06 -0.07 -0.01 17%	obs model diff error
75	8729548	CAMP PINCHOT FLORIDA	-86.593333 30.470000	0.03	0.07 0.07 0.00 6%	0.07 0.07 0.00 6%	-0.06 -0.07 -0.01 14%	-0.07 -0.07 -0.00 7%	obs model diff error
76	8729567	CINCO BAYOU FLORIDA	-86.631667 30.428333	n/a	0.07 0.07 0.00 0%	0.07 0.07 0.01 11%	-0.06 -0.07 -0.01 19%	-0.07 -0.07 -0.00 0%	obs model diff error
77	8729598	HULBERT FIELD FLORIDA	-86.700000 30.406667	n/a	0.18 0.18 -0.00 -0%	0.16 0.18 0.01 9%	-0.15 -0.16 -0.01 8%	-0.17 -0.17 0.01 -5%	obs model diff error
78	8729613	HARRIS, SANTA ROSA SOUND FLORIDA	-86.731667 30.408333	n/a	0.18 0.19 0.02 9%	0.16 0.19 0.03 16%	-0.18 -0.18 0.01 -3%	-0.20 -0.18 0.02 -12%	obs model diff error

No.	Station	Location	Longitude	Obs		Model			Source
	ID	Name	Latitude	rms	MHHW	MHW	MLW	MLLW	ID
79	8729678	NAVARRE BEACH FLORIDA	-86.865000 30.376667	0.02	0.22 0.21 -0.01 -3%	0.20 0.21 0.01 3%	-0.18 -0.19 -0.01 4%	-0.20 -0.20 0.00 -1%	obs model diff error
80	8729679	SANTA ROSA SOUND, EAST END FLORIDA	-86.863333 30.385000	0.02	0.22 0.21 -0.01 -3%	0.20 0.20 0.01 5%	-0.20 -0.19 0.01 -3%	-0.21 -0.19 0.01 -7%	obs model diff error
81	8729736	WOODLAWN BEACH FLORIDA	-86.991667 30.386667	0.01	0.21 0.20 -0.01 -3%	0.20 0.20 0.00 1%	-0.20 -0.19 0.01 -4%	-0.20 -0.19 0.01 -7%	obs model diff error
82	8729747	SHIELD POINT, BLACKWATER RIVER FLORIDA	-87.015000 30.581667	0.01	0.24 0.22 -0.02 -9%	0.21 0.22 0.00 2%	-0.21 -0.21 -0.00 0%	-0.24 -0.21 0.03 -12%	obs model diff error
83	8729753	BLACKWATER RIVER FLORIDA	-87.028333 30.636667	0.02	0.25 0.22 -0.03 -11%	0.21 0.22 0.01 3%	-0.22 -0.21 0.00 -1%	-0.25 -0.21 0.04 -15%	obs model diff error
84	8729757	MILTON FLORIDA	-87.036667 30.626667	n/a	0.24 0.22 -0.02 -7%	0.20 0.22 0.02 8%	-0.20 -0.21 -0.02 8%	-0.24 -0.21 0.03 -11%	obs model diff error
85	8729791	HERNANDEZ POINT NORTH FLORIDA	-87.100000 30.455000	0.01	0.20 0.21 0.01 3%	0.18 0.20 0.02 10%	-0.17 -0.19 -0.02 11%	-0.20 -0.19 0.01 -4%	obs model diff error
86	8729793	MULLATTO BAYOU FLORIDA	-87.103333 30.545000	n/a	0.23 0.21 -0.01 -6%	0.22 0.21 -0.01 -5%	-0.20 -0.20 0.00 -2%	-0.23 -0.20 0.03 -13%	obs model diff error
87	8729806	FISHING BEND, SANTA ROSA SOUND FLORIDA	-87.140000 30.336667	0.02	0.20 0.20 -0.00 -1%	0.18 0.19 0.01 7%	-0.18 -0.18 -0.00 2%	-0.19 -0.18 0.01 -7%	obs model diff error
88	8729808	LITTLE SABINE BAY FLORIDA	-87.146667 30.336667	n/a	0.20 0.19 -0.00 -2%	0.18 0.19 0.01 4%	-0.18 -0.18 -0.00 1%	-0.19 -0.18 0.02 -8%	obs model diff error
89	8729824	FLORIDATOWN, ESCAMBIA BAY FLORIDA	-87.180000 30.581667	0.01	0.23 0.21 -0.01 -6%	0.21 0.21 -0.00 -0%	-0.19 -0.20 -0.01 5%	-0.22 -0.20 0.02 -9%	obs model diff error
90	8729831	FERRY PASS, ESCAMBIA BAY FLORIDA	-87.195000 30.545000	n/a	0.22 0.21 -0.01 -6%	0.21 0.21 -0.01 -4%	-0.17 -0.20 -0.02 12%	-0.20 -0.20 0.00 -0%	obs model diff error
91	8729840	PENSACOLA, PENSACOLA BAY FLORIDA	-87.211667 30.403333	0.02	0.20 0.19 -0.00 -1%	0.19 0.19 0.00 1%	-0.18 -0.18 0.00 -1%	-0.19 -0.18 0.01 -5%	obs model diff error

No.	Station	Location	Longitude	Obs		Model			Source
	ID	Name	Latitude	rms	MHHW	MHW	MLW	MLLW	ID
92	8729849	BAYOU CHICO FLORIDA	-87.251667 30.401667	n/a	0.19 0.19 -0.00 -1%	0.18 0.19 0.00 1%	-0.17 -0.18 -0.01 5%	-0.18 -0.18 0.01 -3%	obs model diff error
93	8729851	CHEMSTRAND PIER FLORIDA	-87.246667 30.598333	n/a	0.22 0.21 -0.01 -4%	0.20 0.21 0.01 4%	-0.20 -0.20 0.00 -1%	-0.22 -0.20 0.03 -11%	obs model diff error
94	8729868	PENSACOLA, NAVAL AIR STATION FLORIDA	-87.273333 30.345000	n/a	0.19 0.18 -0.00 -1%	0.18 0.18 0.01 4%	-0.17 -0.17 0.00 -0%	-0.18 -0.17 0.01 -7%	obs model diff error
95	8729871	WARRINGTON, BAYOU GRANDE FLORIDA	-87.276667 30.375000	n/a	0.19 0.19 0.00 1%	0.17 0.18 0.01 7%	-0.17 -0.18 -0.01 6%	-0.18 -0.18 0.01 -3%	obs model diff error
96	8729882	FORT PICKENS, PENSACOLA BAY FLORIDA	-87.291667 30.330000	n/a	0.18 0.19 0.00 2%	0.18 0.19 0.01 5%	-0.16 -0.16 0.00 -0%	-0.17 -0.16 0.01 -5%	obs model diff error
97	8729889	HEAD OF BAYOU GRANDE FLORIDA	-87.318333 30.370000	n/a	0.19 0.19 -0.00 -0%	0.18 0.19 0.00 2%	-0.18 -0.18 0.00 -1%	-0.18 -0.18 0.01 -5%	obs model diff error
98	8729905	MILLVIEW, PERDIDO BAY FLORIDA	-87.356667 30.418333	0.03	0.14 0.13 -0.01 -7%	0.13 0.13 -0.00 -3%	-0.12 -0.12 -0.00 0%	-0.11 -0.12 -0.00 2%	obs model diff error
99	8729909	BIG LAGOON FLORIDA	-87.356667 30.326667	0.01	0.17 0.16 -0.01 -4%	0.16 0.16 0.00 2%	-0.14 -0.15 -0.01 6%	-0.15 -0.15 0.01 -3%	obs model diff error
100	8729938	TARKLIN BAY FLORIDA	-87.415000 30.350000	n/a	0.10 0.12 0.01 14%	0.10 0.12 0.02 16%	-0.09 -0.11 -0.02 22%	-0.09 -0.11 -0.02 18%	obs model diff error
101	8729941	BLUE ANGELS PARK, PERDIDO BAY FLORIDA	-87.428333 30.386667	0.02	0.13 0.12 -0.01 -7%	0.13 0.12 -0.01 -6%	-0.12 -0.11 0.01 -11%	-0.12 -0.11 0.01 -11%	obs model diff error
102	8729943	HURST HAMMOCK, PERDIDO RIVER FLORIDA	-87.408333 30.458333	0.02	0.13 0.13 0.00 2%	0.12 0.13 0.01 8%	-0.10 -0.12 -0.02 24%	-0.11 -0.12 -0.00 4%	obs model diff error
103	8729949	NORTH PERDIDO RIVER FLORIDA	-87.443333 30.523333	0.02	0.13 0.13 -0.00 -0%	0.12 0.13 0.01 8%	-0.10 -0.12 -0.01 14%	-0.12 -0.12 0.00 -1%	obs model diff error
104	8729962	PERDIDO BAY FLORIDA	-87.425000 30.393333	0.02	0.11 0.12 0.01 7%	0.11 0.12 0.01 11%	-0.10 -0.11 -0.01 9%	-0.10 -0.11 -0.01 6%	obs model diff error

No.	Station	Location	Longitude	Obs		Model			Source
	ID	Name	Latitude	rms	MHHW	MHW	MLW	MLLW	ID
105	8729974	PERDIDO KEY, OLD RIVER FLORIDA	-87.448333 30.300000	0.02	0.13 0.11 -0.02 -16%	0.12 0.11 -0.01 -11%	-0.11 -0.10 0.01 -5%	-0.12 -0.10 0.01 -11%	obs model diff error
106	8730667	ALABAMA POINT, PERDIDO PASS	-87.555000 30.278611	0.02	0.14 0.12 -0.02 -15%	0.12 0.12 -0.01 -7%	-0.12 -0.10 0.02 -14%	-0.13 -0.10 0.02 -19%	obs model diff error
107	8731439	GULF SHORES, ICWW	-87.684278 30.279889	0.01	0.18 0.15 -0.03 -14%	0.17 0.15 -0.02 -12%	-0.15 -0.13 0.01 -9%	-0.17 -0.14 0.04 -21%	obs model diff error
108	8731952	BON SECOUR	-87.735000 30.303300	0.02	0.24 0.22 -0.01 -6%	0.23 0.22 -0.01 -4%	-0.22 -0.21 0.01 -6%	-0.23 -0.21 0.03 -11%	obs model diff error
109	8732828	WEEKS BAY, MOBILE BAY ALABAMA	-87.825000 30.416700	0.02	0.24 0.22 -0.02 -9%	0.21 0.22 0.01 5%	-0.20 -0.21 -0.01 6%	-0.24 -0.21 0.03 -11%	obs model diff error
110	8733821	POINT CLEAR, MOBILE BAY ALABAMA	-87.935000 30.486667	0.01	0.22 0.23 0.01 4%	0.23 0.22 -0.00 -1%	-0.23 -0.21 0.02 -8%	-0.24 -0.21 0.02 -10%	obs model diff error
111	8733839	MEAHER STATE PARK, DUCKER BAY ALABAMA	-87.936667 30.666667	0.01	0.23 0.24 0.01 6%	0.23 0.22 -0.01 -2%	-0.23 -0.22 0.01 -3%	-0.24 -0.23 0.01 -4%	obs model diff error
112	8735180	DAUPHIN ISLAND, MOBILE BAY	-88.075000 30.250000	0.00	0.20 0.20 0.01 4%	0.19 0.20 0.01 7%	-0.17 -0.17 -0.00 1%	-0.17 -0.17 0.00 -1%	obs model diff error
113	8735523	FOWL RIVER	-88.113300 30.443300	0.01	0.22 0.22 -0.00 -2%	0.20 0.21 0.01 4%	-0.20 -0.20 -0.00 2%	-0.22 -0.20 0.01 -6%	obs model diff error
114	8736897	COAST GUARD SECTOR MOBILE, MOBILE BAY	-88.058300 30.648300	0.01	0.25 0.24 -0.01 -4%	0.22 0.22 -0.00 -1%	-0.22 -0.22 0.00 -2%	-0.25 -0.23 0.02 -8%	obs model diff error
115	8737048	MOBILE STATE DOCKS, MOBILE RIVER ALABAMA	-88.043300 30.708300	0.01	0.25 0.24 -0.01 -2%	0.22 0.22 0.00 0%	-0.22 -0.22 0.00 -1%	-0.25 -0.23 0.02 -7%	obs model diff error
116	8737373	LOWER BRYANT LANDING, TENSAW RIVER	-87.873300 30.978300	0.02	0.25 0.27 0.02 9%	0.21 0.23 0.02 8%	-0.24 -0.23 0.02 -7%	-0.26 -0.26 0.01 -2%	obs model diff error
117	8738043	STATE HIGHWAY 188 BRIDGE, W. FOWL RIVER ALABA	-88.158333 30.376667	0.02	0.25 0.22 -0.02 -10%	0.20 0.22 0.02 8%	-0.20 -0.22 -0.01 7%	-0.24 -0.22 0.03 -11%	obs model diff error

No.	Station	Location	Longitude	Obs		Model			Source
	ID	Name	Latitude	rms	MHHW	MHW	MLW	MLLW	ID
118	8740166	GRAND BAY NERR, MISSISSIPPI SOUND MISSISSIPPI	-88.403333 30.413333	0.01	0.25 0.23 -0.02 -8%	0.22 0.22 0.00 1%	-0.20 -0.23 -0.03 15%	-0.24 -0.23 0.01 -4%	obs model diff error
119	8740405	PETIT BOIS ISLAND, MISS. SOUND MISSISSIPPI	-88.441667 30.203333	0.01	0.23 0.22 -0.01 -3%	0.21 0.22 0.00 2%	-0.20 -0.22 -0.02 10%	-0.22 -0.22 -0.00 2%	obs model diff error
120	8740448	POINT OF PINES, BAYOU CUMBEST MISSISSIPPI	-88.440000 30.386700	0.01	0.24 0.23 -0.02 -7%	0.21 0.22 0.01 7%	-0.21 -0.22 -0.01 6%	-0.25 -0.22 0.03 -11%	obs model diff error
121	8741041	DOCK E, PORT OF PASCAGOULA MISSISSIPPI	-88.505400 30.347700	0.01	0.24 0.23 -0.02 -7%	0.21 0.22 0.01 3%	-0.21 -0.22 -0.02 8%	-0.23 -0.22 0.01 -5%	obs model diff error
122	8741196	PASCAGOULA POINT, MISS. SOUND	-88.533300 30.340000	0.01	0.23 0.23 -0.01 -3%	0.21 0.22 0.01 6%	-0.21 -0.22 -0.02 8%	-0.23 -0.22 0.01 -4%	obs model diff error
123	8741533	PASCAGOULA NOAA LAB, PASCAGOULA RIVER MISSISS	-88.563000 30.367900	0.01	0.24 0.23 -0.01 -4%	0.21 0.22 0.01 6%	-0.20 -0.22 -0.02 11%	-0.23 -0.22 0.00 -2%	obs model diff error
124	8742205	GRAVELINE BAYOU ENTRANCE MISSISSIPPI	-88.663333 30.361667	0.01	0.25 0.23 -0.01 -5%	0.22 0.22 0.00 1%	-0.22 -0.23 -0.01 2%	-0.25 -0.23 0.02 -8%	obs model diff error
125	8742221	HORN ISLAND, MISSISSIPPI SOUND	-88.666700 30.238300	0.01	0.24 0.23 -0.01 -4%	0.21 0.23 0.02 8%	-0.21 -0.23 -0.02 11%	-0.24 -0.23 0.01 -6%	obs model diff error
126	8742947	EASTERN OLD FORT BAYOU MISSISSIPPI	-88.726700 30.440000	0.01	0.30 0.26 -0.04 -13%	0.21 0.24 0.03 15%	-0.24 -0.25 -0.00 1%	-0.33 -0.26 0.07 -22%	obs model diff error
127	8743081	HOLLINGSWORTH POINT, DAVIS BAYOU MISSISSIPPI	-88.773300 30.386700	0.01	0.27 0.25 -0.02 -9%	0.24 0.23 -0.01 -5%	-0.24 -0.24 0.01 -2%	-0.28 -0.25 0.03 -10%	obs model diff error
128	8743281	OCEAN SPRINGS MISSISSIPPI	-88.798300 30.391700	0.01	0.26 0.25 -0.01 -5%	0.24 0.23 -0.01 -4%	-0.22 -0.24 -0.02 7%	-0.26 -0.25 0.02 -6%	obs model diff error
129	8743735	BILOXI (CADET POINT), BILOXI BAY MISSISSIPPI	-88.856700 30.390000	0.02	0.27 0.25 -0.02 -7%	0.23 0.23 -0.01 -3%	-0.24 -0.23 0.00 -1%	-0.27 -0.25 0.02 -9%	obs model diff error
130	8744117	BILOXI, BAY OF BILOXI MISSISSIPPI	-88.903300 30.411700	0.02	0.27 0.26 -0.01 -4%	0.24 0.24 -0.00 -2%	-0.23 -0.24 -0.01 6%	-0.28 -0.26 0.02 -7%	obs model diff error

No.	Station	Location	Longitude	Obs		Model			Source
	ID	Name	Latitude	rms	MHHW	MHW	MLW	MLLW	ID
131	8744671	POPPS FERRY, BACK BAY OF BILOXI MISSISSIPPI	-88.975000 30.413333	0.01	0.29 0.26 -0.02 -8%	0.24 0.24 -0.01 -3%	-0.27 -0.25 0.02 -7%	-0.31 -0.27 0.04 -14%	obs model diff error
132	8744756	SHIP ISLAND, MISSISSIPPI SOUND MISSISSIPPI	-88.971700 30.213300	0.01	0.26 0.24 -0.02 -7%	0.22 0.23 0.01 6%	-0.22 -0.24 -0.01 6%	-0.26 -0.24 0.02 -8%	obs model diff error
133	8745375	TURKEY CREEK, BERNARD BAYOU MISSISSIPPI	-89.053300 30.426700	0.02	0.29 0.27 -0.02 -7%	0.25 0.24 -0.00 -1%	-0.26 -0.25 0.00 -1%	-0.32 -0.27 0.04 -14%	obs model diff error
134	8745557	GULFPORT HARBOR, MISSISSIPPI SOUND MISSISSIPP	-89.081700 30.360000	0.01	0.26 0.24 -0.02 -6%	0.23 0.22 -0.01 -4%	-0.24 -0.23 0.01 -3%	-0.27 -0.24 0.03 -9%	obs model diff error
135	8745799	CAT ISLAND, MISSISSIPPI SOUND MISSISSIPPI	-89.116700 30.231700	0.02	0.24 0.23 -0.02 -7%	0.21 0.21 -0.00 -0%	-0.21 -0.22 -0.01 4%	-0.24 -0.22 0.01 -6%	obs model diff error
136	8746487	EASTERN WOLF RIVER MISSISSIPPI	-89.200000 30.396700	n/a	0.16 0.23 0.07 46%	0.15 0.21 0.06 43%	-0.26 -0.22 0.04 -16%	-0.30 -0.23 0.07 -24%	obs model diff error
137	8746724	JOHNSON BAYOU MISSISSIPPI	-89.225000 30.336700	n/a	0.28 0.23 -0.06 -20%	0.23 0.21 -0.02 -10%	-0.23 -0.22 0.02 -6%	-0.29 -0.22 0.07 -23%	obs model diff error
138	8746737	CUEVAS, EASTERN BAYOU PORTAGE MISSISSIPPI	-89.225000 30.360000	n/a	0.28 0.23 -0.06 -21%	0.24 0.21 -0.03 -14%	-0.23 -0.22 0.01 -6%	-0.29 -0.22 0.07 -23%	obs model diff error
139	8746819	PASS CHRISTIAN YACHT CLUB, MISS. SOUND MISSIS	-89.245000 30.310000	0.01	0.26 0.23 -0.03 -12%	0.23 0.21 -0.02 -8%	-0.23 -0.22 0.02 -7%	-0.27 -0.22 0.04 -17%	obs model diff error
140	8746943	HENDERSON AVENUE BRIDGE, BAYOU PORTAGE MISSIS	-89.265000 30.341700	n/a	0.27 0.22 -0.04 -16%	0.22 0.21 -0.01 -4%	-0.23 -0.22 0.01 -5%	-0.28 -0.22 0.06 -20%	obs model diff error
141	8747038	HENDERSON AVENUE BRIDGE, WOLF RIVER MISSISSIP	-89.273300 30.358300	n/a	0.27 0.23 -0.05 -17%	0.22 0.21 -0.01 -4%	-0.23 -0.22 0.01 -4%	-0.28 -0.22 0.05 -19%	obs model diff error
142	8747131	MALLINI BAYOU NORTH MISSISSIPPI	-89.288300 30.326700	n/a	0.27 0.22 -0.04 -15%	0.23 0.21 -0.02 -10%	-0.23 -0.22 0.01 -5%	-0.27 -0.22 0.05 -18%	obs model diff error
143	8747145	MALLINI BAYOU SOUTH MISSISSIPPI	-89.286700 30.311700	n/a	0.26 0.22 -0.04 -15%	0.23 0.21 -0.02 -8%	-0.22 -0.21 0.01 -4%	-0.26 -0.22 0.05 -17%	obs model diff error

No.	Station	Location	Longitude	Obs		Model			Source
	ID	Name	Latitude	rms	MHHW	MHW	MLW	MLLW	ID
144	8747398	NORTH SHORE, BAY OF ST. LOUIS MISSISSIPPI	-89.321700 30.373300	n/a	0.27 0.23 -0.04 -16%	0.22 0.21 -0.01 -4%	-0.23 -0.22 0.01 -3%	-0.27 -0.22 0.05 -19%	obs model diff error
145	8747437	BAY WAVELAND YACHT CLUB, BAY ST. LOUIS MISSIS	-89.325778 30.326389	0.00	0.26 0.22 -0.04 -15%	0.23 0.21 -0.02 -9%	-0.23 -0.22 0.02 -7%	-0.27 -0.22 0.05 -17%	obs model diff error
146	8747739	JOURDAN RIVER ENTRANCE MISSISSIPPI	-89.366700 30.336700	n/a	0.27 0.23 -0.04 -16%	0.22 0.21 -0.01 -4%	-0.23 -0.22 0.01 -4%	-0.28 -0.23 0.05 -19%	obs model diff error
147	8747766	WAVELAND, MISSISSIPPI SOUND MISSISSIPPI	-89.366700 30.281700	0.01	0.24 0.21 -0.03 -12%	0.22 0.20 -0.02 -9%	-0.22 -0.21 0.01 -5%	-0.24 -0.21 0.03 -14%	obs model diff error
148	8747819	WATTS BAYOU, JOURDAN RIVER MISSISSIPPI	-89.373300 30.328300	n/a	0.28 0.23 -0.05 -18%	0.21 0.21 0.00 0%	-0.23 -0.22 0.00 -2%	-0.28 -0.23 0.06 -20%	obs model diff error
149	8749704	PEARLINGTON, PEARL RIVER MISSISSIPPI	-89.615000 30.240000	0.02	0.17 0.17 -0.00 -2%	0.16 0.16 0.00 3%	-0.19 -0.17 0.03 -14%	-0.20 -0.17 0.04 -19%	obs model diff error
150	8760412	NORTH PASS LOUISIANA	-89.036700 29.205000	0.02	0.17 0.19 0.02 12%	0.17 0.19 0.02 15%	-0.16 -0.19 -0.03 18%	-0.17 -0.19 -0.03 16%	obs model diff error
151	8760417	DEVON ENERGY FACILITY, NORTH PASS LOUISIANA	-89.044467 29.200750	0.01	0.18 0.19 0.01 4%	0.18 0.19 0.01 5%	-0.18 -0.19 -0.02 10%	-0.18 -0.19 -0.01 7%	obs model diff error
152	8760551	SOUTH PASS	-89.140000 28.990000	0.01	0.19 0.19 0.01 4%	0.18 0.19 0.01 7%	-0.18 -0.20 -0.02 9%	-0.18 -0.20 -0.01 6%	obs model diff error
153	8760595	BRETON ISLAND LOUISIANA	-89.173300 29.493300	0.02	0.20 0.20 0.01 3%	0.20 0.20 -0.00 -0%	-0.22 -0.21 0.01 -3%	-0.22 -0.21 0.01 -4%	obs model diff error
154	8760668	GRAND PASS LOUISIANA	-89.221700 30.126700	0.01	0.23 0.22 -0.00 -0%	0.21 0.21 0.00 1%	-0.20 -0.22 -0.02 7%	-0.22 -0.22 -0.00 1%	obs model diff error
155	8760742	COMFORT ISLAND LOUISIANA	-89.270000 29.823300	0.01	0.23 0.23 -0.00 -0%	0.22 0.21 -0.01 -3%	-0.23 -0.22 0.01 -3%	-0.25 -0.23 0.02 -7%	obs model diff error
156	8760781	SHELL OIL, EAST BAY LOUISIANA	-89.305000 29.053300	0.01	0.20 0.20 -0.01 -3%	0.20 0.20 -0.00 -1%	-0.19 -0.20 -0.01 4%	-0.20 -0.20 0.00 -1%	obs model diff error

No.	Station	Location	Longitude	Obs		Model			Source
	ID	Name	Latitude	rms	MHHW	MHW	MLW	MLLW	ID
157	8760889	OLGA COMPRESSOR STATION, GRAND BAY LOUISIANA	-89.380139 29.386556	0.02	0.19 0.21 0.02 10%	0.18 0.20 0.02 10%	-0.20 -0.22 -0.02 11%	-0.20 -0.22 -0.01 6%	obs model diff error
158	8760922	PILOTS STATION EAST, SOUTHWEST PASS, LA	-89.407500 28.932200	0.02	0.18 0.19 0.01 7%	0.18 0.19 0.02 9%	-0.18 -0.20 -0.02 11%	-0.18 -0.20 -0.02 9%	obs model diff error
159	8760943	PILOT STATION, SW PASS LOUISIANA	-89.418300 28.925000	0.01	0.19 0.19 0.00 2%	0.18 0.19 0.01 6%	-0.19 -0.20 -0.01 7%	-0.20 -0.20 -0.00 2%	obs model diff error
160	8761108	BAY GARDENE LOUISIANA	-89.618300 29.598300	0.02	0.21 0.20 -0.01 -6%	0.20 0.19 -0.00 -2%	-0.21 -0.16 0.05 -22%	-0.23 -0.16 0.06 -28%	obs model diff error
161	8761198	CHEVRON STATION 289, PELICAN ISLAND LOUISIANA	-89.598300 29.266700	0.01	0.17 0.15 -0.01 -9%	0.16 0.15 -0.01 -8%	-0.17 -0.14 0.03 -20%	-0.17 -0.14 0.04 -22%	obs model diff error
162	8761294	WEST PEARL RIVER LOUISIANA	-89.668300 30.230000	0.02	0.09 0.14 0.05 57%	0.09 0.13 0.05 57%	-0.10 -0.14 -0.04 41%	-0.10 -0.14 -0.04 39%	obs model diff error
163	8761305	SHELL BEACH, LAKE BORGNE LOUISIANA	-89.673250 29.868111	0.02	0.21 0.17 -0.04 -20%	0.19 0.16 -0.04 -20%	-0.21 -0.15 0.06 -28%	-0.22 -0.17 0.06 -26%	obs model diff error
164	8761385	VICINITY OF UNO CHEF MENTEUR PASS LOUISIANA	-89.801667 30.068333	n/a	0.17 0.12 -0.04 -25%	0.16 0.12 -0.04 -27%	-0.16 -0.13 0.03 -21%	-0.18 -0.14 0.04 -24%	obs model diff error
165	8761402	U.S. HIGHWAY 90, THE RIGOLETS LOUISIANA	-89.736700 30.166700	0.02	0.10 0.07 -0.03 -29%	0.10 0.07 -0.03 -27%	-0.11 -0.08 0.03 -29%	-0.12 -0.08 0.04 -34%	obs model diff error
166	8761414	BILLET BAY COMMUNITY, BILLET BAY LOUISIANA	-89.751700 29.371700	0.02	0.16 0.18 0.02 16%	0.15 0.18 0.03 18%	-0.15 -0.17 -0.02 11%	-0.16 -0.17 -0.01 5%	obs model diff error
167	8761426	GREENS DITCH, LAKE ST. CATHERINE LOUISIANA	-89.760000 30.111700	0.02	0.12 0.08 -0.04 -33%	0.11 0.08 -0.03 -30%	-0.12 -0.08 0.04 -32%	-0.12 -0.08 0.04 -32%	obs model diff error
168	8761473	RT. 433, BAYOU BONFOUCA LOUISIANA	-89.793300 30.271700	0.02	0.08 0.04 -0.04 -52%	0.08 0.04 -0.04 -51%	-0.08 -0.03 0.05 -60%	-0.08 -0.03 0.05 -60%	obs model diff error
169	8761484	LEASE VB #4, BAYOU DULAC LOUISIANA	-89.800000 29.456700	0.02	0.16 0.19 0.04 25%	0.15 0.19 0.04 27%	-0.16 -0.19 -0.03 17%	-0.16 -0.19 -0.02 13%	obs model diff error

No.	Station	Location	Longitude	Obs		Model			Source
	ID	Name	Latitude	rms	MHHW	MHW	MLW	MLLW	ID
170	8761487	CHEF MENTEUR, CHEF MENTEUR PASS LOUISIANA	-89.800000 30.065000	0.02	0.15 0.13 -0.02 -13%	0.14 0.12 -0.02 -12%	-0.15 -0.13 0.02 -14%	-0.17 -0.14 0.03 -18%	obs model diff error
171	8761529	MARTELLO CASTLE, LAKE BORGNE LOUISIANA	-89.835000 29.945000	0.01	0.21 0.17 -0.04 -19%	0.17 0.15 -0.02 -12%	-0.19 -0.15 0.04 -20%	-0.21 -0.17 0.04 -20%	obs model diff error
172	8761534	BIG POINT, LAKE PONTCHARTRAIN LOUISIANA	-89.853300 30.228300	0.02	0.07 0.04 -0.03 -47%	0.07 0.04 -0.03 -45%	-0.08 -0.04 0.05 -56%	-0.08 -0.04 0.05 -56%	obs model diff error
173	8761678	MICHOUD SUBSTATION, ICWW LOUISIANA	-89.936700 30.006700	0.01	0.21 0.16 -0.05 -25%	0.19 0.14 -0.04 -24%	-0.19 -0.14 0.04 -23%	-0.21 -0.16 0.06 -27%	obs model diff error
174	8761679	ST. MARYS POINT, BARATARIA BAY LOUISIANA	-89.938300 29.431700	0.01	0.15 0.18 0.04 27%	0.15 0.18 0.04 27%	-0.15 -0.18 -0.03 19%	-0.16 -0.18 -0.02 13%	obs model diff error
175	8761724	GRAND ISLE, EAST POINT LOUISIANA	-89.956667 29.263333	0.00	0.16 0.19 0.03 18%	0.16 0.19 0.03 19%	-0.16 -0.18 -0.02 15%	-0.16 -0.18 -0.02 13%	obs model diff error
176	8761742	MENDICANT ISLAND, BARATARIA BAY LOUISIANA	-89.980000 29.318300	0.01	0.15 0.18 0.03 18%	0.15 0.18 0.03 20%	-0.15 -0.17 -0.02 11%	-0.16 -0.17 -0.01 9%	obs model diff error
177	8761819	TEXACO DOCK, HACKBERRY BAY LOUISIANA	-90.038300 29.401700	0.02	0.13 0.19 0.05 40%	0.13 0.19 0.05 42%	-0.14 -0.18 -0.04 29%	-0.14 -0.18 -0.04 27%	obs model diff error
178	8761826	CHENIERE CAMINADA, CAMINADA PASS LOUISIANA	-90.040000 29.210000	0.01	0.15 0.17 0.02 11%	0.15 0.17 0.02 12%	-0.15 -0.16 -0.01 9%	-0.15 -0.16 -0.01 7%	obs model diff error
179	8761927	USCG NEW CANAL STA., LAKE PONTCHARTRAIN LOUIS	-90.113417 30.027167	0.03	0.08 0.04 -0.03 -43%	0.08 0.04 -0.03 -43%	-0.08 -0.04 0.04 -48%	-0.07 -0.04 0.03 -45%	obs model diff error
180	8761993	TCHEFUNCTA RIVER, LAKE PONT LOUISIANA	-90.160000 30.378300	0.02	0.09 0.05 -0.04 -46%	0.08 0.05 -0.04 -45%	-0.09 -0.04 0.05 -55%	-0.09 -0.04 0.05 -53%	obs model diff error
181	8762273	EAST END, PASS MANCHAC LOUISIANA	-90.311700 30.296700	0.01	0.07 0.05 -0.03 -38%	0.07 0.05 -0.03 -37%	-0.08 -0.04 0.04 -46%	-0.08 -0.04 0.04 -46%	obs model diff error
182	8762372	EAST BANK 1, NORCO, BAYOU LABRANCHE LOUISIANA	-90.368000 30.050333	0.01	0.06 0.05 -0.02 -25%	0.06 0.05 -0.01 -24%	-0.08 -0.04 0.03 -43%	-0.08 -0.04 0.03 -44%	obs model diff error

APPENDIX B TIDAL DATUMS AND SPATIALLY VARYING UNCERTAINTY IN MARINE GRIDS IN VDATUM REGION

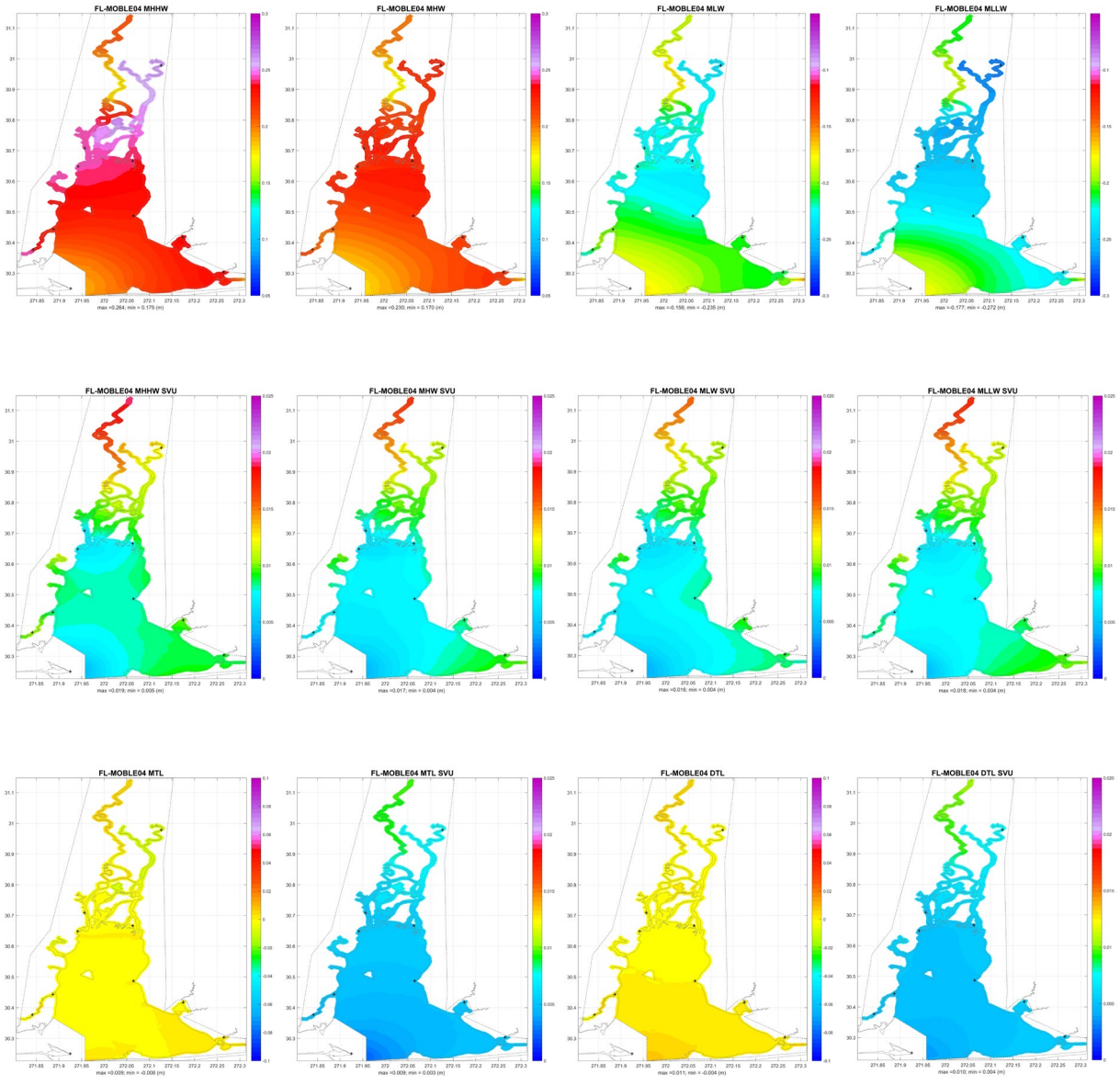

Figure B.1 Datum products and spatially varying uncertainty for the MOBLE marine grid.

(1)

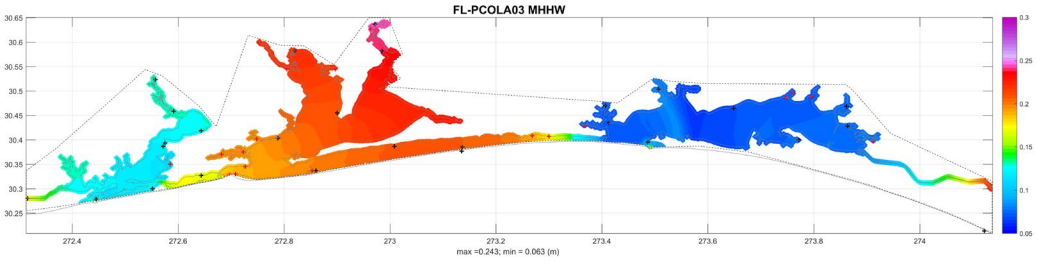
FL-PCOLA03 MHHW
max =0.243; min = 0.063 (m)

(2)

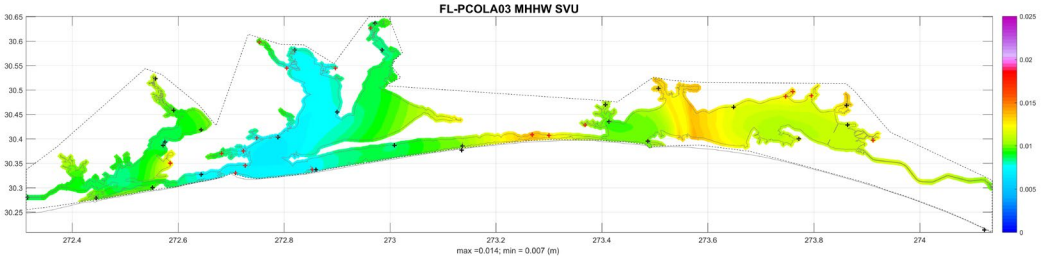
FL-PCOLA03 MHHW SVU
max =0.014; min = 0.007 (m)

(3)

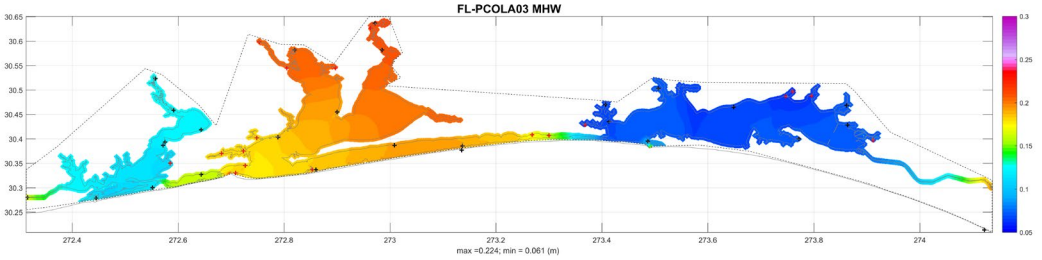
FL-PCOLA03 MHW
max =0.224; min = 0.061 (m)

(4)

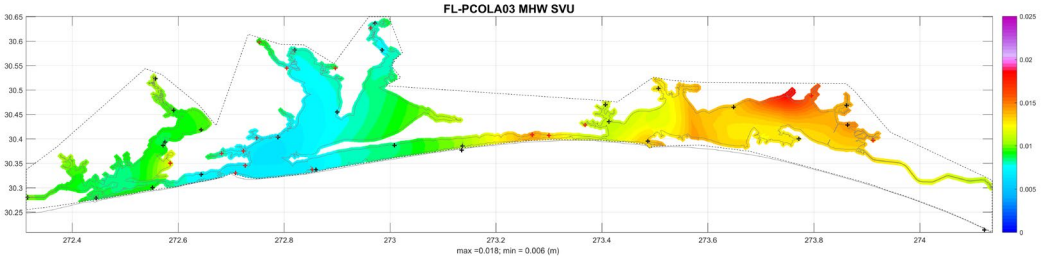
FL-PCOLA03 MHW SVU
max =0.018; min = 0.006 (m)

(5)

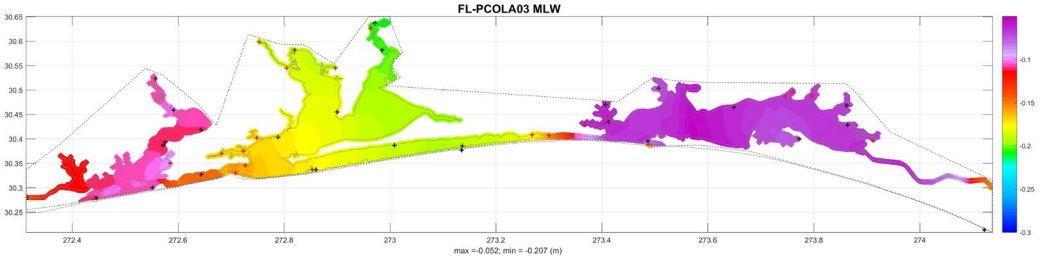
FL-PCOLA03 MLW
max =-0.052; min = -0.207 (m)

(6)

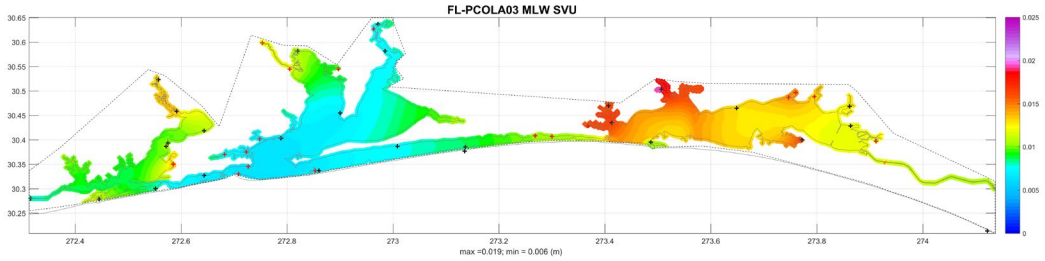
FL-PCOLA03 MLW SVU
max =0.019; min = 0.006 (m)

(7)

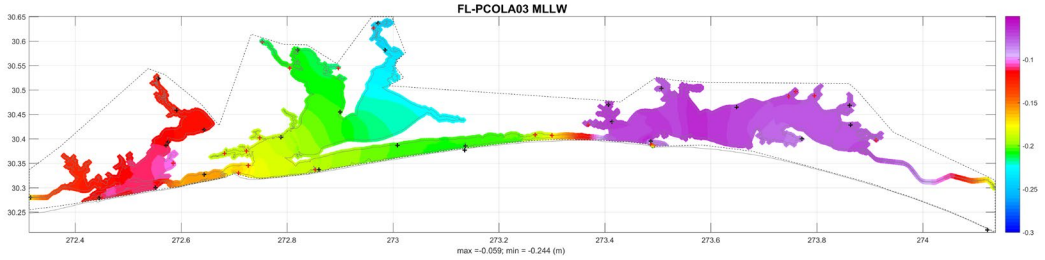
FL-PCOLA03 MLLW
max =-0.059; min = -0.244 (m)

(8)

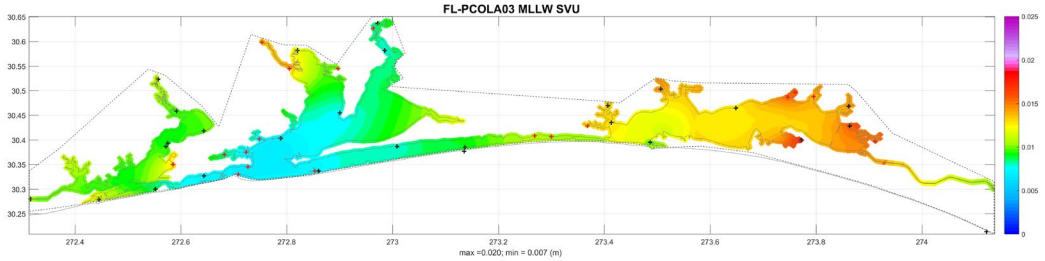
FL-PCOLA03 MLLW SVU
max =0.020; min = 0.007 (m)

(9)

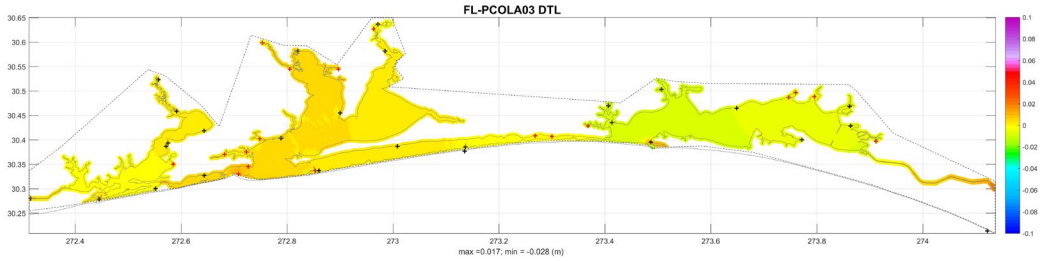
FL-PCOLA03 DTL
max =0.017; min = -0.028 (m)

(10)

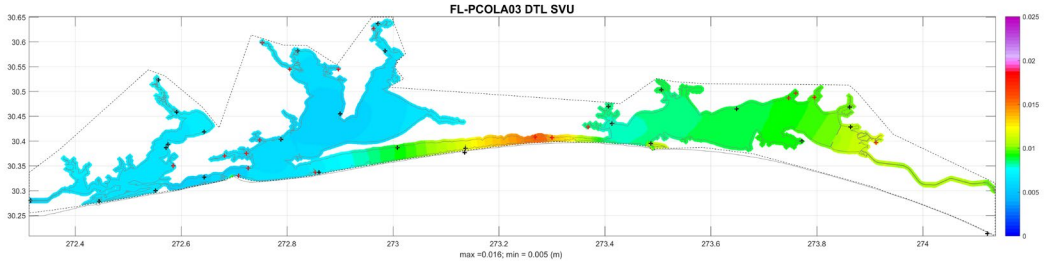
FL-PCOLA03 DTL SVU
max =0.016; min = 0.005 (m)

(11)

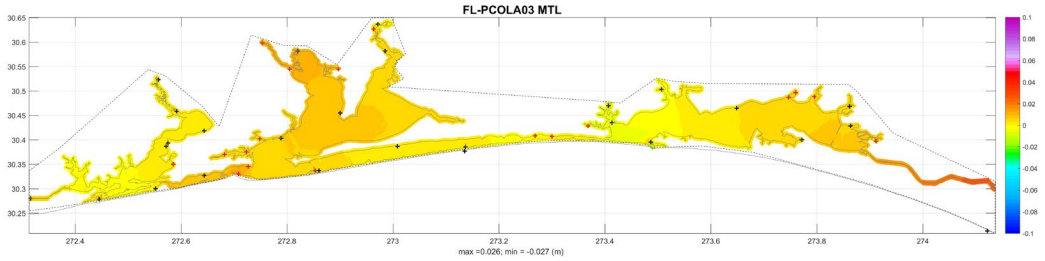

(12)

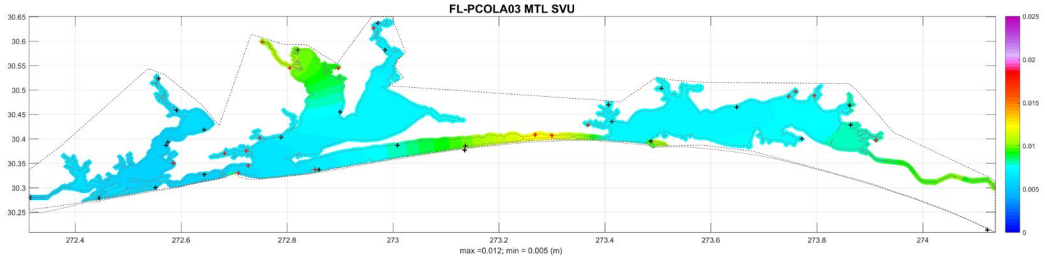

Figure B. 2 Datum products and spatially varying uncertainty for PCOLA marine grid.

(a) **(b)** **(c)**

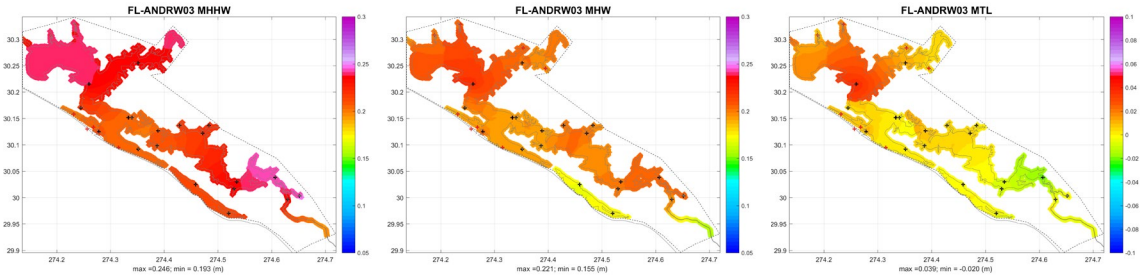

(d) **(e)** **(f)**

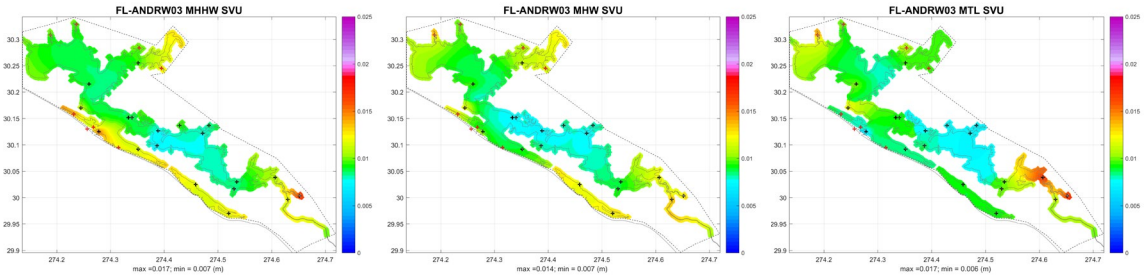

(g) **(h)** **(i)**

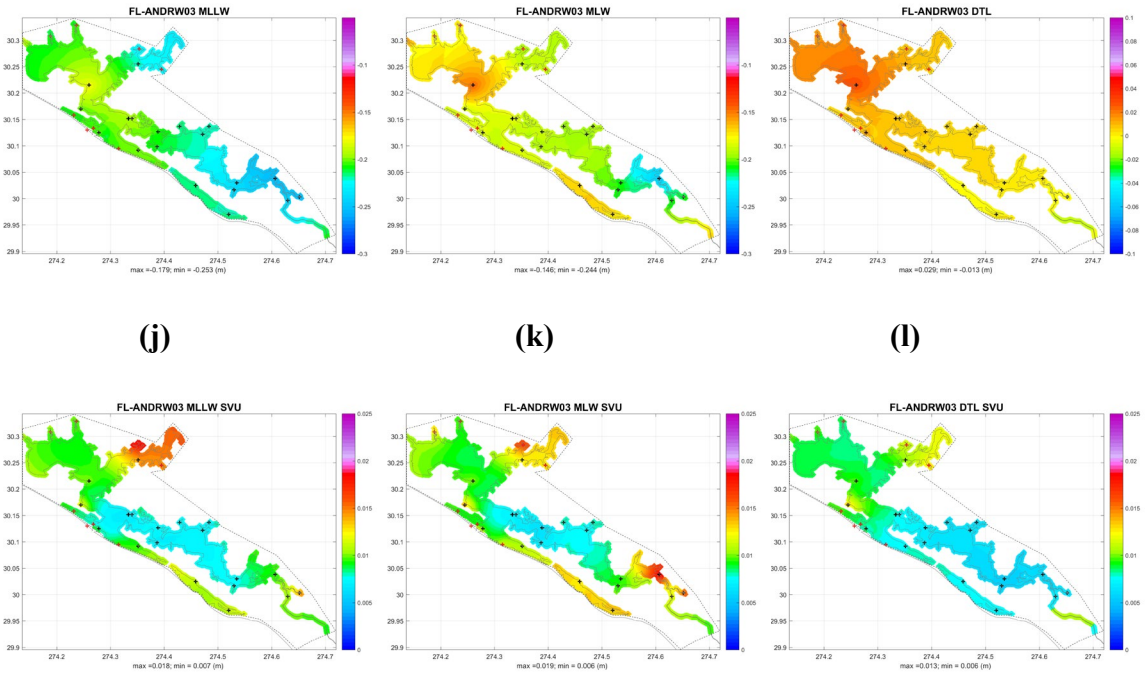

Figure B. 3 Datum products and spatially varying uncertainty for ANDRW marine grid.

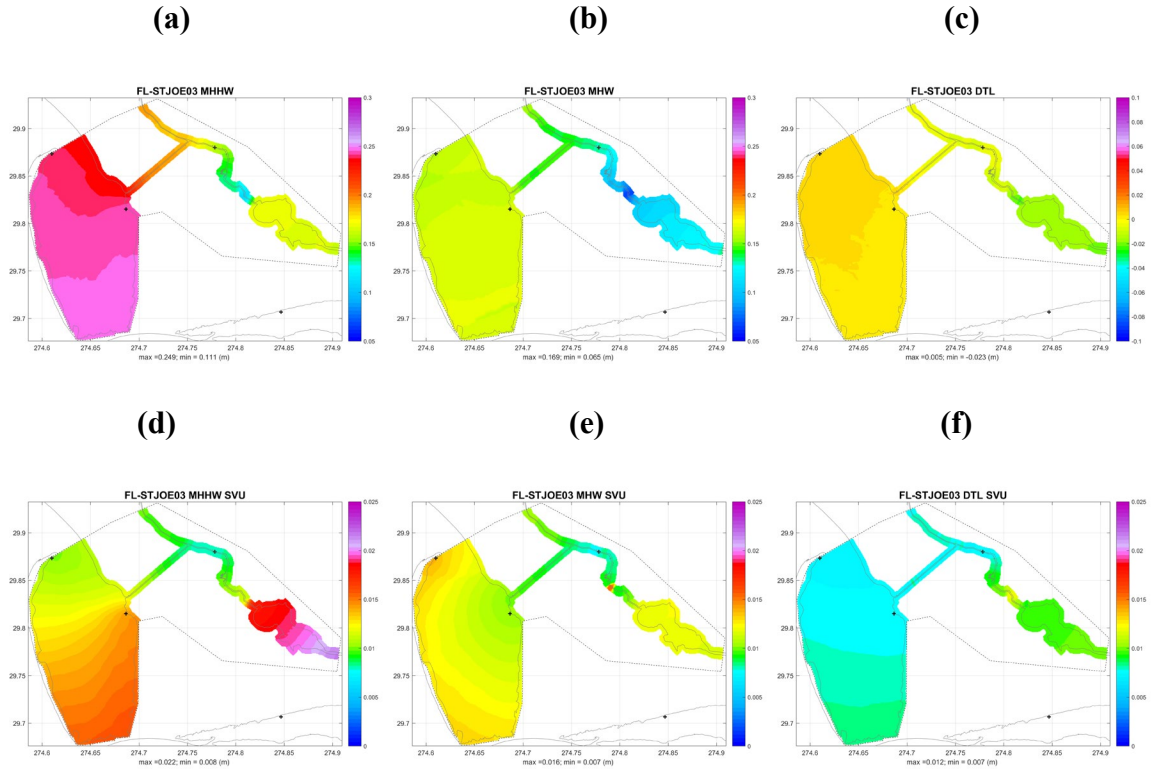

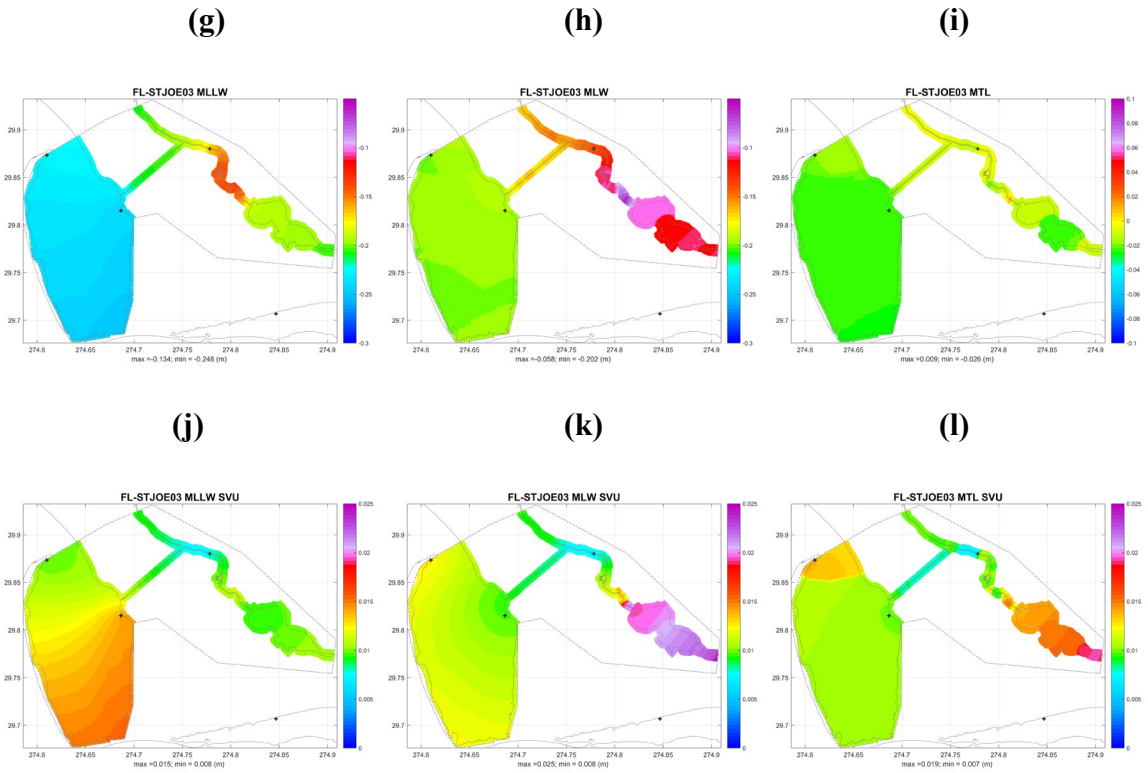

Figure B.4 Datum products and spatially varying uncertainty for STJOE marine grid.

(a) Datum products (b) SVU

(1)

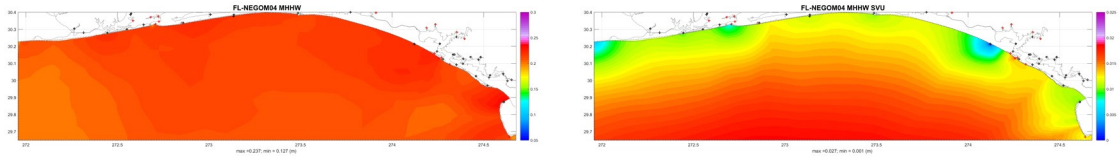

(2)

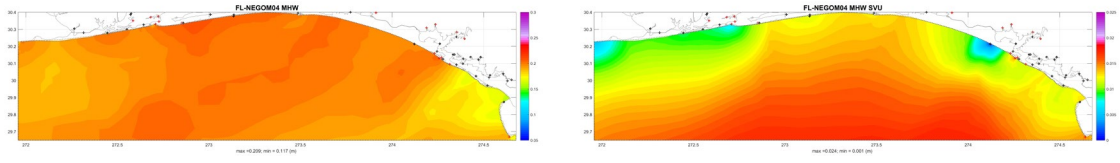

(3)

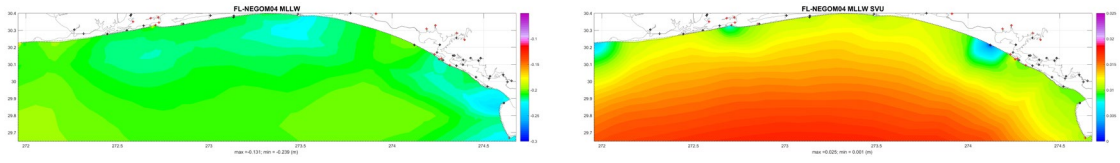

(4)

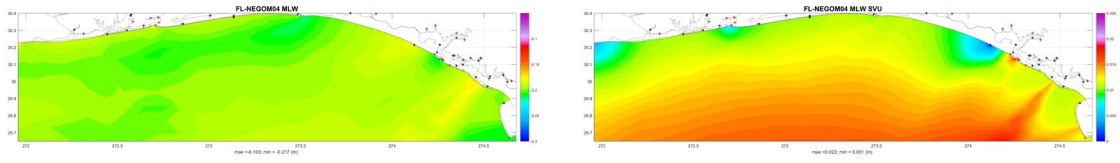

(5)

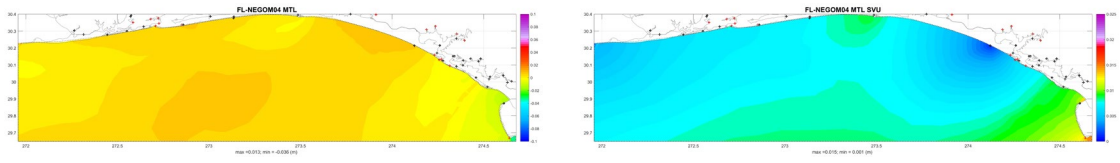

(6)

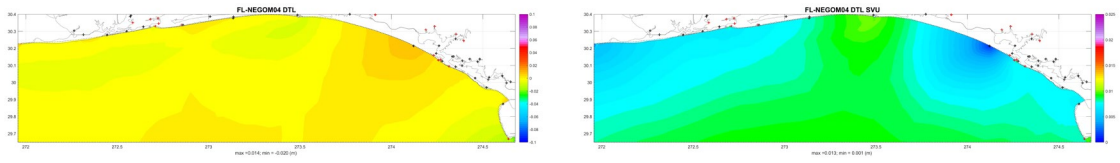

Figure B.5 (a) Datum products and (b) spatially varying uncertainty for NEGOM marine grid.